Permeability and Stability of Base and Subbase Materials

State Job No. 14512(0)

Final Report No. FHWA/OH 2000/017

by

Brian W. Randolph, Andrew G. Heydinger and Jiwan D. Gupta
with contributions by
Jiangeng Cai, Edward Steinhauser and Qinglu Xie

Department of Civil Engineering
The University of Toledo

August 2000

Prepared in cooperation with the
Ohio Department of Transportation
and the
U.S. Department of Transportation
Federal Highway Administration

1. Report No.	2. Government Accession No.	3. Recipient's Catalog No.
FHWA/OH-2000/017		3 1980 00021 9598

4. Title and Subtitle	5. Report Date
PERMEABILITY AND STABILITY OF BASE AND SUBBASE MATERIALS	August, 2000
	6. Performing Organization Code
7. Author(s)	8. Performing Organization Report No.
Brian W. Randolph, Andrew G. Heydinger and Jiwan D. Gupta	10. Work Unit No. (TRAIS)
9. Performing Organization Name and Address The University of Toledo Department of Civil Engineering 2801 West Bancroft Street Toledo, OH 43606-3390	11. Contract or Grant No. State Job No. 14512(0)
	13. Type of Report and Period Covered Final Report
12. Sponsoring Agency Name and Address Ohio Department of Transportation 1980 West Broad Street Columbus, OH 43223	14. Sponsoring Agency Code

15. Supplementary Notes

Prepared in cooperation with the U.S. Department of Transportation, Federal Highway Administration

16. Abstract This study determined the hydraulic conductivities, effective porosities and resilient moduli of several current and proposed drainable base materials. The materials studied were AASHTO No. 57, AASHTO No. 67, ODOT No. 304, ODOT No. 310, Iowa DOT No. 41-21 ('IA mix') and the 'New Jersey mix' studied by Baumgartner (1992). An in situ hydraulic conductivity test was developed for coarse grained materials under existing pavements. This device was tested on test sections of St. Rte. 2 for drainable bases composed of asphalt and Portland cement stabilized AASHTO No. 57, ODOT No. 304, ODOT No. 310, Iowa DOT No. 41-21 and the New Jersey mix. A large scale, horizontal laboratory permeameter and testing procedure were developed to simulate in situ conditions under a pavement. This was used to determine the range of hydraulic conductivities and effective porosities of several drainable bases made up of gravel, limestone and air cooled blast furnace slag over the range of gradations permitted by their specifications. The specifications studied were AASHTO No. 57, AASHTO No. 67, ODOT No. 304, ODOT No. 310, Iowa DOT No. 41-21 and the New Jersey mix. AASHTO No. 57 and AASHTO No. 67 were also stabilized with asphalt or Portland cement and tested. The resilient moduli of both stabilized and unstabilized base and subbase materials as a function of material variation were also investigated for this study. Wide variations exist in the hydraulic conductivities and effective porosities within gradation envelopes. All of the specifications tested can provide hydraulic conductivities in excess of 0.353 cm/s (1000 ft/day) in some portion of their gradation envelope. The lower limit of the gradation envelope (coarser) should be followed for ODOT 304 and ODOT 310. Stabilization reduces the hydraulic conductivity and effective porosity. The effective porosities suggest that most freely drained bases exist in a partially saturated state. Unstabilized No. 57 was found to have an equal or higher resilient modulus than the dense graded bases tested (ODOT 304, 310 and IA mix) for these moist conditions. Gravel generally provided the highest moduli, followed by limestone and air cooled blast furnace slag. Test procedures, equipment lists, data table worksheets, computer codes, field test results and laboratory test results are reproduced in Appendices A through Q, in an accompanying volume.

17. Key Words	18. Distribution Statement
Permeability, Hydraulic Conductivity, Drainage, In Situ Testing, Stability, Resilient Modulus, Drainable Base, Effective Porosity	No Restrictions. This document is available to the public through the National Technical Information Service, Springfield, Virginia 22161

19. Security Classif. (of this report)	20. Security Classif. (of this page)	21. No. of Pages	22. Price
Unclassified	Unclassified	186 (Appendices 338)	

Form DOT F 1700.7 (8-72) Reproduction of completed page authorized

Permeability and Stability of Base and Subbase Materials

State Job No. 14512(0)

Final Report No. FHWA/OH 2000/017

by

Brian W. Randolph, Andrew G. Heydinger and Jiwan D. Gupta
with contributions by
Jiangeng Cai, Edward Steinhauser and Qinglu Xie

Department of Civil Engineering
The University of Toledo

August 2000

Prepared in cooperation with the
Ohio Department of Transportation
and the
U.S. Department of Transportation
Federal Highway Administration

Disclaimer

Acknowledgements

The authors express their gratitude to Mr. Roger Green, Mr. Randy Morris, Mr. Aric Morse and Mr. Brad Young of the Ohio Department of Transportation for their guidance and constructive comments. The assistance of former University of Toledo graduate students Jiangeng Cai, Edward Steinhauser and Qinglu Xie for field and laboratory testing is gratefully acknowledged.

Table of Contents

LIST OF FIGURES

LIST OF TABLES

1. INTRODUCTION AND SCOPE

1.1 Background

Since the advent of the automobile early in the twentieth century and the construction of modern roadways, engineers have recognized that asphalt and concrete roadways need adequate subsurface drainage (Oglesby and Hewes, 1963). Among the reasons cited for pavement failures, the inadequate drainage of pavement structures has been identified as a primary cause of pavement distress. Many of the modern roadway problems are associated with inadequate subsurface drainage. For a pavement, even a jointless asphalt pavement, surface water can penetrate and accumulate in the base and subbase. A high groundwater table and capillary rise of groundwater are other sources of subgrade moisture. The inadequate drainage of the accumulated water under the pavement causes mud pumping, adverse stress redistribution in the subgrade and lowers the shear strength of subgrade soils. Freezing action of a saturated base is also detrimental. These factors result in serious damage and undermine the serviceability of pavements (Moulton, 1980). Therefore, adequate drainage is now considered essential for the long service life of a pavement. As a result, permeable bases have become more popular in the design and construction of pavements.

The AASHTO Guide for the Design of Pavement Structures (1986) addresses inadequate drainage as a problem by including drainage as an essential element of pavement design. Also, the Federal Highway Administration's (FHWA) pavement management and design policy encourages performing a drainage analysis for each new rehabilitation and reconstruction of a pavement. In order to minimize pavement distress, it is necessary to drain accumulated water out from pavement bases and subbases fast enough, and to a sufficient degree, as to prevent subgrade soils from becoming saturated.

The Ohio Department of Transportation (ODOT) specifies the gradational characteristics of unstabilized dense and open-graded aggregates, as well as aggregates stabilized with asphalt or Portland cement, in order to ensure adequate drainage and structural stability. However, direct measurement of important engineering properties such as resilient modulus and hydraulic conductivity of the materials have not been

determined. Therefore, this project was initiated to investigate several of these aggregates for hydraulic conductivity and resilient modulus.

Modern roads generally consist of three layers 1) subgrade, 2) aggregate base course material and 3) the pavement. The subgrade is the soil that underlies the site upon which the road is built. The aggregate base course material is a layer consisting of crushed stone or coarse gravel materials to provide drainage under the road and may include a subbase layer. The pavement layer is the top layer of the road, which usually consists of asphalt concrete or Portland cement concrete.

Many of the problems associated with asphalt concrete pavements are due to the same basic issue, inadequate subsurface drainage. In the absence of adequate drainage, rainwater and groundwater remain under the pavement, saturating the subsurface materials (e.g. aggregate base courses). Repetitive highway loadings of saturated subsurface materials cause the temporary development of very high pore pressures which causes a loss in strength in the unbound materials (Cedergren, 1974). The water and fine material is pumped out of the pore space by pavement flexure during repetitive highway loadings (see Figure 1.1). This phenomenon causes the void space under the pavement to be enlarged. Subsequent collapse of these void spaces reduces support for the pavement, causing potholes, rutting, and cracking (Yoder and Witczak, 1975).

The problems associated with Portland cement concrete pavements include broken joints and cracking of the pavement. Portland cement concrete pavements are susceptible to failure at their joints, often due to the pumping phenomenon. Groundwater and rainwater invade the subsurface materials, saturating these layers. Due to high pore pressures during repetitive highway loadings, water and fine material are pumped out of the subsurface due to deflection at the joints (see Figure 1.2). The void space increases in the subsurface under the joint due to the loss of the fine material. The subbase does not support the pavement slabs at the joints and the continuing stresses of the highway loadings at the joints. This subsequently causes their failure and cracking in the pavement (Spellman, 1972).

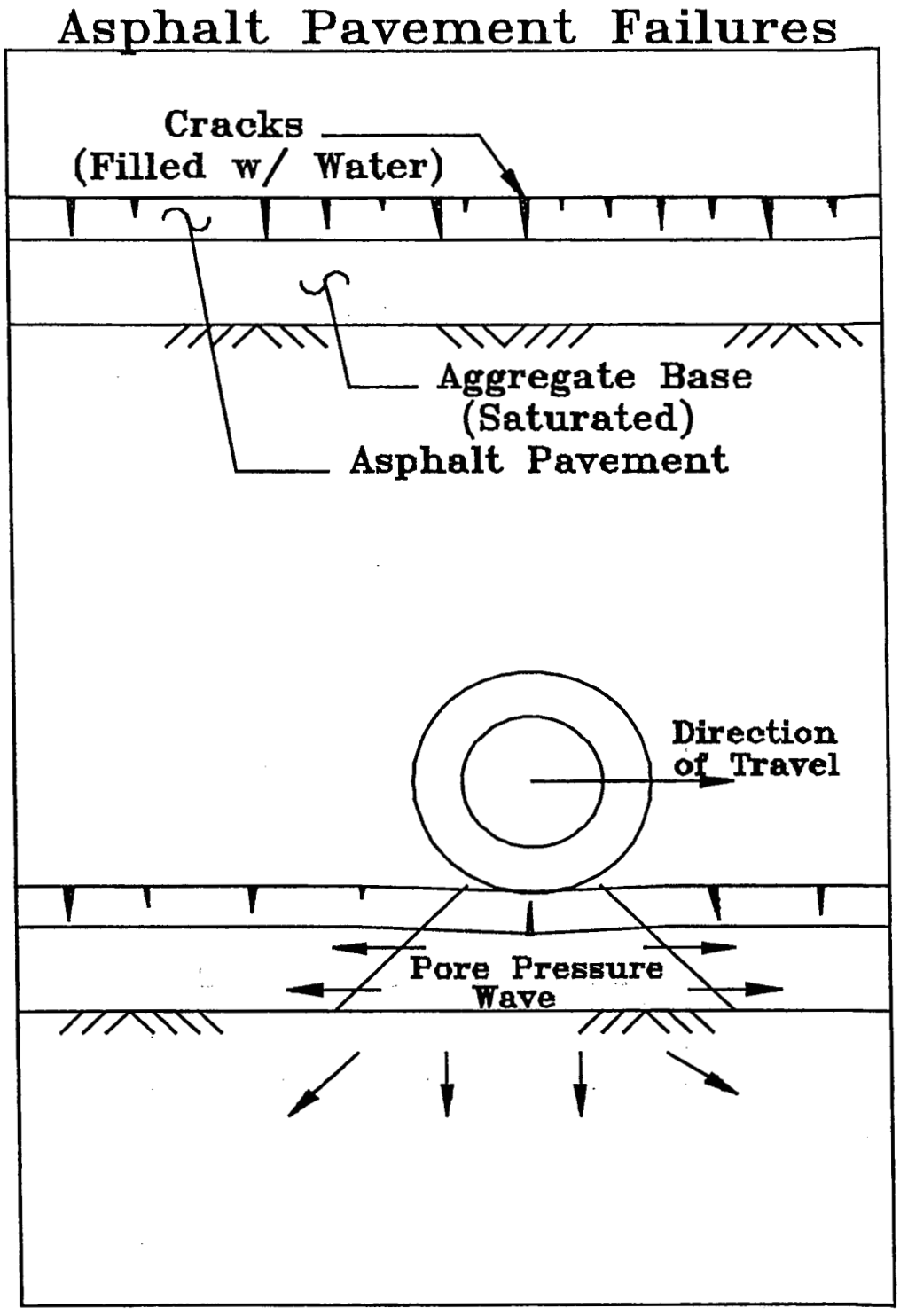

Figure 1.1: Asphalt pavement failure (from Moulton, 1980)

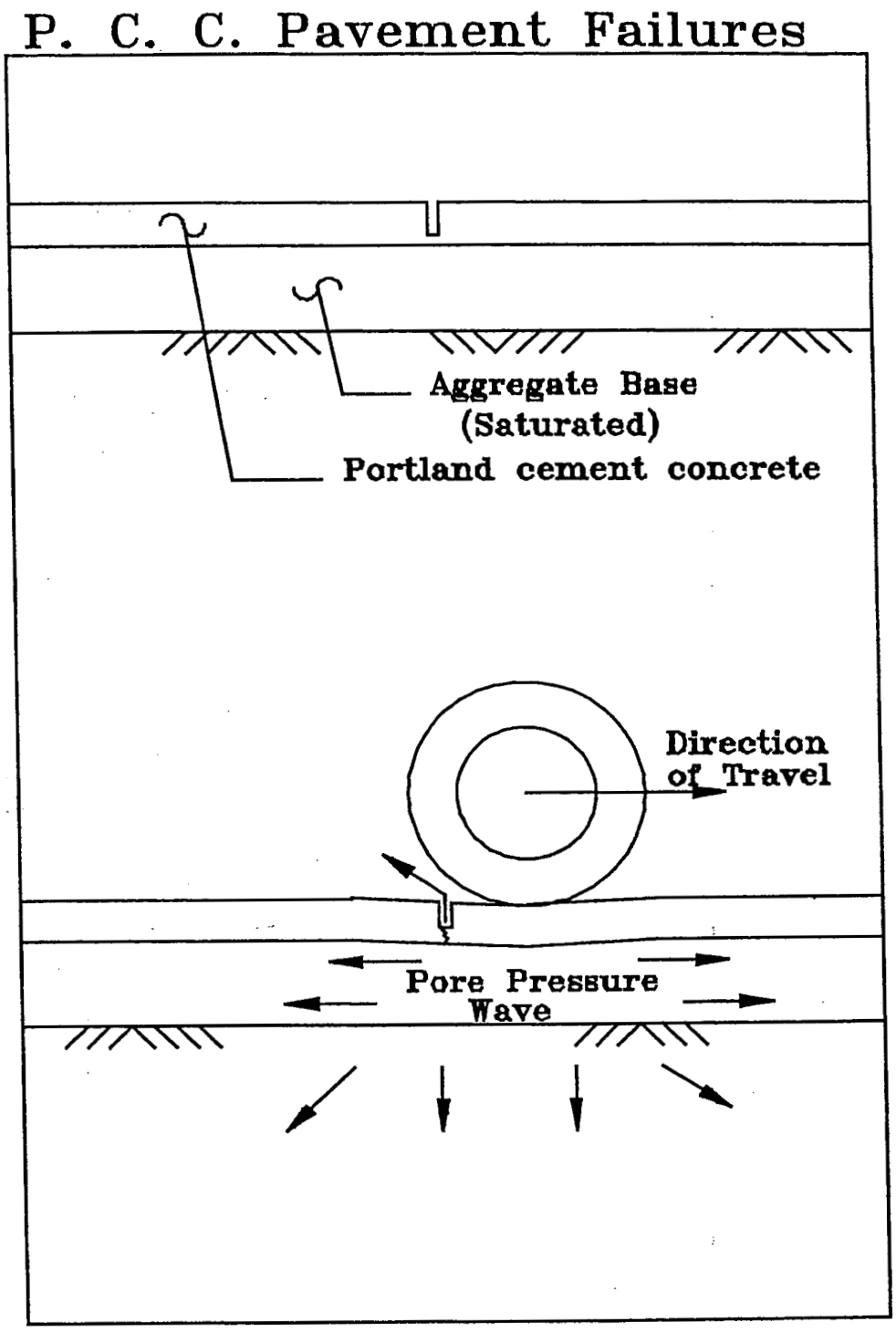

Figure 1.2: P. C. C. pavement failure (from Moulton, 1980)

Another problem associated with both types of pavements is frost heave. A pavement with insufficient subsurface drainage is susceptible to frost heave. Water that remains in the roadway base material freezes in the void space and forms an ice lens. Water is drawn to the ice lens by capillary action and expands as it freezes, lifting the pavement. After the ice lens melts, the subgrade becomes saturated and the pavement failures mentioned above occur.

Current methods of improving the subsurface drainage characteristics are to use aggregate base materials in combination with shallow pipe underdrains. Aggregate base materials typically have a higher hydraulic conductivity than subgrade materials. This increases the permeability of the drainage layer and permits the gravity flow of water in the base materials to a collection system. Therefore, aggregate bases used in conjunction with shallow pipe underdrains help to remove water from the subsurface. The use of these methods is more effective than laying the pavement directly on the subgrade. However, these materials are still susceptible to the same problems mentioned above if water is not removed.

Newer methods of improving the subsurface drainage characteristics of pavements are the use of open-graded asphalt or Portland cement stabilized aggregate base materials in combination with shallow pipe underdrains. These materials have been designed to have a significantly higher hydraulic conductivity than dense graded non-stabilized materials and a higher strength than coarse graded non-stabilized materials. Strength properties and hydraulic conductivities of base materials have yet to be studied extensively. Hence, it is not yet known whether these materials are adequate for subsurface drainage and pavement support.

Data required for analyzing the adequacy of subsurface drainage are: geometric properties, material properties, climatology data, and other miscellaneous considerations (Moulton, 1980). One important material property in the design of subsurface drainage is the hydraulic conductivity. At the present time, there is uncertainty about the hydraulic conductivity of current and proposed subsurface materials. Due to this, engineers are less confident in their subsurface drainage designs.

Currently, materials satisfying a certain gradation specification for a subbase or drainage layer are expected to have an acceptable value of hydraulic conductivity.

However, large variations in hydraulic conductivity within such a gradation envelope have been observed (Wu et al., 1987). For typical graded aggregates meeting generous gradation specifications, there is no reliable relation between hydraulic conductivity and gradation characteristics. Therefore, it is necessary to determine the ranges of hydraulic conductivity possible within a gradation envelope to furnish reliable information for use in drainage design. Hydraulic conductivity of stabilized bases which are asphalt bound or Portland cement bound need to be investigated also. An additional benefit would allow the designer to calculate the 'time to dewater' which indicates the adequacy of drainage when these materials are used in proposed typical cross sections.

While coarse grained materials tend to drain more freely, they also exhibit a decreased capability to support the pavement. A balance must be struck between using open graded material to drain the base in an attempt to increase support for the pavement and losing some of that support due to the open grading. One measure of the structural stability of a base or subbase material is its resilient modulus. The resilient modulus is an elastic modulus obtained from dynamic loading, defined as the ratio of the cyclic deviator stress to the resilient (recoverable) strain. It provides an indication of the degree of compliance of a layer in a pavement system under repeated traffic loading. Generally, a high resilient modulus for a base material will result in a long usable pavement life. Therefore, it is very important to have knowledge about the resilient properties of the pavement materials.

1.2 Scope

The first purpose of this research was to develop a standard in situ hydraulic conductivity test for coarse grained materials under pavements that yields reliable and consistent hydraulic conductivity values in the field. The research involved two principle tasks: first, the design and the procedure for an in situ hydraulic conductivity testing device and, second, the testing of this device to determine if it yields consistent and reliable hydraulic conductivity values for drainage materials used by the Ohio Department of Transportation. With accurate and consistent determination of the hydraulic conductivity of these materials, engineers can be more confident in their subsurface drainage designs.

The second purpose of this study was to design and construct a suitable laboratory permeameter, develop an appropriate testing procedure and produce valid, repeatable and accurate results for drainage materials used by the Ohio Department of Transportation over the range of gradations permitted by the specifications. The design should reproduce in situ conditions to the extent that laboratory results accurately represent the field behavior of the same drainage materials within acceptable limits.

The third purpose of this study was to use the in situ hydraulic conductivity test device to determine hydraulic conductivity values for various drainage materials present in pavement test sections in Ohio. The laboratory permeameter was also tested for consistency with the in situ hydraulic conductivity measurements. Once consistency was established, the laboratory test could be used to determine hydraulic conductivities over the full range of gradations permitted by the specifications.

The materials studied are AASHTO No. 57, AASHTO No. 67, ODOT No. 304, ODOT No. 310, Iowa DOT No. 41-21 ('Iowa mix') and the 'New Jersey mix' studied by Baumgartner (1992). Some of these materials were stabilized with asphalt or Portland cement. Comparisons are made between the in situ field test results for test pavement sections of Route 2, the results of the laboratory method and the results of other research, including an empirical formula and nomograph, for similar base and subbase materials.

The fourth purpose of this study was to determine the structural stability properties of some of the same drainable base and subbase materials tested for hydraulic conductivity. The resilient moduli of both stabilized and unstabilized base and subbase materials were investigated as a function of material variation for this study.

1.3 Organization of the Report

Chapter 2 contains the information which has been obtained through an extensive literature review of materials related to the research. Chapter 3 outlines the development of an in situ testing device and procedure for use under existing pavements, as well as its application for field tests to evaluate the hydraulic conductivity of base test sections. Chapter 4 details the development of a compatible laboratory device and procedure, as well as extensive testing of aggregate bases. Chapter 5 covers the stability testing of the same base materials, principally

using the resilient modulus test. Chapter 6 summarizes the results, outlines the conclusions drawn from this study and presents recommendations and suggestions for implementation. Chapter 7 has a comprehensive list of the literature cited in this work. Test procedures, equipment lists, data table worksheets, computer codes, field test results and laboratory test results are reproduced in Appendices A through Q, in an accompanying volume.

2.0 LITERATURE REVIEW

2.1 Darcy's Law

Darcy's Law was used in order to quantify the flow of water through porous media. The next two sections describe Darcy's Law in detail and discuss the conditions necessary for Darcy's Law to be valid.

2.1.1 Background on Darcy's Law

The first person to determine a relation to quantify the flow of water through porous media was Henry Darcy in 1856 (Bear, 1972). Darcy conducted a flow experiment on a column of sand. He found the flow of water through the column of sand was proportional to the cross-sectional area and proportional to the change in potential. The flow was also found to be inversely proportional to the length of sand in the column. This relationship, now known as Darcy's Law, is expressed mathematically as:

$$Q \propto \frac{A \, x \, \Delta\phi}{L} \qquad (2.1)$$

where: Q - the volumetric flow rate through the porous media $(\frac{L^3}{T})$

A - the cross sectional area (L^2)

$\Delta\phi$ - the change in potential = $(h_1 - h_2)$ (L)

L - the length of the specimen (L)

To make Darcy's Law an equality, a coefficient of proportionality is added to the relationship. This coefficient of proportionality is known as the hydraulic conductivity. The mathematical equation for Darcy's Law is now expressed as:

$$Q = \frac{K \, x \, A \, x \, \Delta\phi}{L} \qquad (2.2)$$

where: K - the hydraulic conductivity $(\frac{L}{T})$

Dividing equation 2.2 by area on both sides yields:

$$q = K \, x \, i \qquad (2.3)$$

where: q - specific discharge $(\frac{L^3}{T \, L^2})$

$i = \frac{\Delta \phi}{L}$ - the hydraulic gradient

For anisotropic, inhomogeneous, three dimensional flow Darcy's Law can be expressed in tensor notation as:

$$q_i = - K_{ij}(x_i) \frac{\partial \phi(x_i)}{\partial x_j} \quad for\ all\ i, j = 1,3 \qquad (2.4)$$

where: q_i - the specific discharge in the i direction

$K_{ij}(x_i)$ - the hydraulic conductivity tensor

$\frac{\partial \phi(x_i)}{\partial x_j}$ - the hydraulic gradient tensor

The Darcy column experiment is a very popular and well accepted method for determining the hydraulic conductivity of porous media. However, it is not well suited to in situ testing and must be carefully applied to high conductivity materials. The problem in this research is that the boundary conditions of the field are not always known because flow is unconfined and the gradient may be variable. This complicates the application of Darcy's law. Test conditions in situ and in laboratory experiments must not invalidate the limitations of Darcy's law. Hence, there was a need to develop an in situ hydraulic conductivity test and a complementary laboratory device and proceedure that comply with the limitations assumed in the development of Darcy's law.

2.1.2 *Range of Validity of Darcy's Law*

The value of hydraulic conductivity in equation 2.3 becomes nonconstant at higher values of specific discharge due to turbulent head losses. The general relationship of specific discharge as a function of hydraulic gradient is curved. However, for low gradients, the function can be treated as linear (Figure 2-1). This represents Darcy's law, on which the calculation of hydraulic conductivity in laboratory measurements is based ($K = \tan \alpha$). If a high hydraulic gradient is applied and it is misinterpreted as linear flow, then the calculated hydraulic conductivity ($K' = \tan \beta$) will be lower than the true hydraulic conductivity of linear flow. Linear behavior is associated with laminar flow, while deviations are attributed to inertial forces and turbulent head losses in smaller and smaller voids (Dudgeon, 1966; Lindquist, 1933; Hubbert, 1956; Scheidegger, 1960; Wright, 1968). It is necessary to define laminar and turbulent flow regimes if experimental results are to be correctly interpreted.

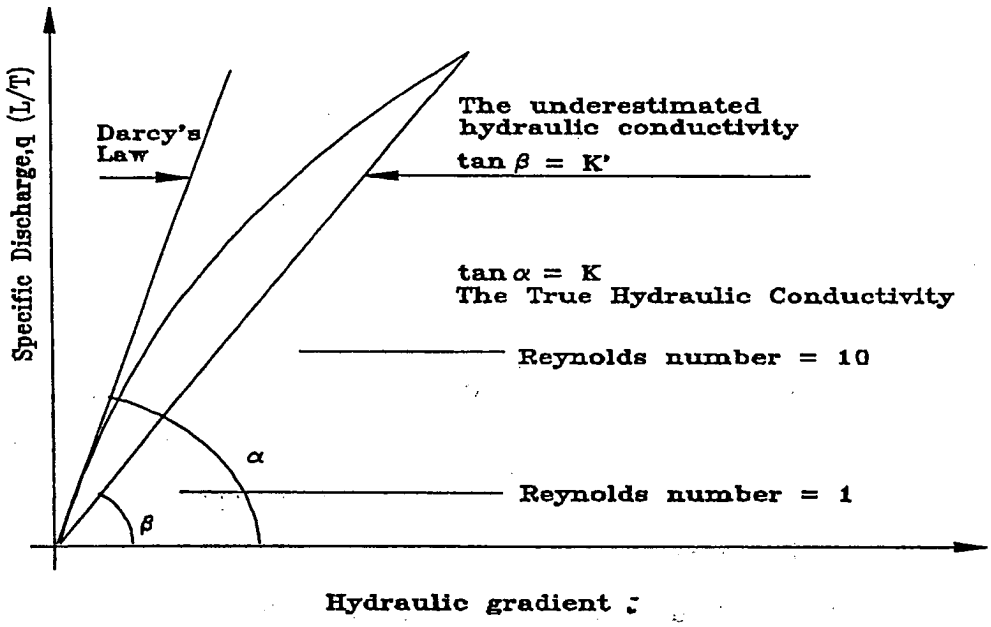

Figure 2-1: Experimental relationship between specific discharge and hydraulic gradient (After Bear, 1972; Jones and Jones, 1989).

The range of validity of Darcy's Law is determined by finding the critical gradient. The critical gradient corresponds to the limiting velocity that maintains laminar

flow conditions. The critical gradient was determined as a function of the Reynold's number, R_e, for porous media by Fancher and Lewis (1933):

$$R_e = \frac{q\, d_{mean}}{\nu} \leq 10 \qquad (2.5)$$

where: d_{mean} - the mean grain diameter of the media *(L)*

ν - the kinematic viscosity of the permeant $(\frac{L^2}{T})$

The mean grain diameter is calculated as follows (Muskat, 1937):

$$d_{mean} = \sqrt[3]{\frac{\sum n_s d_s^3}{\sum n_s}} \qquad (2.6)$$

where n_s - the number of particles of diameter, d_s

From the literature, it was found that $d_{mean} \approx D_{10}$ (Bear and Verruijt, 1987). This nomenclature signifies that ten percent (by weight) of a material's particles have a diameter less than D_{10}.

Therefore, a Reynold's number of less than or equal to ten at the expected or measured discharge velocity can be used to determine the actual hydraulic conductivity. Underestimation of hydraulic conductivity will occur when using Darcy's Law under turbulent conditions (see Figure 2-1).

The critical gradient can also be determined in laboratory experiments. Experimental results (Rose, 1945) show that there are three flow regions that may be present in flow through porous media as the Reynolds number increases (i.e. q increases for a certain porous media and fluid).

(1) Linear flow

At low Reynolds numbers, the flow is laminar and viscous forces are predominant. Darcy's law is valid. The upper limit of this range is at a value of Reynolds number between 1 and 10.

(2) Transition zone

As the Reynolds number increases, flow progresses from a laminar regime, where viscous forces are predominant, to another laminar regime where inertial forces govern the flow, then gradually passes to turbulent flow. This is referred to as the nonlinear laminar flow regime. As the Reynolds number is in the range of 60 to 150, turbulence occurs (Dudgeon,1966; Wright, 1968). Most experiments indicate that actual turbulence occurs at values of Reynolds number at least one order of magnitude higher than the Reynolds number at which deviation from Darcy's law is observed (Scheidegger, 1960).

(3) Turbulent flow

At high Reynolds number, turbulent flow occurs.

The deviation from Darcy's law in the transition zone (nonlinear laminar flow regime) has been attributed to inertial forces, which at low Reynolds number are negligible in comparison with viscous forces (Hubbert, 1956; Scheidegger, 1960). The inertial forces are proportional to the square of the specific discharge and are independent of the viscosity. As a result of various theoretical or experimental investigations, a large number of nonlinear motion equations appear in the literature (Scheidegger, 1960). Most of them have the form suggested by Forchheimer (1901)

$$i = W \cdot q + b \cdot q^2 \qquad (2.7)$$

The linear term stands for the viscous resistance and the quadratic term expresses the inertial resistance. Both W and b are constant. These values can be found by fitting the function to experimental data.

2.2 Factors Affecting Hydraulic Conductivity

Hydraulic conductivity is dependent on both soil matrix and fluid properties. The hydraulic conductivity of a homogeneous, isotropic soil mass depends primarily on the following factors:

1. Temperature. As the temperature increases, the viscosity and density of the fluid decrease. Thus, the flow rate increases and therefore, the hydraulic conductivity increases. The measured hydraulic conductivity can be corrected to a standard temperature, which is usually $20^0 C$, with the following :

$$K_{20} = K_T(\frac{\eta_T}{\eta_{20}}) \qquad (2.8)$$

where, K_{20} and K_T are the hydraulic conductivities, and η_{20} and η_T are the viscosities at $20^0 C$ and at temperature T, respectively. They can be found in reference tables such as Bowles (1992).

2. The void ratio of the soil. The ways in which a soil is placed or compacted has a considerable effect on the size and disposition of the voids between the particles, and hence the hydraulic conductivity. Void ratio can be used for an empirical approximation of hydraulic conductivity of sands by the Kozeny-Carmen equation (Head, 1982).

$$K = \frac{\rho_w g}{C\eta_w S^2} x \frac{e^3}{1+e} \qquad (2.9)$$

where ρ_w = density of water,

g = the acceleration due to gravity

η_w= viscosity of water,

S = specific surface of soil grains,

e = void ratio of soil, and

C = shape factor (C=5 for spherical particles).

3. Particle size distribution, shape and texture. The smaller the particles, the smaller the voids between them, and therefore, the resistance to flow increases with decreasing particle size. The effective grain size, D_{10}, can be used to predict the hydraulic conductivity of sands and gravel by Hazen's formula (Bowles, 1992)

$$K = \alpha D_{10}^2 \qquad (2.10)$$

where α is a factor which is approximately 100 (dimensions $cm^{-1}\,sec^{-1}$),

D_{10} is the effective particle size in centimeters.

A wide range of particle sizes creates the lowest void ratios and therefore, lower hydraulic conductivities.

The shape and texture of soil grains also affect hydraulic conductivity. Elongated or irregular particles create flow paths which are more tortuous than those around nearly spherical particles. Particles with a rough surface texture provide more frictional resistance to flow than do smooth textured particles. Both of theses conditions tend to reduce the rate of flow through the soil, and therefore, to reduce its hydraulic conductivity.

4. The degree of saturation. The degree of saturation of the tested sample is crucial in the measurement of hydraulic conductivity. Bubbles of air can block seepage channels between particles, thus appreciably reducing the hydraulic conductivity. If the degree of saturation is less than approximately 80%, air is likely to be continuous, instead of being in isolated bubbles, which dramatically lowers hydraulic conductivity (Head, 1982).

2.3 Sources of Variability in Laboratory Measurement of Hydraulic Conductivity

A number of sources of variability in laboratory testing of hydraulic conductivity of saturated cohesive soils have been identified. They are also encountered in the testing of granular and coarse materials.

2.3.1 Variation of samples in the laboratory

For cohesive soils, the most significant error is due to nonrepresentative samples. Laboratory samples may not include desiccation cracks, fissures and associated macrofabric defects. Also, the orientation of the in-situ stratum to the flow of water is probably not duplicated in the laboratory. Surface texture, tortuosity and compactive effort may all vary throughout a sample. Although the materials investigated in this study were mixed according to the gradation specifications, the variations of materials still exist and affect test results.

2.3.2 *Compactive effort and methods*

Previous studies have shown that water content at the time of compaction, compactive effort, and compaction method influence the hydraulic conductivity (Lambe, 1958). In the standard methods, using a vibrating tamper (dynamic method) or sliding weight tamper (static method), maximum compaction is usually carried out at a moisture content close to the optimum value. In order to obtain a reproducible density, the compactive effort should be adjusted in a process of trial and error. In spite of reflecting field practice, moist compaction runs the risk of occluding air bubbles which block pores, prevent full saturation and reduce hydraulic conductivity. Therefore, moist compaction must be followed by careful saturation if it is used for testing (Jones and Jones, 1989). In Jones and Jones' study (1989), a dry compaction method was used and it obtained maximum density for coarse materials. However, dry compaction gives rise to significant amounts of fines as dust and results in possible segregation problems.

2.3.3 *Degree of saturation*

Lack of complete saturation has also been shown to reduce the measured value of hydraulic conductivity (Irmay, 1954; Wallace, 1948; Wyckoff and Botset, 1936). In flexible-wall permeameters, a back pressure can be applied to provide improved saturation. However, this method is impractical for large sized rigid wall permeameters that are usually preferred for granular soils. The saturation procedure in the standard methods involves applying a vacuum to a dry specimen and filling with water from the bottom upward while under vacuum (ASTM D 2434-68). This has been shown to create full saturation. Besides standard methods, other procedures used to saturate soil specimens in rigid wall permeameters are

(1) to moisten soil by capillarity,

(2) to saturate specimens from the bottom upward under a hydraulic head greater than the length of the specimen,

(3) to saturate specimens from the top, with the air being evacuated from the bottom.

It has been shown (Christiansen, 1944; Smith and Browning, 1942; Chapuis, et al., 1989) that these methods give a degree of saturation between 75% and 97%.

Christiansen (1944) obtained saturation in the range of 85% to 90% with method 1, which is most suitable for fine-grained soils. He obtained a lower degree of saturation with method 3. An average of 91% saturation with low value of 78% was obtained by Smith and Browning (1942) using method 2 to saturate 200 soil samples. The experiments by Chapuis, et al. (1989), in which method 2 was used with de-aired water, gave degrees of saturation between 75% and 90% for sand specimens.

To reduce the dissolved air in the inflow water, the standard methods recommend the use of de-aired water during the test. Another technique is to use water warmer than the soil sample during the test so that the water cools as it percolates through the soil. This will attract air from the sample into solution. The standard methods also recommend connecting the tap water supply to a constant head filter tank. The filter in the tank can reduce the dissolved air in the tap water.

The use of de-aired water can improve the test results because the influence of a bubble of air coming out of solution in a small laboratory sample may be very significant considering the relative size of the bubble. However, the cost of producing a large volume of de-aired water is high. The use of de-aired water will produce a higher value of hydraulic conductivity in the laboratory than in the field because in situ water is neither de-aired nor distilled. As a simple expedient, the method of passing tap water through a sand filter and warming can be used when testing coarse materials (Bowles, 1992).

Even when the standard procedures have been carefully followed, it is possible that the degree of saturation is less than 100% if the permeameter is watertight but not airtight or if the air dissolved in the water is not completely removed (Chapuis, et al., 1989). The standard methods do not provide a practical procedure to check the real degree of saturation in a rigid wall permeameter. Chapuis, et al. (1989) proposed a method to determine the degree of saturation, S_r. The following measurements are made:

M_{tot} = the total mass of the system (permeameter and all fittings, filled with soil, water and air),

M_1 = the mass of the dry permeameter,

M_2 = the mass of the dry permeameter filled with dry soil,

M_e = the mass of the permeameter filled with de-aired water.

Then, the mass of dry soil is

$$M_s = M_2 - M_1 \qquad (2.11)$$

The mass of moist soil is

$$M_{ms} = M_{tot} - (M_e - V\rho_w) \qquad (2.12)$$

where V is the total volume of the sample. The mass of water in the soil specimen is

$$M_w = M_{ms} - M_s \qquad (2.13)$$

The volume of voids in the specimen is

$$V_v = V - \frac{M_s}{G\rho_w} \qquad (2.14)$$

where, G is the specific gravity of the tested soil. The degree of saturation is

$$S_r = \frac{V_w}{V_v} = \frac{M_w}{\rho_w V_v} = \frac{M_{tot} - M_e + V\rho_w - M_s}{V\rho_w - \frac{M_s}{G}} \qquad (2.15)$$

where V_w is the volume of the water in the saturated sample.

This method can be used to check if the saturation procedure used has obtained a high degree of saturation.

2.3.4 Temperature

It has been shown that small changes in laboratory temperature may not significantly affect the measured values of hydraulic conductivity (Olson and Daniel, 1979). However, temperature corrections can be made using equation 2.8 to correlate between laboratory and in situ results when the temperatures are appreciably different .

2.3.5 Hydraulic gradient

As the applied hydraulic gradients increase, flow velocity and Reynolds number will increase. Above a certain critical hydraulic gradient the flow becomes more turbulent and Darcy's law for flow in a saturated domain is no longer valid. There is an upper limit of hydraulic gradient for a material, below which Darcy's law is valid as stated in section 2.1.2. If the hydraulic gradient is greater than this limit, the ratio of specific discharge to hydraulic gradient decreases and deviates from the initial straight

line due to the increasing inertial resistance or turbulence. An underestimation of the hydraulic conductivity is obtained if a test, carried out beyond the range of validity of Darcy's law, is interpreted as if the law were valid. The error could easily be half an order of magnitude (Jones and Jones, 1989).

2.3.6 Permeameter dependent variables

A study was conducted to investigate the effect of permeameter type, flow direction, sample size, storage time, and desiccation cracking on measured hydraulic conductivity (Daniel, et al., 1985). Both fixed-wall permeameters and flexible-wall permeameters were examined. Among fixed-wall permeameters investigated were compaction mold permeameters, double-ring permeameters, consolidation cell permeameters, and fixed-cylinder permeameters.

Sidewall leakage was possible in the compaction mold device, but was relatively low in the double-ring permeameter that separates outflow through the central part of a sample from the flow along the sidewall. The sidewall leakage was minimized in the consolidation-cell permeameter because the applied vertical pressures squeezed the soil against the side wall. In fixed-cylinder permeameters the sidewall leakage was reduced by outfitting the end plates with undersized porous disks to capture the flow through the central portion of the sample.

The void ratio was relatively high in compaction mold permeameters because the applied vertical stresses during the test were zero. It was relatively low in the consolidation cell device because a vertical stress was applied. It was found that not only side-wall leakage but also applied stress cause differences in measured hydraulic conductivities.

In summary, applied vertical stress plays an important role in reducing sidewall leakage and void ratio. However, the applied vertical stress should not exceed the vertical stress in field conditions. A flexible wall permeameter can also reduce the effect of sidewall leakage. Flexible-wall permeameters not only tend to minimize sidewall leakage but also are convenient for testing with back pressure to obtain full saturation. For all rigid-wall permeameters, the specimen may remain unsaturated. Whether the factors above were significant to the test results was also dependent upon the material

properties, such as density, void ratio, chemical content, etc., according to the literature. It was suggested that one should take into account the advantages and disadvantages of a permeameter when selecting the type of cell to use for a particular project.

2.4 In Situ Hydraulic Conductivity Tests

In order to determine the best method to test in situ hydraulic conductivity, an extensive literature search was conducted with specific parameters of this research in mind. The criteria for the device were: its use for layered, non-homogeneous, anisotropic porous media and it's capability of measuring the hydraulic conductivity of layers of varying thickness of the same material. It was desirable to adopt a technique that was non-destructive or would create a minimal disturbance to the layer being evaluated. It was also desirable to create a device capable of accurately determining the hydraulic conductivity that would then be compared to results from a laboratory permeameter specifically designed to simulate conditions in the field.

2.4.1 Individual Boreholes and Wells

The first class of in situ hydraulic conductivity test methods investigated were individual borehole and well tests. There were three types of in situ hydraulic conductivity test methods that were investigated under this heading; (a) uncased individual boreholes and wells, (b) partially cased individual boreholes and wells, and (c) fully cased individual boreholes and wells (See Figure 2-2).

The different types of partially cased borehole and well tests that were identified are: (1) piezometer method, (2) well point method, (3) Soil Testing Engineers, Inc. testing method (STEI device), (4) constant head permeameter, and (5) porous probes. The piezometer method is a test that has to occur below the groundwater table, is used primarily for fine grained soils and is not good for rocky soil (Moulton and Seals, 1979). The well point method is another in situ hydraulic conductivity test for a soil below the groundwater table. This method is poor in rocky soil but good for fine grained soils (Moulton and Seals, 1979). The STEI device is an in situ hydraulic conductivity testing device that measures both horizontal and vertical hydraulic conductivity above the groundwater table. This device is generally used for fine grained soils (Soil Testing

Engineers, 1983; Boutwell and Derick, 1986; Daniel, 1989; Sai and Anderson, 1990). The constant head permeameter is a device that measures unsaturated horizontal hydraulic conductivity. This device measures only a small volume of soil and is primarily used for fine grained soils (Moulton and Seals, 1979; Olsen and Daniel, 1981; Stephens and Neuman, 1982a,b,c,d; Phillips, 1985; Reynolds et al., 1985; Reynolds and Elrick, 1986; Baumgartner et al., 1987; Stephens et al., 1987; Elrick et al., 1988; Stephens, 1988). The porous probe method is for unsaturated flow and determines horizontal hydraulic conductivity for fine grained soils (Moulton and Seals, 1979; Olson and Daniel, 1981; Torstenson, 1984; Chen and Yamamoto, 1987).

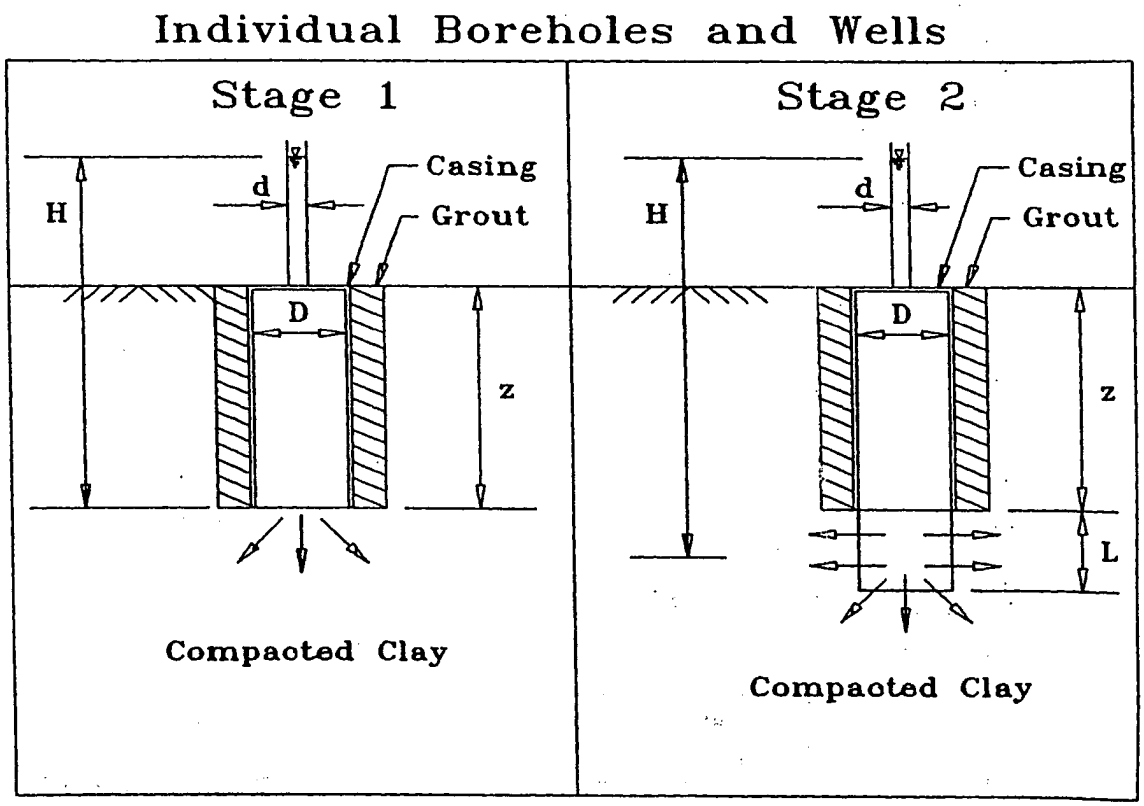

Figure 2-2: General schematic for individual boreholes and wells (from Daniel, 1989).

The final type of test method under the heading of individual boreholes and wells is the fully cased borehole test. The fully cased boreholes and well test method measures horizontal and vertical hydraulic conductivity. These devices are used below the groundwater table and determine the hydraulic conductivity in rocky soil (Moulton and

Seals, 1979). See Table 2-1 for the advantages and disadvantages of the individual borehole methods for this research.

Table 2-1 Advantages and disadvantages of individual borehole and well tests (after Moulton and Seals, 1979)

Test Method Uncased	Advantages	Disadvantages
(1) Packer Tests	measures horizontal hydraulic conductivity	only used for rock or cemented soil, below GWT, high disturbance
(2) Pumping Tests	measures horizontal hydraulic conductivity	costly, high disturbance, below GWT
(3) Auger Hole Method	measures horizontal and vertical hydraulic conductivity	high disturbance, below GWT
(4) Shallow Well Pump-in	above GWT, measures horizontal hydraulic conductivity	high disturbance, requires a large amount of water

Partially Cased	Advantages	Disadvantages
(1) Piezometer Method	horizontal hydraulic conductivity	not good for rocky soils; below GWT, high disturbance
(2) Well Point Method	horizontal hydraulic conductivity	not good for rocky soils; below GWT, high disturbance
(3) STEI	low cost, horizontal and vertical hydraulic conductivity, above GWT	used for fine grained soils, tests only small volume of soil, not good for unsaturated soils
(4) Constant Head Permeameter	low cost, horizontal and vertical hydraulic conductivity, above GWT	test small volume of soil, for fine grained soils, medium disturbance

Fully Cased	Advantages	Disadvantages
(1) Fully Cased	horizontal and vertical hydraulic conductivity	below GWT, high disturbance

2.4.2 *Multiple well systems*

The second class of in situ hydraulic conductivity tests that were assessed are multiple well systems. There are three types of in situ hydraulic conductivity testing methods that were investigated under this heading: (a) pumping test with observation wells, (b) two well, one pumping out and the other recycling the discharge, and (c) four well system (see Figure 2-3).

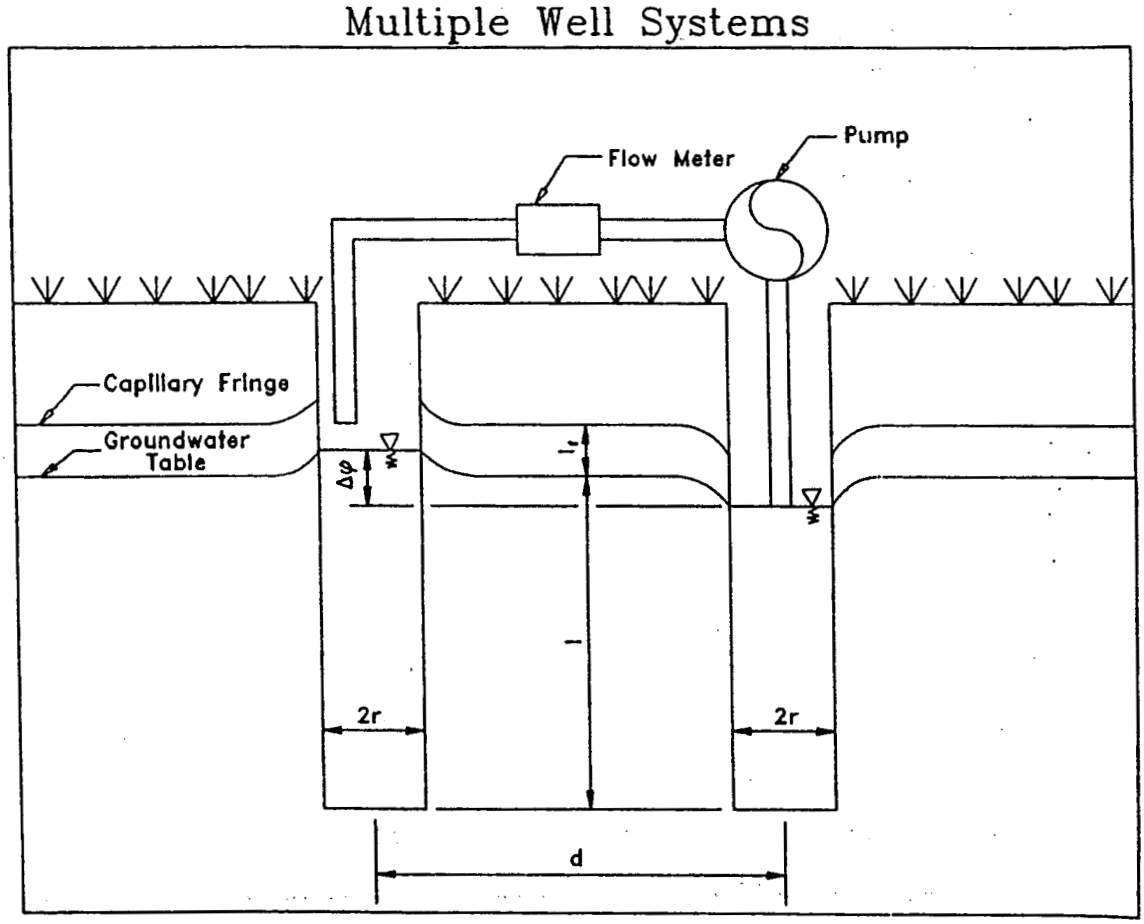

Figure 2-3: General schematic for multiple well systems (from Daniel, 1989).

The pumping tests with observation wells is a method of testing that occurs below the groundwater table which measures primarily horizontal hydraulic conductivity (Moulton and Seals, 1979). The two well system with one well pumping out and the other well recycling the discharge is another method of testing in situ hydraulic conductivity below the groundwater table. This method primarily measures horizontal

hydraulic conductivity but has problems with hole clogging (Moulton and Seals, 1979). The four well system is a method which is run on soils that are below the groundwater table. This method measures horizontal hydraulic conductivity (Moulton and Seals, 1979). See Table 2-2 for advantages and disadvantages of these devices for this research.

Table 2-2 Advantages and disadvantages of multiple well system tests (after Moulton and Seals, 1979)

Test Method	Advantages	Disadvantages
(1) Pumping Test with Observation Wells	horizontal hydraulic conductivity	high disturbance, below GWT
(2) Two Well System with One Pumped into the Other Well	horizontal hydraulic conductivity	below GWT, high equipment cost, hole clogging, long time, medium disturbance
(3) Four Well System	horizontal hydraulic conductivity	below GWT, high equipment cost, long time, medium disturbance

2.4.3 Infiltrometers

The third class of in situ hydraulic conductivity test methods that were assessed are infiltrometers. There are five types of testing methods that were investigated under this heading: (a) single ring, (b) cylinder permeameter, (c) double ring, (d) gradient intake, and (e) seepage meter (see Figure 2-4).

The single ring infiltrometer is the first method of testing that was investigated. The single ring infiltrometer can be either open or sealed and measures vertical hydraulic conductivity in soil located above the groundwater table (Moulton and Seals, 1979; Olson and Daniel, 1981; Amerman, 1983; Daniel, 1984; Day and Daniel, 1985; Stewart and Nolan, 1987; Daniel, 1989; Fernuik and Haug, 1990; Sai and Anderson, 1990).

The cylinder permeameter is the next method of testing that was assessed. This method is primarily for testing fine grained soils in the vertical direction (Moulton and Seals, 1979).

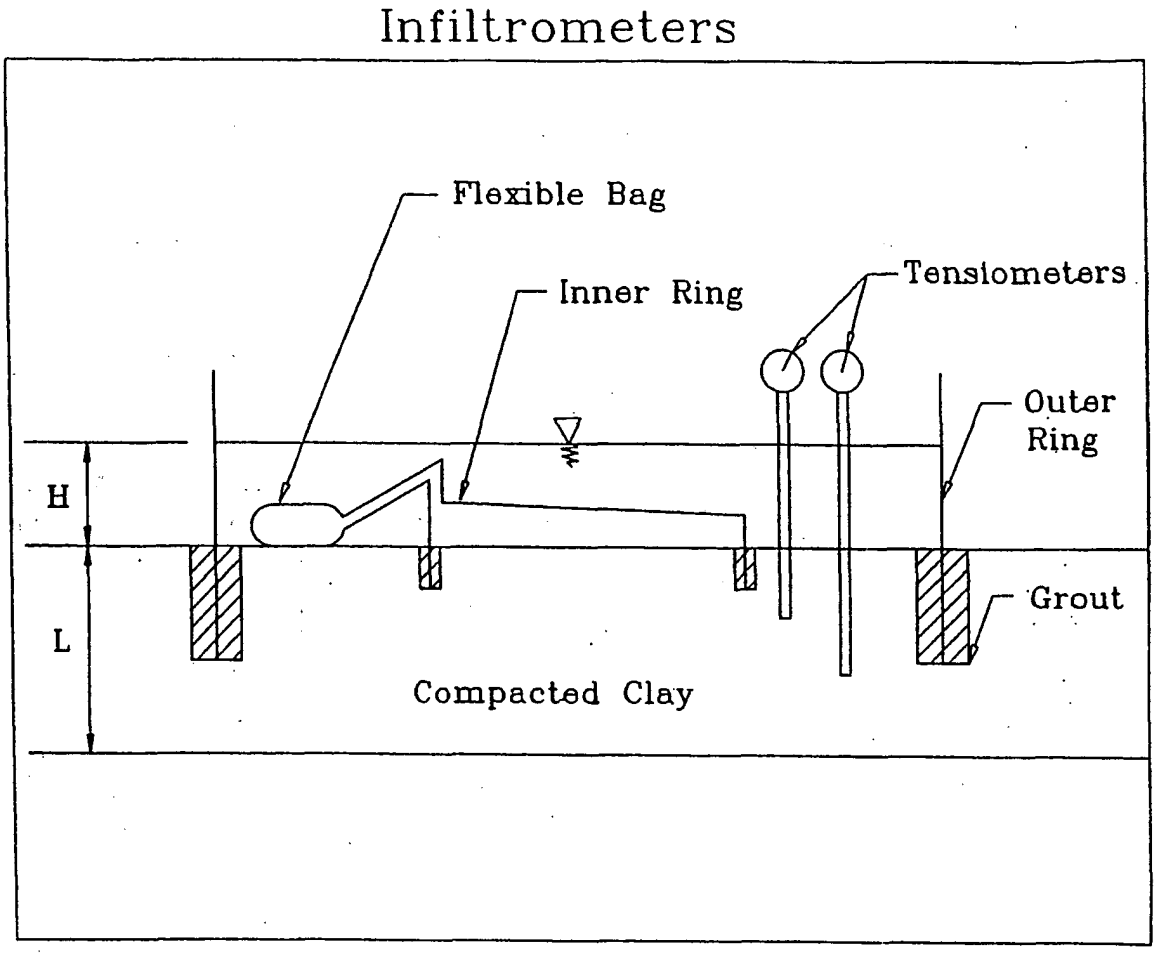

Figure 2-4: General schematic for infiltrometers (from Daniel, 1989)

The third in situ hydraulic conductivity testing method that is investigated was the double ring infiltrometer. The double ring infiltrometer is similar to the single ring infiltrometer in that it can be open or sealed and primarily measures vertical hydraulic conductivity. However, it has an outer ring to help define a vertical flow field from the inner ring. This device is primarily used for fine grained soils such as compacted clays (Moulton and Seals, 1979; Daniel, 1984; Daniel and Trautwein, 1986; Day and Daniel, 1985; Chen and Yamamoto, 1987; Fernuik, 1987; Elsbury and Smith, 1988; Daniel, 1989; Fernuik and Haug, 1990).

A fourth type of infiltrometer is the gradient intake infiltrometer. This method of testing is for soils above the groundwater table and determines vertical hydraulic conductivity. This device is inadequate for testing the in situ hydraulic conductivity of

coarse gravel because the wetting front can not be maintained in highly porous materials (Moulton and Seals, 1979).

The final type of infiltrometer is the seepage meter. This device is primarily used for fine grained soils below the groundwater table (Moulton and Seals, 1979). See Table 2.4.3 for advantages and disadvantages of infiltrometer methods to this research.

Table 2-3 Advantages and disadvantages of infiltrometers (after Moulton and Seals, 1979)

Test Method	Advantages	Disadvantages
(1) Single Ring Infiltrometer	above GWT, medium disturbance	vertical hydraulic conductivity, for fine grained soils, long time
(2) Cylinder Permeameter	above GWT	vertical hydraulic conductivity, long time, equipment, for fine grained soils
(3) Double Ring Infiltrometer	above GWT	high disturbance, vertical hydraulic conductivity, long time, expensive equipment, for fine grained soil
(4) Gradient Intake Infiltrometer	above GWT	high disturbance, vertical hydraulic conductivity, expensive equipment, for fined grained soils
(5) Seepage Meter Infiltrometer		below the GWT, vertical hydraulic conductivity, high disturbance

2.4.4 Air entry permeameter

The fourth class of in situ testing methods that were assessed is air entry permeameters (see Figure 2-5). The air entry permeameter is similar to the single ring infiltrometer except a vacuum gage is attached for the determination of soil suction pressure. This device is mainly used for fine grained soils above the groundwater table to measure vertical hydraulic conductivity (Moulton and Seals, 1979; Knight and Haile, 1984; Bouwer, 1986). See Table 2-4 for advantages and disadvantages of these methods for this research.

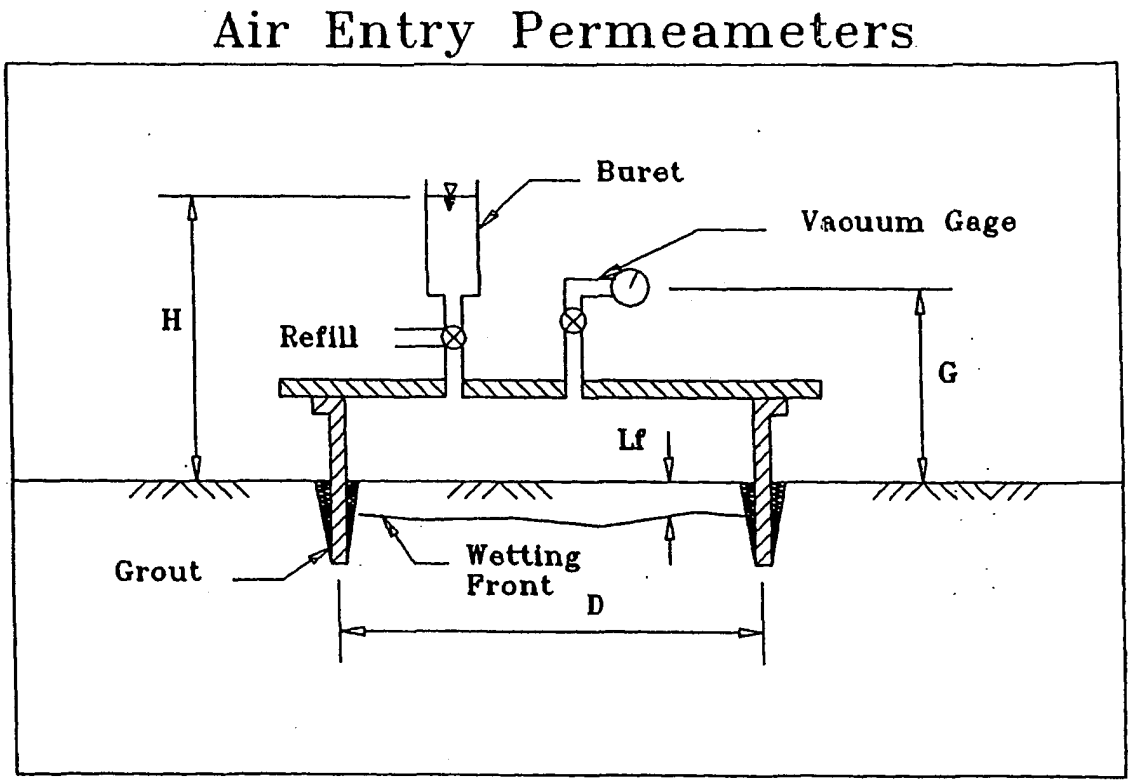

Figure 2-5: General schematic for air entry permeameters (from Daniel, 1989).

Table 2-4 Advantages and disadvantage of air entry permeameters (after Moulton and Seals, 1979)

Test Method	Advantages	Disadvantages
Air Entry Permeameter	above GWT, inexpensive	high disturbance, vertical hydraulic conductivity

2.4.5 Direct velocity techniques using a tracer in a well

The fifth class of in situ hydraulic conductivity testing methods that were assessed are the direct velocity techniques using a tracer in an injection well (see Figure 2-6). This method injects water into the ground and uses probes to measure the difference in potential and the time required for the water to travel from one probe to the next probe. Determining the travel time is accomplished by the injection of an electrolytic solution and noting the time required for a change in measured electrical resistance as the solution passes each probe. The device can be used for material above or below the groundwater

table to measure horizontal hydraulic conductivity with low to medium disturbance of the layer of soil being tested (Maytin, 1962; Moulton and Seals, 1977, 1979, 1980; Roy and Sayer, 1989).

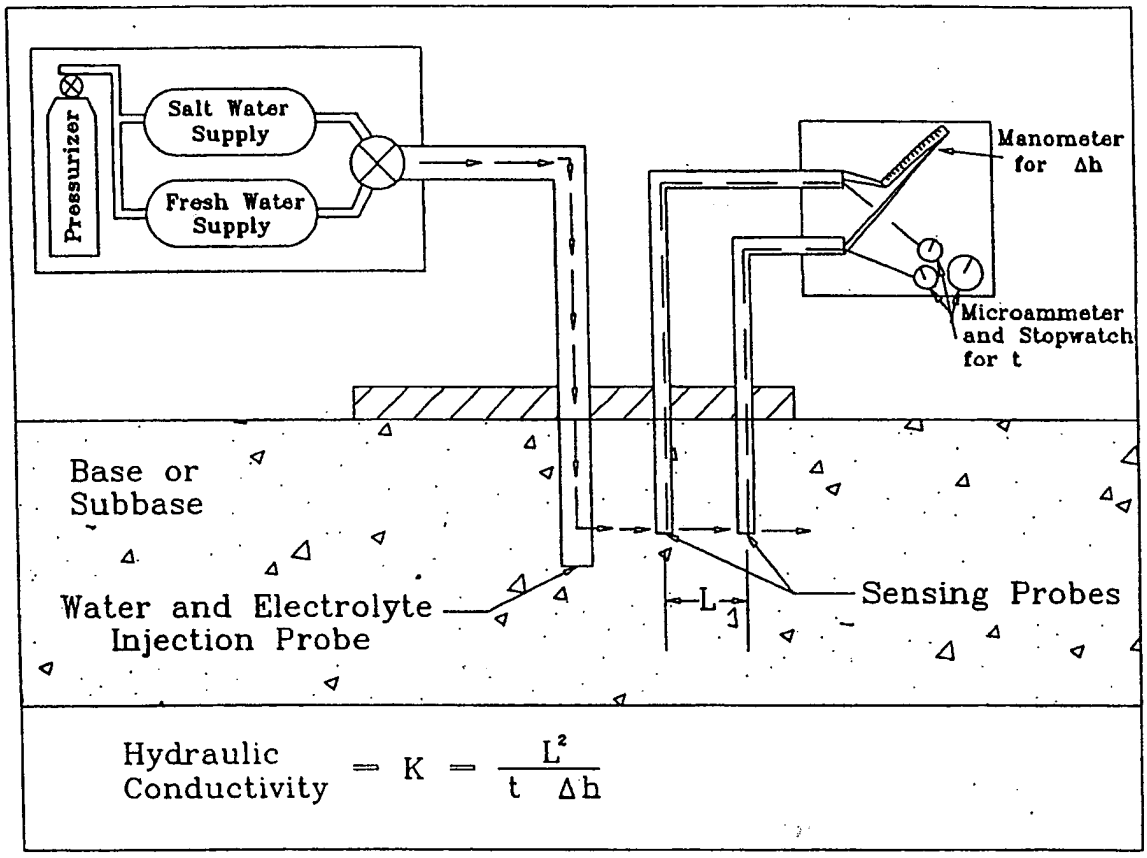

Figure 2-6: Direct velocity technique (from Moulton and Seals, 1979).

The first device of this type was the roadway shoulder permeability test developed by Maytin (1962). This device allowed a simple test to determine the in situ hydraulic conductivity by correlating the in situ velocities through shoulders of roadways to the laboratory hydraulic conductivity results of the same material. This device consisted of an injection well and neon light control panel attached to the probe setup. The neon lights were then set up in a grid so the operator was able to see the rate of advance of the water envelope as the water passed each probe (Maytin, 1962). A stop watch was used to determine the flow time between probes and thereby the velocity.

The device by Moulton and Seals (1977, 1979, 1980) was developed for the Federal Highway Administration and is called the field permeability testing device (FPTD). The device was created to test a layer of a layered, inhomogeneous, anisotropic media. The layer of porous media can range from 3 inches to 18 inches in thickness. It was designed to measure a range of hydraulic conductivities from 0.0001 cm/s to 10 cm/s under various boundary conditions. The test was designed to cause little disturbance to the medium that is tested.

The FPTD uses the velocity technique to determine the in situ hydraulic conductivity. This technique is a direct application of Darcy's law given by equation 2.3. The hydraulic gradient is rewritten:

$$i = \frac{\Delta h}{L} \qquad (2.16)$$

where: Δh - the loss in total head between two points

L - the distance between the two points

$$q = \frac{L}{t} \qquad (2.17)$$

The discharge velocity is rewritten:

where: t - the travel time for water between the two points

Rewriting equation 2.3:

$$K = \frac{q}{i} \qquad (2.18)$$

Hence, substituting Equation 2.16 and 2.17 into 2.18, Darcy's law can be rewritten:

$$K = \frac{L^2}{\Delta h \, x \, t} \qquad (2.19)$$

In order to determine the hydraulic conductivity, a perforated injection tube is used to develop saturated steady state radial flow. Electrical resistance is used to measure the macroscopic velocity between the two probes. Once the soil is saturated, a slug of electrolytic solution is introduced into the aquifer at the injection point. The time required for the slug of electrolytic solution to go from the upstream probe to the downstream probe is recorded.

The loss in total head is determined by directly measuring the fluid pressures at the ends of the two probes. This is accomplished by using either a differential manometer or a differential pressure transducer. See Table 2-5 for the advantages and disadvantages of the velocity technique for this research.

Table 2-5 Advantages and disadvantages of the direct velocity technique

Test Method	Advantages	Disadvantages
(1) Shoulder Permeability Test	above GWT, horizontal hydraulic conductivity, low disturbance	large amount of time
(2) FPTD	above GWT, horizontal hydraulic conductivity, low disturbance	fine grained soils

2.5 Large Scale Laboratory Permeameters

A few large scale permeameters for coarse materials have been reported in the literature (Head, 1982; Jones and Jones, 1989; Chapuis et al, 1989).

Head (1982) described a large scale permeameter of 406 mm (16 inches) diameter, suitable for gravel containing particles up to 75 mm (3 inches). The permeameter was 964 mm (34 inches) long. The sample could be compacted or vibrated into the cell. A water supply tank of 900 liters ($0.9\,m^3$ or $3.188\,ft^3$) with several overflow levels was connected to the permeameter so that the inlet head could be changed. Water was taken to and from the permeameter by 75 mm (3 inches) diameter rubber hoses. The principle of the test is the same as for the standard permeability test on sands. It was

reported that the large scale permeameter provided a realistic representation of the likely behavior of these materials in situ.

Jones and Jones (1989) introduced a horizontal permeameter for drainage layers with a median particle size, D_{50}, of up to 30 mm (1.2 inches). The sample size was 1 m × 0.3 m × 0.3 m (39.37 inches × 11.81 inches × 11.81 inches) and was compacted using a vibrating hammer. The permeameter was a rectangular galvanized steel box. A piece of impermeable neoprene foam sheet was placed on the top of the compacted aggregate. A lid with bar stiffeners was bolted tightly to the flanges of the cell and the bars pressed into the foam firmly to prevent flow around the specimen. The specimen was slowly saturated with de-aired water. Settled water was used during the testing. The tests were conducted over a range of hydraulic gradients. Crushed limestone, sandy gravel and crushed granite were used in the study. Fine, medium and coarse gradation within Type 1 subbase grading limits of the British Department of Transportation were tested for each aggregate type. It was concluded that the apparatus and the test procedure provided a satisfactory basis for the measurement of hydraulic conductivity. The test results varied less than one order of magnitude between nominally identical specimens. This was attributed to slightly different compacted densities and degrees of saturation. Further investigation was suggested to develop a repeatable and reproducible test method.

Chapuis, et al. (1989) developed a horizontal permeameter for sandy and gravelly non-cohesive soils. Its cross-section was 150 mm × 150 mm (5.9 inches × 5.9 inches) 12 and its length was 30 cm (11.8 inches). The design details were compatible with those of the vertical permeameter recommended by ASTM standard D2434-68 (1974), except a flexible rubber membrane was placed on the top wall. A water pressure was applied behind the rubber sheet to maintain positive effective stresses everywhere within the soil sample, reducing the side-wall leakage. All joints of the permeameter were detailed carefully to make it airtight. De-aired water was used for the initial saturation and during the tests. The degree of saturation was checked by means of the volume-and-mass method mentioned in section 2.3.3. Full saturation was obtained without the application of back pressure in all tests reported.

2.6 Published Laboratory Hydraulic Conductivity Values

Moulton's (1980) nomograph for predicting hydraulic conductivity was developed by statistically correlating the measured hydraulic conductivity for a large number of samples (Barber and Sawyer, 1952; Chu, Davidson, and Wickstrom, 1955; Smith, Cedergren and Reyner, 1964) with those properties known to exert an influence on hydraulic conductivity. The three parameters needed to predict hydraulic conductivity are the effective grain size, D_{10}, the porosity, n, and the percent passing the No. 200 sieve, P200. The nomograph (Figure 2-7) was developed from data on granular bases and subbases, therefore it is limited to these types of materials. For open graded bases and filter materials, Moulton (1980) suggested that a figure (developed by Cedergren, 1974), relating gradation distribution and hydraulic conductivity might be an aid to estimate hydraulic conductivity (Figure 2-8).

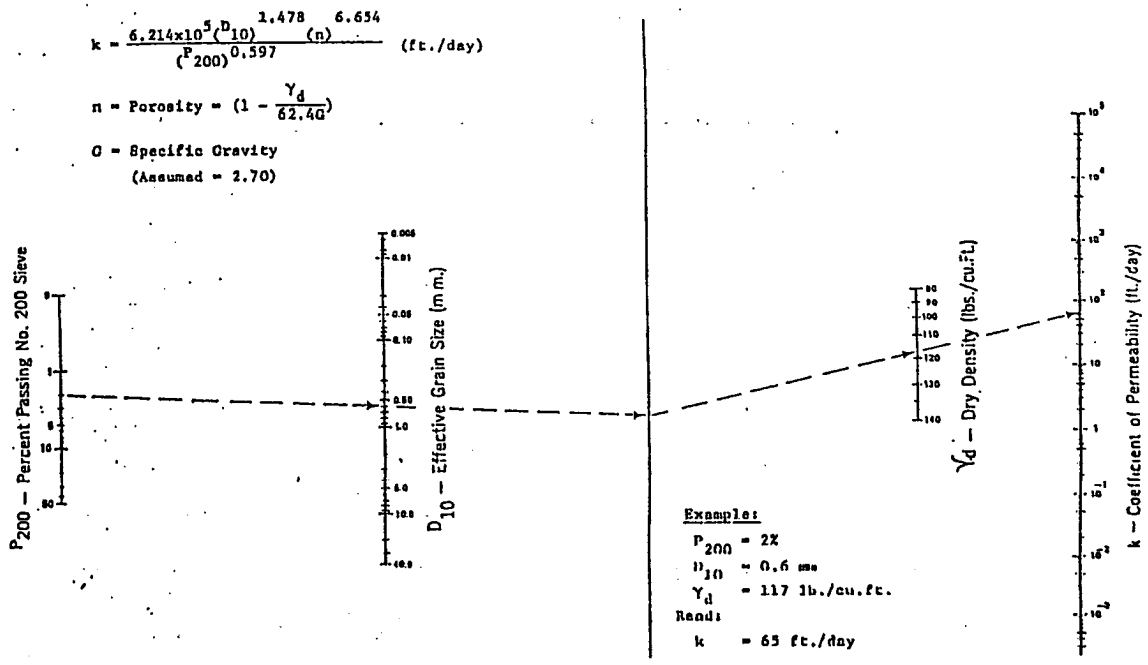

Figure 2-7: Nomograph for estimating hydraulic conductivity of granular drainage and filter materials (Moulton, 1980).

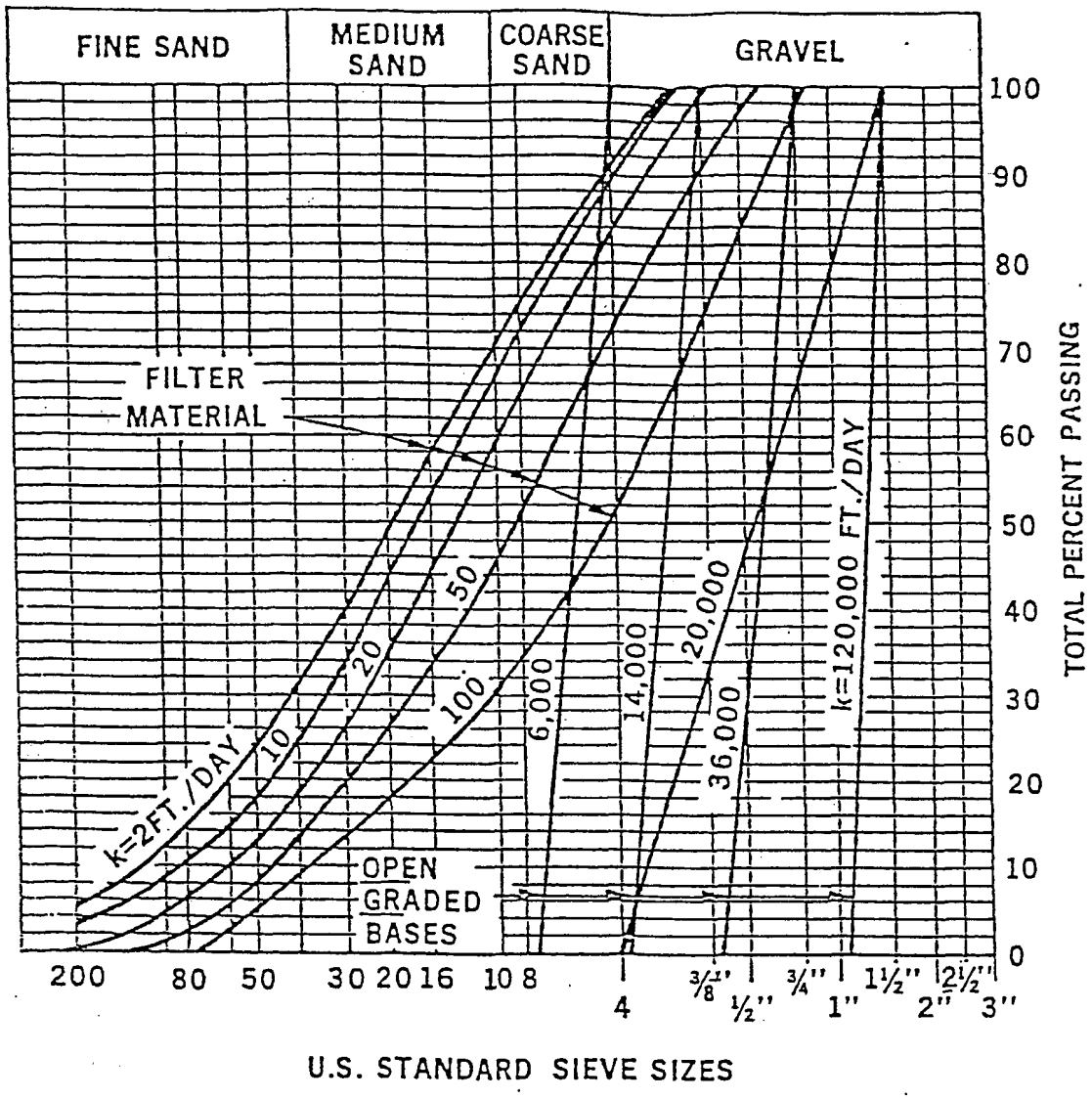

Figure 2-8: Typical gradations and hydraulic conductivities of open graded bases and filter materials (Cedergren, 1974).

Additional research on the hydraulic conductivity of base and subbase materials can be found in the literature. However, only a few studies on open-graded bases and subbases have been done since the popularity of open-graded bases and subbases started in the late 1980's.

Jones and Jones (1989) conducted research on the laboratory measurement of hydraulic conductivity of aggregate used in pavement bases and subbases. Their

permeameter is described in section 2.5. Crushed limestone, sandy gravel and crushed granite were used in the study. Fine, medium and coarse gradation within Type 1 subbase grading limits of the British Department of Transportation were tested for each aggregate type. By comparison, the coarse grading of their materials is close to the coarse grading of ODOT 304, and the fine grading of their materials falls between the fine grading and middle grading of ODOT 304. The test results range from about 10 ft/day to 5000 ft/day. They also compared their results with Hazen's empirical formula. Hazen's formula gave higher values than their test results, but the difference is within one order of magnitude. The permeameter and the procedure worked well, but further study was recommended to verify its repeatability.

From the literature review, it was found that research on laboratory hydraulic conductivity had been performed on the specific materials that were tested in this research. The materials that were tested in this research are Ohio Department of Transportation (ODOT) specification No. 304 and No. 310, AASHTO M 43 specification No. 57, Iowa Department of Transportation (IDOT) granular subbase specification 41-21, and a New Jersey Department of Transportation (NJDOT) test subbase mix referenced by Kozlov (1984) and Baumgartner (1992).

In 1981, Majidzadeh and Elmitiny completed laboratory research on vertical hydraulic conductivity of No. 310, No. 304, and No. 57. They tested two gradations of No. 57, four gradations of No. 304, and two gradations of No. 310. They used specimens of 4 inches diameter and 4.5 inches height. The samples were compacted vertically. There was no detailed description of the permeameter or the procedure. The values of hydraulic conductivity for ODOT 57 ranged from 5000 ft/day to 8000 ft/day. For ODOT 304 and ODOT 310, only those samples with 0% and 4% passing sieve No. 200 produced results, with others yielding no flow. For those with 0% passing No.200, the results agreed well with Moulton's nomograph for predicting hydraulic conductivity. For those with 4% passing No. 200, the results differed from those estimated from Moulton's nomograph. For those without water coming out, the authors attributed it to some errors which might have occurred in the permeameter. Results of their research is listed in Tables 2-6 and 2-7.

Table 2-6 Percent finer by weight and vertical laboratory hydraulic conductivity of AASHTO M 43, No. 57 (follows Majidzadeh and Elmitiny, 1981).

Sieve	No. 57 A	No. 57 B
$1\frac{1}{2}$"	100	100
1"	100	100
$\frac{3}{4}$"	82	75
$\frac{1}{2}$"	60	46
$\frac{3}{8}$"	42	25
No. 4	0	0
Average Hydraulic Conductivity, cm/s (ft/day)	2.37 (6720)	2.79 (7900)

Table 2-7 Percent finer by weight and vertical laboratory hydraulic conductivity of ODOT specification No. 304 (follows Majidzadeh and Elmitiny, 1981).

Sieve	No. 304-1	No. 304-2	No. 304-3	No. 304-4
1"	100	100	100	100
3/4"	67	67	67	68
1/2"	58	58	58	59
3/8"	49	50	50	52
No. 4	40	41	42	44
No. 8	29	31	32	35
No. 16	21	23	25	28
No. 30	15	18		
No. 50	9	12	15	19
No. 100	4	8	11	15
No. 200	0	4	8	12
Average Hydraulic Conductivity, cm/s $x\ 10^{-3}$ (ft/day)	8.05 (22.8)	2.26 (6.4)	No Flow Reported	No Flow Reported

Some of the limitations of their research are that sample saturation was not described, a non-standard method of compaction was employed, a small sample size was tested, and vertical hydraulic conductivities were determined. Unfortunately, hydraulic conductivities were not determined for No. 310 in this report. This was due to the relatively low hydraulic conductivity of this material. Water had not passed through the No. 310 specimens after three hours performing a constant head test. Therefore, the authors aborted the test. However, sample saturation and deairing procedures were not reported. It is possible that the specimens were not fully saturated at the start of these tests and that infiltration was still taking place when the tests were ended.

The Iowa Department of Transportation conducted laboratory research on horizontal hydraulic conductivity of IDOT specification 41-21. A range of values were reported ranging from 0.177 to 0.706 centimeters per second (500 to 2000 feet per day) (McWaters, pers. comm., 1994).

The test performed by Iowa DOT as described by McWaters was a laboratory constant head unconfined hydraulic conductivity test. This test was performed in a one foot wide by six foot long flume which had holes drilled in the bottom along the centerline of the width at one foot intervals. Piezometers were attached to these holes in order to measure the gradient at these specified intervals. The water draining from the base was collected and measured for a certain time interval. Hydraulic conductivity could then be determined.

Limitations of this device are that sample saturation and gradients at which the hydraulic conductivities were reported were not described. It is likely from the description by McWaters that sample saturation was not consistent from test to test and the gradient at which the hydraulic conductivity was measured may have exceeded the critical gradient in other tests causing disparity in the reported results.

A value of hydraulic conductivity for the NJDOT test subbase was estimated from a report by Baumgardner (1992). The estimated value reported is 0.353 centimeters per second (1000 feet per day). The New Jersey mix has yet to be adopted by a state department of transportation. This is a test base created by combining fifty percent of AASHTO M 43 specification No. 57, and fifty percent of AASHTO M 43 specification No. 9 into a mixture (Kozlov, 1984).

2.7 Resilient Modulus Testing

Design for pavements and rehabilitation of layered pavement systems uses resilient modulus as an essential parameter for designing pavements. Design procedures for determining layer thicknesses for flexible pavements includes resilient moduli (AASHTO, 1993; Yoder and Witczak, 1975). The resilient modulus is an important parameter determined from non-destructive pavement testing and back-calculation analysis (Sargand, et al., 1991). According to the AASHTO 1993 Design Guide for

Roadbed Materials, the standard resilient modulus test must be performed on representative samples in stress and moisture conditions simulating those of the primary moisture seasons. The Long-Term Testing and Pavement Performance program initiated during the Strategic Highway Research Program (SHRP) specifies resilient modulus testing for SHRP test pavements.

Standardized test procedures have been developed for testing base and subgrade materials. Standard test method AASHTO T 274 was developed for resilient modulus testing of subgrade materials (AASHTO, 1986; The Asphalt Institute, 1986; ASTM, 1989). An interim test method for laboratory testing of unbound materials, SHRP Protocol P46 (AASHTO DESIGNATION: T 294-92 I), has been developed (FHWA, 1992).

Other investigators have reported the results of resilient modulus testing. Albright (1986) reported on an investigation to evaluation gradation specifications in Alaska. Resilient properties of pavement materials were reported (Monismith, et al., 1972; Kaspyapa and Lytton, 1988; Zhou et al., 1992). Attempts have been made to evaluate resilient modulus test results (Rada and Witczak, 1981; Thompson, 1989; Thompson and Smith, 1990).

3. IN SITU HYDRAULIC CONDUCTIVITY TEST

3.1 Introduction

A great deal of research has been performed on the development of in situ hydraulic conductivity test devices. Most of the previous research was primarily concerned with developing a device for fine grained materials with great thickness and regional groundwater flow. The hydraulic conductivity device required for this research is one for materials with very small thickness when compared to their length and width. Because of the relatively small thickness of the coarse grained material layer and the great difference between the hydraulic conductivity of the coarse grained material when compared with the underlying subbase layers, the primary direction of travel would be in the horizontal direction. Therefore, this device must primarily measure horizontal hydraulic conductivity. The device that is most promising for the determination of in situ hydraulic conductivity for these coarse grained materials is a device utilizing the velocity technique, such as that by Moulton and Seals (1977, 1979, 1980).

The device by Moulton and Seals (1977, 1979, 1980) was developed primarily for fine grained soils (See Figure 2-6). The in situ hydraulic conductivity testing occurs during the construction of roadway bases, prior to paving. The device is laid directly on the layer of soil to be tested and a small region of the soil is saturated. Once the soil is saturated and steady state is achieved, a slug of salt solution is introduced into the soil. The time for the slug of saline solution to pass two points in the radial direction at known distances away from the injection well is recorded. The two probes are saturated and attached to a differential pressure transducer to determine the pressure difference between the two probes. The hydraulic conductivity can then be calculated using equation 2.19.

Because the device developed by Moulton and Seals (1977, 1979, 1980) was primarily developed for fined grained soils, modifications had to be made to this technique to determine the in situ hydraulic conductivity accurately for coarse grained materials. One primary modification that had to be made to the device was that it had to be fabricated so that it could test the base course material below a layer of existing pavement. A second aspect that was considered was the dispersion of the electrolytic solution. Due to high pore water velocities and near critical gradients in coarse materials, dispersion presents more difficulty

than with fine grained materials. The dispersion coefficient is larger for coarse grained soil than for fine grained soil. Hence, a method of determining the median resistance of the saline solution that reaches a probe had to be determined instead of an arbitrary resistance which signals that the saline solution has reached the probe.

This portion of the research involved three primary steps:

1 Computer modeling of the problem for use in the design of the in situ hydraulic conductivity testing device for coarse materials.

2. Testing of the hydraulic conductivity device to verify that it worked.

3. Make recommendations for the further development of an in situ hydraulic conductivity test device.

3.1.1 Test sections

This device was tested in highway test sections prepared by the Ohio Department of Transportation. The highway test sections were located on Ohio State Route 2 near the city of Vermilion, Ohio (see Figure 3.1). Six different coarse grained aggregate base materials were tested, including asphalt and Portland cement stabilized aggregate bases.

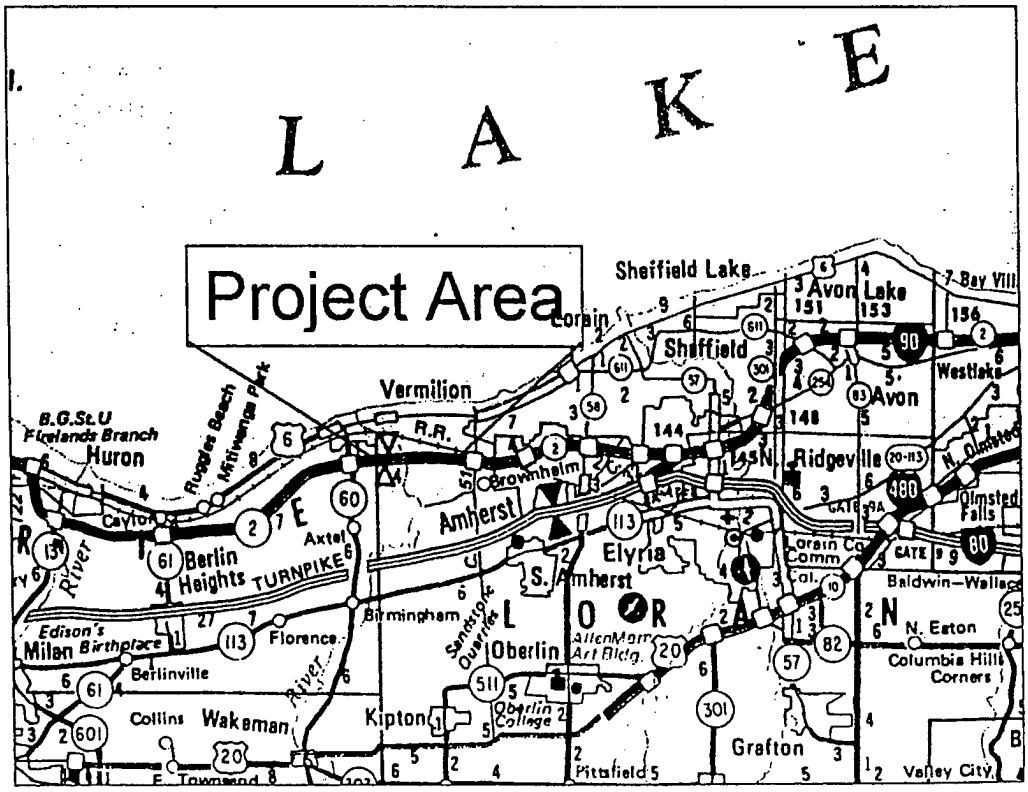

Figure 3.1 – Location of Test Sections

Six highway test sections were constructed by ODOT to evaluate the drainage characteristics and durability of five different base materials. The test sections are located in the counties of Erie and Lorain on Ohio State Route 2 near the city of Vermilion, Ohio (see Table 3-1 for other location details). The six test sections consist of four unstabilized drainable aggregate bases and two stabilized aggregate bases. The four unstabilized aggregate bases consist of two ODOT specified materials, No. 304 and No. 310 (current aggregate bases being used in the state of Ohio), and materials used in two other states, the New Jersey test base and the Iowa Department of Transportation granular base specification 41-21. The two stabilized free draining base courses are AASHTO M 43 specification No. 57. One of these test sections is Portland cement stabilized and the other test section is asphalt cement stabilized. These stabilized bases are being tested for possible widespread use in the state of Ohio. See Table 3-2 and Appendices E-J for further details about the materials that were placed in the test sections.

Table 3-1: Location of test sections on Ohio State Route 2, Erie and Lorain counties.

Construction Stationing From	To	Side	Length	Material Type
1835+00	5+00	W.B.	819.49'	No. 310
5+00	14+60	W.B.	960.00'	Iowa drainable base
56+06.25	64+60	W.B.	853.75'	No. 304
64+60	73+14	W.B.	854.00'	New Jersey base
73+14	81+68	W.B.	854.00'	Asphalt treated No.57
81+68	90+23	W.B.	855.00'	Cement treated No. 57

State Route 2 is in the northern part of the state of Ohio. At the test section location, State Route 2 is a four lane limited access highway with two lanes in both directions, separated by a sixty foot grass median. The westbound and eastbound lanes are typically crowned at a slope of three sixteenths of an inch per foot. All the test sections are in straight sections of the highway. The pavement system consists of a six

inch bottom aggregate base layer of No. 304 (the plans specified that eight percent pass the No. 200 sieve), overlain by a bituminous prime coat, overlain by a four inch test base (one of the test materials mentioned above), and overlain by a ten inch reinforced Portland cement concrete pavement layer. A longitudinal pipe underdrain is located along the edge of the pavement. See Figure 3-2 for further details.

Table 3-2: Percentage by weight finer for standard sieves.

Sieve	No. 304	No. 310	No. 57*	N.J.	Iowa
$2\frac{1}{2}"$	-	100	-	-	-
$2"$	100	-	-	-	-
$1\frac{1}{2}"$	-	-	100	100	-
$1"$	70 - 100	70 - 100	95 - 100	95 - 100	100
$\frac{3}{4}"$	50 - 90	-	-	-	-
$\frac{1}{2}"$	-	-	25 - 60	60 - 80	50 - 80
No. 4	30 - 60	25 - 100	0 - 10	40 - 55	-
No. 8	-	-	0 - 5	5 - 25	10 - 35
No. 16	-	-	-	0 - 8	-
No. 30	7 - 30	-	-	-	-
No. 40	-	5 - 50	-	-	-
No. 50	-	-	-	0 - 5	0 - 15
No. 200	0 - 13	0 - 10	-	0	0 - 6

* Asphalt and Portland cement stabilized

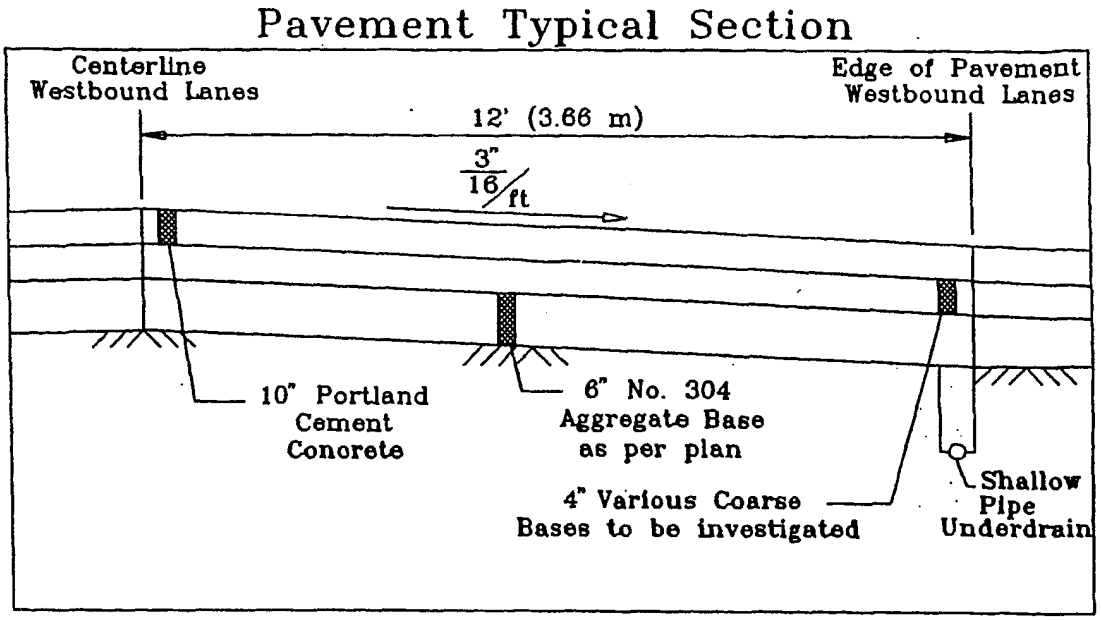

Figure 3-2: Pavement typical section.

3.1.2 Estimated values of hydraulic conductivity for design

Approximate values of hydraulic conductivity had to be estimated in order to model the test sections. The laboratory portion of this research had not yet been completed, so values were estimated from the literature. From the literature review in section 2.6, it was found that research on the hydraulic conductivity of ODOT specified No. 304 and No. 310, AASHTO M 43 specification No. 57, IDOT specified 41-21, and the New Jersey test mix had all been performed or the values had been estimated. The values obtained from these reports were taken as approximate values to use in the test design and modeling, due to uncertainty about factors affecting the accuracy of the reported values.

Values for No. 304 and No. 57 could be found from the report by Majidzadeh and Elmitiny (1981). The estimated values for No. 304 and No. 57 were taken as 0.00364 and 0.400 centimeters per second (10.4 and 7310 feet per day), respectively, based on the average values reported. Since results were not reported for the hydraulic conductivity of No. 310, and empirical formula developed by Moulton (1980) was used to estimate values for No. 310:

$$K = \frac{6.214 \times 10^{5} \, d_{10}^{1.478} \, n^{6.654}}{P_{200}^{0.597}} \qquad (3.1)$$

where: $n = 1 - \frac{\gamma_d}{\gamma_w G_s}$ - the porosity

γ_d - the dry unit weight of the soil

γ_w - the unit weight of water

d_{10} - the particle size of ten percent passing

P_{200} - the percent passing the No. 200 sieve

G_s - the specific gravity of the porous media (assumed to be equal to 2.70)

The value of hydraulic conductivity for No. 310 from this equation is 0.00351 centimeters per second (10.2 feet per day).

Values for IDOT granular subbase specification 41-21 could be found from the report compiled by the Iowa Department of Transportation in 1989. The reported values range from 0.177 to 0.706 centimeters per second (500 to 2000 feet per day). From the empirical equation by Moulton (1980), a value of 0.049 centimeters per second (150 feet per day) was determined. Since there was a wide range of values reported and the value from the Moulton equation did not agree, a value of 0.353 centimeters per second (1000 feet per day) was selected.

The value of hydraulic conductivity for the New Jersey mix was estimated from the report by Baumgardner (1992) as 0.353 centimeters per second (1000 feet per day). Since the gradation specification for this material specified that zero percent pass the No. 200 sieve, the Moulton equation yielded a value of infinity. Therefore, the value of 0.353 centimeters per second (1000 feet per day) was used for design.

The range of 0.000353 to 3.53 centimeters per second (1 to 10000 feet per day) was used to encompass expected design values of hydraulic conductivity of coarse grained materials for the in situ hydraulic conductivity device.

3.1.3 Test setup

After deciding which technique to use, the next step was to determine how to adapt the technique to the specific conditions of this research. There were four considerations that were investigated before design could proceed: 1) what pavement region to place the device for testing, 2) how to develop steady state saturated, laminar flow, 3) how to account for the mechanical dispersion effect of the flow of the electrolytic solution as it passes through the flow domain, and 4) determination of probe placement within the testing region.

The first consideration on the set up of the test was where on the pavement to place the device. Since State Route 2 is an active four lane limited access highway, large volumes of traffic using this roadway prevented testing both west bound lanes of traffic simultaneously. Therefore, placing the device along the centerline of the pavement was impossible. Closing down the driving lane and testing near the centerline is dangerous because of vehicles traveling at high speeds within a short distance of the equipment and personnel. Closing down the driving lane and testing near the outer edge of the pavement is also disadvantageous because the underdrain is located directly below the edge of the pavement. The underdrain would remove the water from under the pavement quickly, limiting the region available to place the probes and inducing vertical flow between the point of entry for the flow and the underdrain trench. A reasonable solution to the problem is to place the device in the center of the driving lane. In this way, there is enough distance from the point of entry of the flow to the edge of the underdrain trench to induce laminar horizontal flow.

The second consideration given to the setup of the test device was how to develop steady state saturated flow. The first thought was to directly connect the fresh water inlet to a pump to develop flow within the testing region. Pumping the water directly into the base material was abandoned due to the fact that there was no guarantee that a steady laminar flow could be induced in the test materials. Also, head conditions at the inlet would be varying and difficult to record. The idea that was chosen is the use of a standpipe. The fresh water supply tank is connected to a pump, which is connected to two ball valves. The ball valves are used for metering the flow of water. One of the valve branches is connected to the standpipe to regulate the head and the other branch is

used to discharge excess flow. By maintaining a constant head at the point of entry for the water, a constant flow could be developed.

The third consideration that was given to the setup of the test device was accounting for the mechanical dispersion of the electrolytic solution as it passes through the test material. In previous research this effect was neglected and was considered to have little or no consequence. This was due to the fact that the materials that were tested were mainly fine grained, tightly packed materials where pore water velocities were relatively small. The materials tested in this research were coarse materials where high pore water velocities are created, causing a greater error due to the mechanical dispersion. The continual monitoring of the electrical resistance versus time permits accounting for the mechanical dispersion effect.

The final consideration that was given to the setup of the test device was determination of probe placement within the test region. One of the essential considerations to the placement of the probes was the critical gradient. The critical gradient corresponds to the limiting velocity that maintains laminar flow conditions. Darcy's Law remains valid only for laminar conditions. The critical gradient is determined as a function of Reynolds number, R_e, as seen in section 2.1.2. The Reynolds number is then used to determine if the flow through the porous media was laminar or turbulent at the expected velocities. Since Darcy's Law is necessary to compute the hydraulic conductivity with the velocity technique, it is imperative to place the probes within an area of the pavement where the flow is laminar.

3.2 Numeric Modeling

Once the setup of the test was determined and the material hydraulic conductivities were estimated, numeric modeling could be done to investigate the necessary flow rates, velocities, and potentials to make the test device operate properly. This information was necessary to size tanks, pipes, hoses, valves and pumps for the testing device. This modeling also serves as a tool to adjust the test operation to suit the in situ conditions.

3.2.1 Modeling of the hydraulic potentials

As stated in Chapter 2, one of the main concerns in determining the hydraulic conductivity is the determination of the critical gradient as an upper bound for testing conditions. Before determining gradients to compare with the critical gradient, the potential or hydraulic head at any point within the domain has to be known. The governing partial differential equation for non-steady state, inhomogeneous and anisotropic flow is as follows (in radial and Cartesian coordinates, respectively) (Bear, 1972):

$$\frac{S^*}{K}\frac{\partial \phi}{\partial t} = \frac{\partial^2 \phi}{\partial r^2} + \frac{1}{r}\frac{\partial \phi}{\partial r} + \frac{1}{r^2}\frac{\partial^2 \phi}{\partial \theta^2} + \frac{\partial^2 \phi}{\partial z^2} \qquad (3.1)$$

$$S^*\frac{\partial \phi}{\partial t} = \frac{\partial}{\partial x_i}\left\{\rho K_{ij}\frac{\partial \phi}{\partial x_j}\right\} \qquad for\ i, j = 1\text{-}3 \qquad (3.2)$$

where: $r, \theta, z (= x_3)$ - the coordinate points in a cylindrical coordinate system

$x_1, x_2, x_3 (x, y, z)$ - the coordinate points in a Cartesian coordinate system

S^* - the specific mass storage coefficient

The first attempt to determine the potential at any point within the base was through the use of Aquifer Simulation Model (ASM), a computer software package developed by Kinzelbach and Rausch (1989). Note that from a hydrologic standpoint, a pavement drainage layer behaves as an aquifer. This program uses a user selected finite differencing technique (either the iterative alternating direction implicit method or the conjugate gradient method) to solve the partial differential equation. The program has the following options: steady or nonsteady state flow conditions; homogeneous or inhomogeneous aquifer; confined, phreatic, or leaky aquifers; isotropic or anisotropic conditions; injection or pumping wells with constant or time varying flow rates; constant

boundary fluxes; temporally and spatially variable groundwater recharge from precipitation; infiltration or exfiltration due to surface water bodies; permanent or instantaneous solute injection; pathlines; isochrones around pumping wells; and a water balance for the whole model area or selected parts of the model area.

A domain was formulated that matched the test scenario described in section 3.1.3. After a number of simulations under confined conditions, it was determined that the potentials near the pavement edges were below the thickness of the base, indicating phreatic flow conditions occurring in these areas. Simulations were tried under phreatic flow conditions but the values of potential near the inlet standpipe were not deemed reliable because the potential could not be any higher than the thickness of the base layer if the phreatic solution was to be valid. Since both a combined confined and phreatic flow solution was not available through the use of this software, another solution had to be found.

From an extended literature review, a combined shallow confined and phreatic flow solution was found presented by Strack (1989). This solution is for homogeneous, isotropic, steady state flow to a discharge well in an infinite aquifer. However, the solution does not include edge boundary conditions that need to be included for this research. The two assumed boundary conditions are 1) a constant head boundary condition at the edge of the pavement due to the underdrain system and 2) a no flow boundary condition at the centerline of the pavement due to the break in side slope.

The Strack (1989) solution was further developed by making assumptions about the material homogeneity, isotropy, steady state flow, and the use of image wells to create boundary conditions. Since the materials were mixed and well graded, it was assumed that they are homogeneous. Due to the way the materials were compacted there is hydraulic anisotropy. It is expected that the anisotropy varies only between the horizontal and vertical directions. Since the device was designed to induce and determine horizontal flow only, anisotropy should not account for a great error. Steady state conditions are a reasonable assumption if the experiment takes place only when steady state saturated flow conditions have been reached. Strack (1989) describes the creation of boundary conditions desired for this solution by the use of image well theory (superposition of imaginary wells to create mathematical boundary conditions).

With the ideas presented by Strack (1989), a solution was developed. The governing partial differential equation for homogeneous, isotropic, steady state flow is the Laplace equation (in cartesian and radial coordinates, respectively):

$$\frac{\partial^2 \Phi}{\partial x^2} + \frac{\partial^2 \Phi}{\partial y^2} = 0 \qquad (3.3)$$

$$\frac{\partial^2 \Phi}{\partial r^2} + \frac{1}{r}\frac{\partial \Phi}{\partial r} = 0 \qquad (3.4)$$

where: Φ - the potential function (a function of, ϕ the actual potential)

The potential functions for confined and phreatic flow are, respectively:

$$\Phi = K H \phi + C_c \qquad (\phi \geq H) \quad (3.5)$$

$$\Phi = \frac{1}{2} K \phi^2 + C_p \qquad (\phi < H) \quad (3.6)$$

where: H - the thickness of the aquifer

C_c - the constant of integration for confined flow

C_p - the constant of integration for phreatic flow

To link the solutions, Strack suggests an interzonal boundary between the confined and phreatic regions where the thickness of the aquifer is equal to the actual hydraulic head:

$$\phi = H \qquad (3.7)$$

To determine the constants of integration at the interzonal boundary, equations 3.5 and 3.6 are set equal and equation 3.7 is substituted, which yields:

$$K H^2 + C_c = \frac{1}{2} K H^2 + C_p \qquad (3.8)$$

Solving equation 3.8 for C_p, it follows:

$$C_p = C_c + \frac{1}{2} K H^2 \qquad (3.9)$$

One of the two constants is arbitrarily set to zero which yields:

$$C_p = \frac{1}{2} K H^2 \qquad C_c = 0 \qquad (3.10)$$

Finally, substituting the constants of integration back into the original potential functions, they became:

$$\Phi = K H \phi \qquad (\phi \geq H) \qquad (3.11)$$

$$\Phi = \frac{1}{2} K \phi^2 + \frac{1}{2} K H^2 \qquad (\phi < H) \qquad (3.12)$$

The next step in the solution process is to use image well theory to create the desired boundary conditions, a constant head boundary along the edge of the pavement, and a no-

flow boundary along the centerline of the pavement (see Figure 3-3 for the location of the real and image wells). This involves superimposing recharge and pumping well solutions at different points outside the domain to mathematically create boundary conditions. The general well solution for the wells in Figure 3-3 is (positive - discharge well, negative - recharge well):

$$\Phi_i = +_- \frac{Q_i}{2\pi} \ln r_i + C_i \qquad (3.13)$$

where: Q_i - the volumetric flow rate into the well

r_i - the coordinate transformations from polar to Cartesian

C_i - the constant of integration

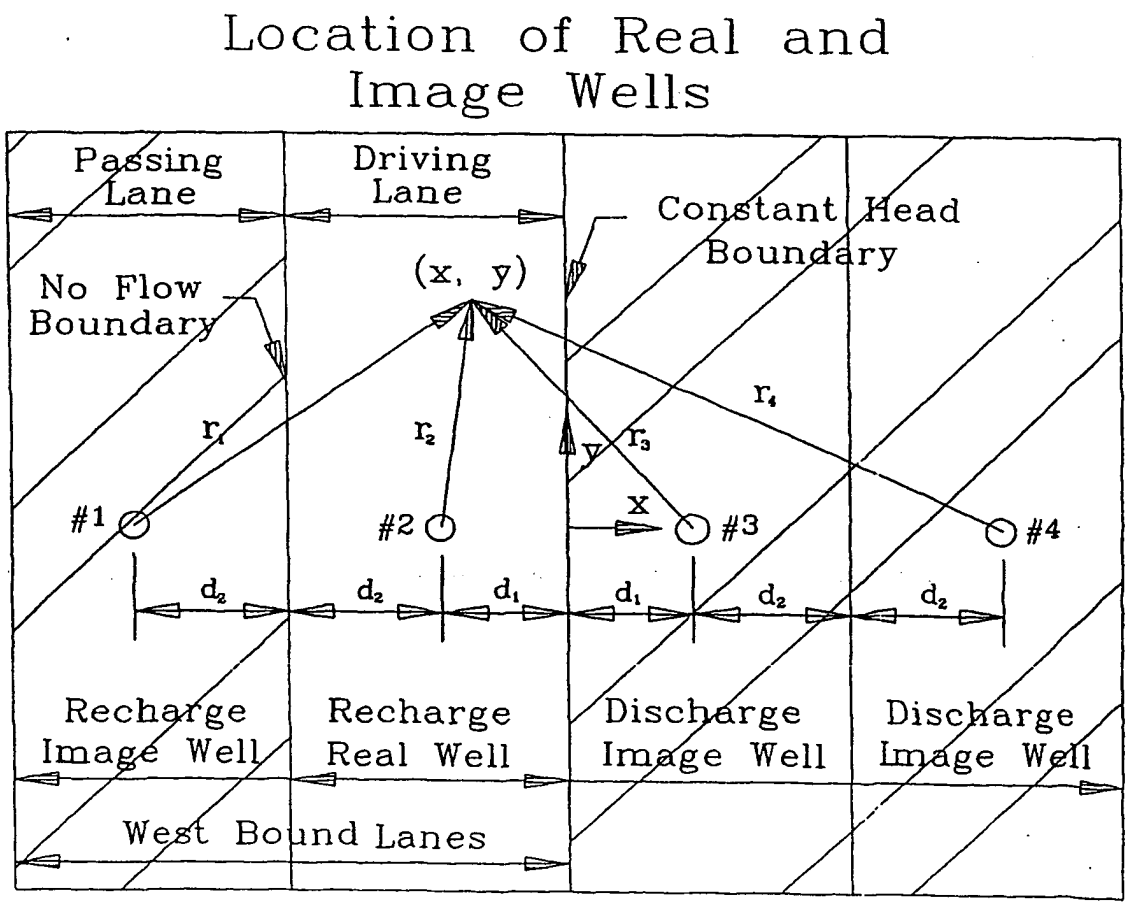

Figure 3-3: Location of real and image wells.

The polar to Cartesian coordinate transformations were derived using the Pythagorean theorem and are as follows (refer to Figure 3-3):

$$r_1 = \sqrt{(x + d_1 + 2\,d_2)^2 + y^2} \qquad (3.14)$$

$$r_2 = \sqrt{(x + d_1)^2 + y^2} \qquad (3.15)$$

$$r_3 = \sqrt{(x - d_1)^2 + y^2} \qquad (3.16)$$

$$r_4 = \sqrt{(x - d_1 - 2\,d_2)^2 + y^2} \qquad (3.17)$$

In order for the image wells to represent the appropriate boundary conditions, the following had to be true:

$$Q_1 = Q_2 = Q_3 = Q_4 = Q \qquad (3.18)$$

$$C_1 = C_2 = C_3 = C_4 = C \qquad (3.19)$$

To determine the general solution to equation 3.13, the well solutions are superimposed:

$$\Phi = \sum_{i=1}^{4} \Phi_i = \frac{Q}{2\pi} \ln \frac{r_3 r_4}{r_1 r_2} + C \qquad (3.20)$$

The next step is to impose the constant head boundary which occurs at the pavement edge ($x=0$):

$$\Phi(0, y) = \Phi_0 \qquad (3.21)$$

Substituting this boundary condition into the general solution, the following result is obtained:

$$\Phi = \frac{Q}{2\pi} \ln \frac{r_3 r_4}{r_1 r_2} + \Phi_0 \qquad (3.22)$$

In order to determine the actual potential in the confined region (Equation 3.11), the potential function for confined flow and the constant head potential function are substituted into equation 3.22:

$$K H \phi = \frac{Q}{2\pi} \ln \frac{r_3 r_4}{r_1 r_2} + \frac{K}{2}(\phi_0^2 + H^2) \qquad (3.23)$$

Solving for actual potential in the confined region yields:

$$\phi = \frac{\frac{Q}{2\pi} \ln \frac{r_3 r_4}{r_1 r_2} + \frac{K}{2}(\phi_0^2 + H^2)}{K H} \qquad (\phi \geq H) \qquad (3.24)$$

In order to determine the actual potential in the phreatic region, the potential function for phreatic flow (Equation 3.12) and the constant head potential function are substituted into equation 3.22:

$$\frac{K}{2}(\phi^2 + H^2) = \frac{Q}{2\pi}\ln\frac{r_3 r_4}{r_1 r_2} + \frac{K}{2}(\phi_0^{\,2} + H^2) \qquad (3.25)$$

Solving for actual potential in the phreatic region yields:

$$\phi = \sqrt{\frac{\frac{Q}{\pi}\ln\frac{r_3 r_4}{r_1 r_2} + K(\phi_0^{\,2} + H^2)}{K} - H^2} \quad (\phi < H) \qquad (3.26)$$

Finally, the flow rate into the well as a function of the potential at the well needs to be determined. At the well radius (r_w) the coordinate transformations are as follows:

$$r_1 = 2d_2 + r_w \qquad (3.27)$$

$$r_2 = r_w \qquad (3.28)$$

$$r_3 = 2d_1 + r_w \qquad (3.29)$$

$$r_4 = 2d_2 + 2d_1 + r_w \qquad (3.30)$$

In order to determine the flow rate into the well, the potential function at the well (in a confined region, Equation 3.11), the constant head potential function (Equation 3.12), and equations 3.27 through 3.30 are substituted into equation 3.22:

$$K H \phi_w = \frac{Q}{2\pi} \ln [\xi] + \frac{K}{2}(\phi_0^2 + H^2) \qquad (3.31)$$

where: $$\xi = \left[\frac{(2 d_2 + r_w)(2 d_2 + 2 d_1 + r_w)}{(2 d_2 - r_w)(r_w)} \right]$$

Solving for the flow rate into the well yields:

$$Q = \frac{2\pi \left[K H \phi_w - \frac{K}{2}(\phi_0^2 + H^2)\right]}{\ln \left[\frac{4 d_1 (d_2 + d_1 + r_w) + 2 d_2 r_w + r_w^2}{2 d_2 r_w - r_w^2} \right]} \qquad (3.32)$$

Equations 3.24, 3.26, 3.32 were incorporated into a BASIC program. For a given potential at the well and at the constant head boundary, a given hydraulic conductivity, well radius and, location of the well, the flow rate into the well and, the potential at any point within the domain of the analytic solution can be determined. The computer program calculates potential every 0.24 meters (9.5 inches) in both the x and y directions for a 3.6 meter by 7.2 meter (12 foot by 25 foot) pavement slab. These values of potential can be imported into a computer software package such as Surfer that is capable of creating piezometric contours. The computer program also calculates the flow rate into the pavement based on the potential at the well. This is a helpful design tool for simulation of the test device. See Appendix A for details of the computer program listing.

3.2.2 Modeling of the solute concentration

A numeric or analytic model for tracer concentration had to be found in order to predict the time required for discharge velocity measurements at any location in the aquifer . Recall that this velocity affects the design of the permeameter and the test. In order to determine the discharge velocity, an electrolytic solution is pumped into the base. The electrolytic solution registers a change in the resistance at the upstream probe

and a timer is started. Once the electrolytic solution reaches the downstream probe the timer is stopped. The velocity is then determined by dividing the distance between the two probes by the time it takes for the electrolytic solution to travel between the two probes.

The electrolytic solution provides a change in resistance in the water passing through the base, therefore it was important to find a predictive mathematical tool to determine the concentration at a particular point and time within the flow domain to predict the in kind resistance of the water. This information was needed to select a device with the proper range of resistances to record both the upper limit resistance (where fresh water is flowing in the base) and the lower limit resistance (when the full strength concentration of the electrolytic solution is flowing in the base).

The governing partial differential equation for convective, dispersive, diffusive mass transport for a single well is (Ogata, 1958):

$$\frac{\partial C}{\partial t}+\frac{A}{r}\frac{\partial C}{\partial r}=\alpha_l\frac{A}{r}\frac{\partial^2 C}{\partial r^2}+\frac{D_m}{r}\frac{\partial}{\partial r}\left(r\frac{\partial C}{\partial r}\right) \qquad (3.33)$$

where: $A = \dfrac{Q}{2\pi H n}$

C - the concentration of the tracer solution

Q - the flow rate into well

H - the thickness of the material being tested

n - the porosity of the material being tested

α_l - the longitudinal dispersivity coefficient

D_m - the molecular diffusion coefficient

An analytical solution to the radial flow problem of convective, dispersive, diffusive mass transport for confined flow is known. This solution was developed by Hoopes and Harleman (1967) and is as follows:

$$C(r,t) = \frac{C_0}{2} erfc\left[\frac{\left(\frac{r^2}{2} - A\,t\right)}{\left(\frac{4}{3}\alpha_{l'} r^3 + \frac{D_m}{A} r^4\right)^{\frac{1}{2}}}\right] \qquad (3.34)$$

where: $erfc\,[x]$ - is the complimentary error function

$$erfc\,[x] = 1 - \frac{2}{\sqrt{\pi}} \int_0^x e^{-t^2}\,dt$$

C_o - the initial concentration of the tracer solution

From an experimental evaluation by Hoopes and Harleman (1967) it was determined that:

$$\alpha_{l'} = 0.86\, D_{50} \qquad (3.35)$$

where: D_{50} - the material diameter with fifty percent (by weight) passing

Assumptions that Hoopes and Harleman (1967) made in their solution are no regional groundwater flow occurs and steady state, saturated, laminar flow conditions have been developed by an injection well. The assumption that no regional groundwater flow occurs is valid for the pavement if the roadway is built above the natural groundwater table. The assumption that steady state, saturated, laminar flow conditions occur within the base is reasonable. These conditions must occur to measure the differential pressure between to flow points within the base accurately. Therefore, the electrolytic solution should be introduced into the base only after steady state conditions occur.

In order to model this solution in Cartesian coordinates, a transformation had to be made using the Pythagorean theorem (see Figure 3-4):

$$r = \sqrt{(x+d)^2 + y^2} \qquad (3.36)$$

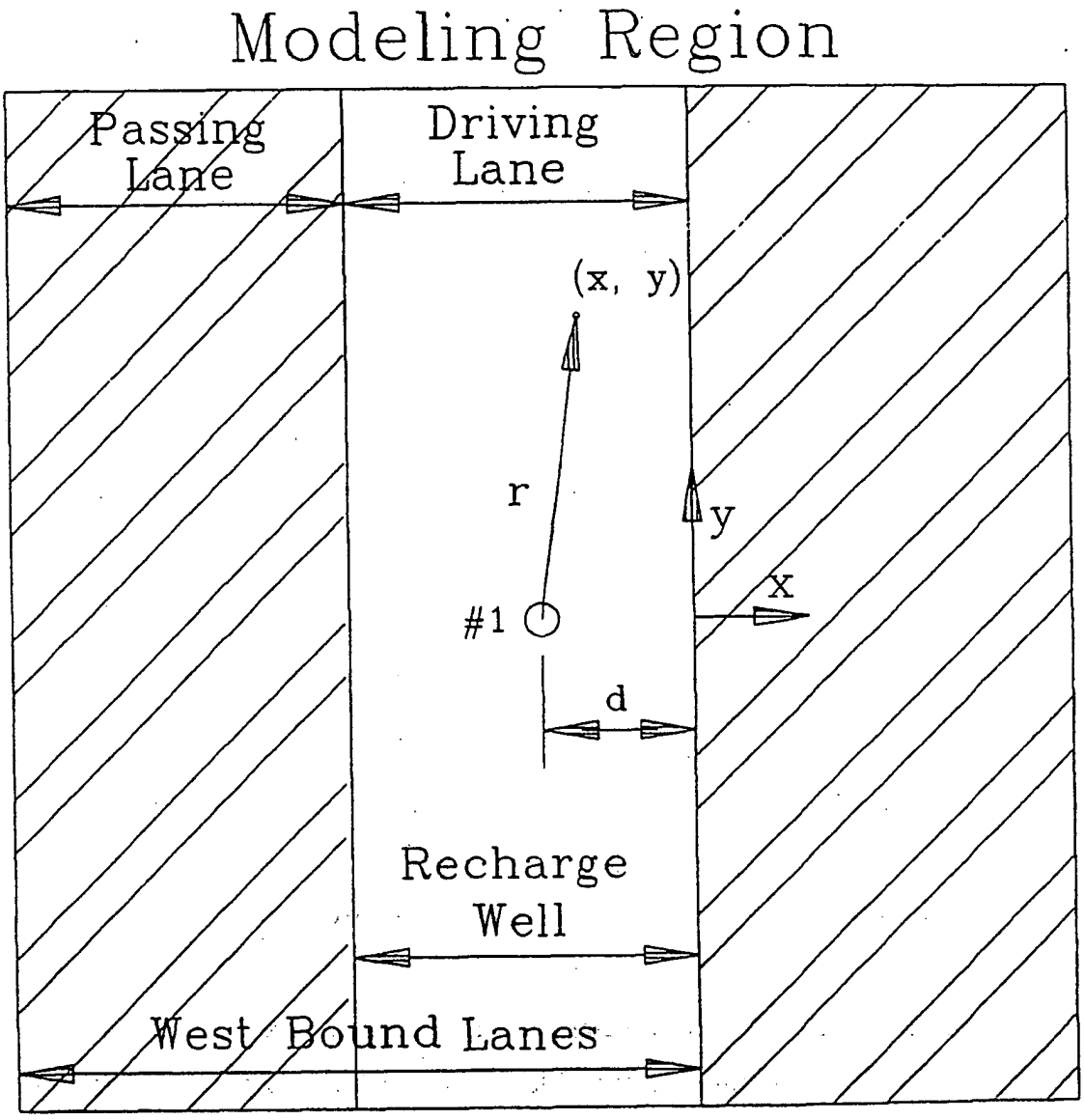

Figure 3-4: Computer modeling for solute concentration.

Because the diffusion coefficient has a negligible effect on the mass transport solution at high velocities, this value is taken to be zero. Hence, equation 3.34 reduces to:

$$C(r,t) = \frac{C_0}{2} erfc\left[\frac{\left(\frac{r^2}{2} - At\right)}{\left(\frac{4}{3}\alpha_l r^3\right)^{\frac{1}{2}}}\right] \qquad (3.37)$$

Some of the known properties of the error function and the complimentary error function are as follows:

$$erf\,[x] = 1 - erfc\,[x] \qquad (3.38)$$

$$erf\,[-x] = -erf\,[x] \qquad (3.39)$$

$$erfc\,[0] = 1 \qquad (3.40)$$

$$erfc\,[\infty] = 0 \qquad (3.41)$$

$$erfc\,[-\infty] = 2 \qquad (3.42)$$

A rational approximation from Hastings (1955) to evaluate the function is:

$$erf\,(x) = 1 - [\zeta] \qquad (0 \le x < +\infty) \qquad (3.43)$$

where:
$$\zeta = \frac{1}{[1 + a_1 x + a_2 x^2 + a_3 x^3 + a_4 x^4]^4}$$

$a_1 = 0.278393$

$a_2 = 0.230389$

$a_3 = 0.000972$

$a_4 = 0.078108$

Knowing the properties of the error function and the complimentary error function and using the rational approximation from Hastings, the complimentary error function was evaluated as follows:

$$erfc[x] = [\zeta] \qquad (0 \le x < +\infty) \qquad (3.44)$$

$$erfc[x] = 2 - [\beta] \qquad (-\infty < x < 0) \qquad (3.45)$$

where: $$\beta = \frac{1}{[1 + a_1|x| + a_2|x^2| + a_3|x^3| + a_4|x^4|]^4}$$

A computer program was developed in order to evaluate the mass transport solution more efficiently. The program input values are well flow rate, porosity of the base, thickness of the base, the longitudinal dispersivity coefficient and the initial tracer concentration. Electrolyte concentration at a given time and position is the output. See Appendix A for the program source code.

3.3 Design of the In Situ Test

The permeameter design was approached after the proper analytic models had been determined for simulation of the test device. The tasks involved in the design were: 1) determination of the well standpipe head level and determination of the probe placement, 2) design of the fresh water supply for the test, 3) selection of a device to determine the discharge velocity and 4) determination of a device to measure differential pressure.

3.3.1 Determination of well potential level and probe placement

A calculation procedure was developed in order to determine the level of potential at the point of entry into the pavement (the well or standpipe location) and the placement of the probes where appropriate values had been selected. Selection of appropriate

values for these two variables was based on critical gradient, travel time of the electrolytic solution, and the deflection of the pavement due to the imposed uplift pressures.

The critical gradient was the first criterion to ensure appropriate values of well potential and probe placement. No. 304 was the first material to be evaluated. The material values used for No. 304 came from Table 3-3. Note that the hydraulic conductivities were assumed from the information outlined in Chapter 2. The values of the potential at the well and the potential at the constant head boundary were assumed to be:

$$\phi_w = 2.0\ m \qquad \textit{(at the well)}$$

$$\phi_o = 0.001\ m \qquad \textit{(at the constant head boundary)}$$

Table 3-3: Material properties (assuming a median material gradation)

Material	No. 304	No. 310	Iowa	N. J.	No. 57
K (m/s) $x\,10^{-5}$	4.23	3.52	352	352	3500
H (m)	0.254	0.102	0.102	0.102	0.102
$D_{10}(mm)$	0.23	0.11	0.42	1.80	5.20
$D_{50}(mm)$	6.2	2.1	7.1	5.3	10.4
n	0.415	0.415	0.415	0.413	0.377
$\alpha_l(m)$ $x\,10^{-3}$	5.33	1.81	6.11	4.56	8.94

The input values were entered into the computer program that determined the confined/phreatic analytic solution. The output file of potential values generated by this program was then imported into the program Surfer that determines equipotential lines

from the matrix of output values. From the plot of equipotential contours, stream functions could then be drawn by hand to determine flow paths. Knowing the direction of the flow under the pavement, an appropriate position for probe placement was chosen. The position chosen to place the probes was in the region where the flow paths were straight.

The values of potential determined were next imported into a spreadsheet, Quattro Pro. From the contour map it was evident that the region where the flow path was straight, was the path from the standpipe flowing directly to the underdrain. These values of potential were then graphed, where x varied from -3.6 meters to 0 meters and y equalled 0 meters. Note that this profile includes the standpipe at x = -1.8 m. Finally, two points from this plot were selected for the probe placement. These positions were:

$$x_1 = -1.7\,m, \quad y_1 = 0 \quad at \quad \phi = 1.75\,m$$

$$x_2 = -1.6\,m, \quad y_2 = 0 \quad at \quad \phi = 1.55\,m$$

The Reynold's number was calculated to determine that the critical gradient was not exceeded (that laminar flow was occurring). The first value that had to be calculated was the length between the two probes. This was determined by the following equation:

$$L = \sqrt{(x_1 - x_2)^2 + (y_1 - y_2)^2} \qquad (3.46)$$

$$L = \sqrt{(-1.7 - (-1.6))^2 + (0 - 0)^2} = 0.1\,m$$

The hydraulic gradient was then determined:

$$i = \frac{\Delta\phi}{L} = \frac{1.75\,m - 1.55\,m}{0.1\,m} = 2$$

Next, the expected discharge velocity was determined:

$$q = ki = (4.23 \times 10^{-5}\ \frac{m}{s})(2) = 8.46 \times 10^{-5}\ \frac{m}{s}$$

At a temperature of $25^{o}C$: $\nu = 0.893 \times 10^{-6}\ \frac{m^2}{s}$

From these calculations the Reynold's number was determined from equation 2.5:

$$R_e = \frac{q\,D_{10}}{\nu} = \frac{(8.46 \times 10^{-5}\ \frac{m}{s})(2.30 \times 10^{-3}\,m)}{0.893 \times 10^{-6}\ \frac{m^2}{s}} = 0.22 \leq 10$$

Therefore, at these probe locations the critical gradient was not greater than the value indicating turbulent conditions. This calculation procedure was then carried out for the rest of the materials to determine the well potential and probe placement according to the critical gradient. Refer to Table 3-4 for the calculated values of the other materials.

The next check was to determine the travel time of the electrolytic solution from the point of entry to each probe. This was analyzed by using the computer program developed to solve the convective, dispersive mass transport and by direct hand calculation. The computer program determines the concentration at a particular point for given coordinates and a given time.

Table 3-4: Calculated material design values

Material	No. 304	No. 310	Iowa	N. J.	No. 57
$\phi_w(m)$	2.0	2.0	1.8	1.5	0.5
$\phi_o(m)$	0.001	0.001	0.001	0.001	0.001
$Q(\frac{m^3}{s}) \times 10^{-5}$	2.53	0.881	19.8	32.8	198
$Q(cfs) \times 10^{-4}$	8.94	3.11	69.9	115.8	699.3
$Q(\frac{gal}{\min})$	0.4	0.1	3.1	5.2	30.0
$x_1(m)$	-1.70	-1.65	-1.50	-1.50	-1.50
$y_1(m)$	0	0	0	0	0
$x_2(m)$	-1.60	-1.50	-1.25	-1.25	-3.0
$y_2(m)$	0	0	0	0	0
$L(m)$	0.10	0.15	0.25	0.25	0.25
$\phi_1(m)$	1.750	1.540	1.120	0.940	0.295
$\phi_2(m)$	1.550	1.250	0.830	0.700	0.290
i	2.00	1.93	1.93	0.95	0.02
$q(\frac{m}{s}) \times 10^{-5}$	8.46	23.5	170	168	73.2
R_e	0.22	< 0.1	0.8	3.4	4.0

From a design standpoint of this research, the probes were placed at points where it took a reasonable amount of time (less than forty minutes) for the median concentration of the electrolytic solution to reach the downstream probe. This involved looking at the mechanical dispersion of the electrolytic solution. To determine when the median concentration passed each probe, the ten and ninety percent concentration times were determined, then an average of these times were determined. Determination of the ten and ninety percent concentrations was also important for selecting a device capable of recording the change in electrical resistance.

It took many iterations using the developed computer program to determine these values of time. A quicker way to solve for these values was by the use of hand calculations and the use of the complimentary error function table listed in Appendix A.

The convective, dispersive, mass transport solution (equation 3.37) can be rewritten as follows:

$$C(r, t) = \frac{C_o}{2} erfc[\xi]$$

where: $\xi = \dfrac{(\frac{r^2}{2} - A t)}{(\frac{4}{3}\alpha_l r^3)^{\frac{1}{2}}}$ and $A = \dfrac{Q}{2\pi H n}$

Solving for the complimentary error function:

$$erfc[\xi] = 2\frac{C}{C_o}$$

At a ten percent concentration it followed:

$$erfc[\xi] = 2(0.10) = 0.20$$

Going to the complimentary error function table listed in Appendix A, it followed that ξ corresponded to 0.90.

Similarly, at ninety percent concentration it followed:

$$erfc\,[\xi] = 2(0.90) = 1.80$$

Going to the complimentary error function chart it followed that ξ corresponded to 0.90. For No. 304 at a ten percent concentration it followed:

$$x_1 = -1.7\,m \qquad y_1 = 0\,m$$

$$A = \frac{2.53 \times 10^{-5}\ \frac{m^3}{s}}{2\,\pi(0.254\,m)\,(0.415)} = 3.82 \times 10^{-5}\ \frac{m^2}{s}$$

$$r = \sqrt{(x_i - d)^2 + y_i^2} = \sqrt{(-1.7 + 1.8)^2 + 0^2} = 0.1\,m$$

$$\xi = 0.90 = \frac{(\frac{(0.1m)^2}{2} - (3.82 \times 10^{-5}\ \frac{m^2}{s}\,t))}{(\frac{4}{3}\,(0.005332\,m)\,(0.1\,m))^{\frac{1}{2}}}$$

Solving for the time at a ten percent concentration:

$$t_{10\%} = 68.0\,s$$

The ninety percent calculation for No. 304 and the ten and ninety percent calculations for the other materials were performed by the same calculation procedure at both probe locations. The results of these calculations are listed in Table 3-5.

Table 3-5: Mass transport design results

Material	No. 304	No. 310	Iowa	N. J.	No. 57
$x_1(m)$	-1.70	-1.65	-1.50	-1.50	-2.75
$y_1(m)$	0	0	0	0	0
$A(\frac{m^2}{s}) x 10^{-5}$	3.82	3.31	74.4	124	836
$r(m)$	0.10	0.15	0.30	0.30	0.95
$t_{10\%}$ (sec)	68.0	262.0	43.0	27.0	43.0
$t_{10\%}$ (min)	1.1	4.4	0.7	0.5	0.7
$t_{90\%}$ (sec)	194.0	417.0	78.0	46.0	65.0
$t_{90\%}$ (min)	3.2	7.0	1.3	0.8	1.1
$x_2(m)$	-1.60	-1.50	-1.25	-1.25	-3.00
$y_2(m)$	0	0	0	0	0
$A(\frac{m^2}{s}) x 10^{-5}$	3.82	3.31	74.4	124	836
$r(m)$	0.20	0.30	0.55	0.55	1.20
$t_{10\%}$ (sec)	346.0	1140.0	159.0	99.0	71.0
$t_{10\%}$ (min)	5.8	19.0	2.6	1.6	1.2
$t_{90\%}$ (sec)	701.0	1579.0	248.0	145.0	102.0
$t_{90\%}$ (min)	11.7	26.3	4.1	2.4	1.7

From the results listed in Table 3-5, the times appear to be reasonable. The only exception might be No. 310. Under this evaluation, the first probe was six inches away from the well and the second probe was six inches away from the first probe. Because of the physical limitations on how close the probes could be from the standpipe (greater than five inches), it was determined that the probe spacing for No. 310 was satisfactory.

The final check to determine if an appropriate value of well potential was selected, was to check the maximum deflection of the pavement due to induced uplift

pressures. If the upward deflection of the pavement due to the piezometric forces was greater than the size of the average void space of the base, water would short circuit the base leading to erroneous results of hydraulic conductivity.

To evaluate for the deflection of the pavement, forces acting on the pavement had to be determined. Two forces act on the pavement: the weight of the pavement acting down and the opposing piezometric force acting up. The weight of the pavement was taken as the unit weight of Portland cement concrete, multiplied by the thickness of the pavement. This was as follows:

$$q_{down} = \gamma_{conc}(t_{pave}) \qquad (3.47)$$

$$q_{down} = 23{,}500 \frac{N}{m^3}(0.254\ m) = 5969 \frac{N}{m^2}$$

The piezometric force acting up against the pavement was determined from the confined portion of the solution for potential developed in section 3.2.1 multiplied by the unit weight of water. For simplicity of analysis, the pavement was assumed to lie flat (no slope). Therefore, the confined portion of the solution simplifies as follows (Strack, 1989):

$$q_{up} = \phi \gamma_w = \frac{\gamma_w Q}{2\pi K H} \ln\left[\frac{|r - 3.81\ m|}{R}\right] \qquad (3.48)$$

$$Q = \frac{2\pi K H \phi_w}{\ln[\frac{r_w}{R}]}$$

where:

The worst-case scenario of upward force acting against the pavement was in No. 304 or No. 310, which had a well potential of two meters. For No. 304, the flow rate into the

$$Q = \frac{2\pi(4.23 \times 10^{-5}\ \frac{m}{s})(0.254\ m)(2\ m)}{\ln(\frac{0.0508\ m}{1.8288\ m})} = -3.77 \times 10^{-5}\ \frac{m^3}{s}$$

well was:

From this the piezometric force acting up could then be calculated:

$$q_{up} = \frac{(9800\ \frac{N}{m^3})(-3.77 \times 10^{-5}\ \frac{m^3}{s})}{2\pi(4.23 \times 10^{-5}\ \frac{m}{s})(0.254\ m)} \ln[\frac{|r - 3.81\ m|}{1.8288\ m}]$$

$$q_{up} = -5472.8 \ln[\frac{|r - 3.81\ m|}{1.8288\ m}]\ \frac{N}{m^2}$$

The pavement was then analyzed as a plate. The dimensions of the pavement are 7.62 meters by 3.66 meters with a thickness of 0.254 meters. Some assumptions were made to determine the deflection of the pavement. The first assumption was that the pavement would deflect upward. From this assumption it followed that the pavement could be analyzed in three steps: 1) find the deflection upward due to the piezometric forces, 2) find the deflection downward due to the weight of the slab, and 3) by using superposition add the two deflections together to get the net upward deflection (if it exists).

The second assumption was that the pavement is simply supported at the joints. This is a conservative assumption since the joints actually may have some moment resisting capacity. Simply supported edge conditions will yield more deflection than moment resisting edge conditions, and are therefore conservative.

Determination of the upward deflection of the pavement can be derived for this specific case by the use of the general Navier solution for simply supported rectangular plates (Timoshenko and Woinowsky-Krieger, 1959). This derivation is a lengthy one which involves numerous numerical integrations to determine Fourier series coefficients and a lengthy process to evaluate Navier's Fourier series solution. Because of this a simplification was made for ease of analysis.

The simplification was to approximate the piezometric force acting upward by a partial uniform square loading acting upward over the center of the pavement. This load was approximated by calculating the volume under the centerline force distribution of the piezometric force function and equating it to a rectangular distribution spread over one meter. This followed:

$$Area_{piezo.} = Area_{rect.}$$

$$19461.9 \frac{N}{m} = q_{up} (1\ m)$$

$$q_{up} = 19461.9 \frac{N}{m^2}$$

A solution to this problem was found by Hsu (1990). The maximum deflection was calculated as follows:

$$w_{max} = \frac{q u v a^2}{100 E t^3} K_w \qquad (3.49)$$

where w - the deflection of the plate (L)

q - the magnitude of the uniform load distribution ($\frac{F}{L^2}$)

u and v - the length and width of the partial uniform load distribution, respectively (L)

a - the width of the pavement (L)

b - the length of the pavement (L)

K_w - a coefficient based on $\frac{b}{a}, \frac{u}{a}, \frac{v}{a}$ (see Appendix B)

E - the modulus of elasticity ($\frac{F}{L^2}$)

t - the thickness of the pavement (L)

Determining the upward deflection then followed:

$$K_w \cong 18.1 \qquad for \ \frac{b}{a} = 2.08, \ \frac{u}{a} = 0.27, \ \frac{v}{a} = 0.27$$

$$w_{max} = \frac{19461.9 \ \frac{N}{m^2}(1\ m)(1\ m)(3.66\ m)^2(18.1)}{100(1.72 \times 10^{10} \ \frac{N}{m^2})(0.254\ m)^3} = 1.67 \times 10^{-4}\ m$$

The downward deflection could be found in a similar manner by using the same equation and extending the partial loading across the entire plate to represent slab weight. This followed:

$$K_w \cong 5.92 \qquad for \ \frac{b}{a} = 2.08, \ \frac{u}{a} = 1.00, \ \frac{v}{a} = 2.08$$

$$w_{max} = \frac{5969\ \frac{N}{m^2}(3.66\ m)(7.62\ m)(3.66\ m)^2(5.92)}{100(1.72 \times 10^{10}\ \frac{N}{m^2})(0.254\ m)^3} = 4.71 \times 10^{-4}\ m$$

The assumption that the pavement would deflect upward is therefore wrong, since the value of deflection due to the weight of the pavement is greater than the deflection due to the piezometric force. The pavement will not deflect upward because the piezometric forces are not enough to overcome the weight of the Portland cement concrete pavement. Therefore, the maximum well potential used is satisfactory for this specific case and should not lead to short circuiting and erroneous results.

3.3.2 Design of the fresh water supply for the test

There were three considerations for the design of the fresh water supply system for the test, 1) how to store enough water to run the test, 2) determine the necessary energy levels to take the water from the storage tank to the layer being tested and 3) how to supply additional energy to the fresh water when needed, if gravity flow is inadequate.

The first consideration was how to store enough water to run the test. Considerations for the storage tank were that it had to be portable, non-corrosive, and large enough to carry a sufficient amount of water. Recall from Table 3-4 and Table 3-5 that No. 57 needed 0.00198 cubic meters per second (worst case scenario) for at least two minutes after steady state flow was established. Therefore, about three hundred to five hundred gallons were necessary. One idea was the use of an agricultural water supply tank. Since this storage tank was designed to be hauled around in a pick-up truck and water is relatively heavy (9.8 kN per cubic meter), a 1230 liter portable agricultural water supply tank was selected, so as not to overload the pick-up truck.

3.3.3 Design of a device to measure the discharge velocity

From previous research done by Moulton and Seals (1979) and Roy and Sayer (1989), the discharge velocity was determined through the use of a tracer solution. This method involves measuring the change in resistance at two radial points away from the point of entry of the water before and after the introduction of the tracer solution. To

determine the discharge velocity, the distance between the two points is measured and divided by the difference in time for abrupt changes in resistance to occur at each probe. Two considerations were taken in the present design, 1) the probe system and 2) the device to measure resistance.

The first consideration in the determination of the discharge velocity was the probe system. From the research by Moulton and Seals (1979) it was determined that a two wire probe was the best method to measure resistance. The probes were then designed accordingly, fabricating two sets of probes for the specific field conditions of this research. The probes were made out of rugged materials to withstand field installation conditions. A three-eighths inch diameter stainless steel tube was used to house a three-sixteenths inch diameter stainless steel rod, effectively creating a coaxial electrode. The center rod was threaded at one end to screw into a stainless steel tip. A nylon bushing was placed in between the rod and the tubing to act as an electrical insulator. At the top of the probe a three-eighths inch Swagelok female branch tee and a female quick connect fitting were placed for a tap for the differential pressure system. The stainless rod was separated from the pipe fitting and the tubing at the top of the probe by a nylon bushing. Terminal screws were tapped into the branch tee and the top of the rod to attach wires for the electronics to measure the change in resistance the probe would experience when water closed an electrical gap between the tube and the tip. For a detailed drawing of the probe refer to Figure 3-5.

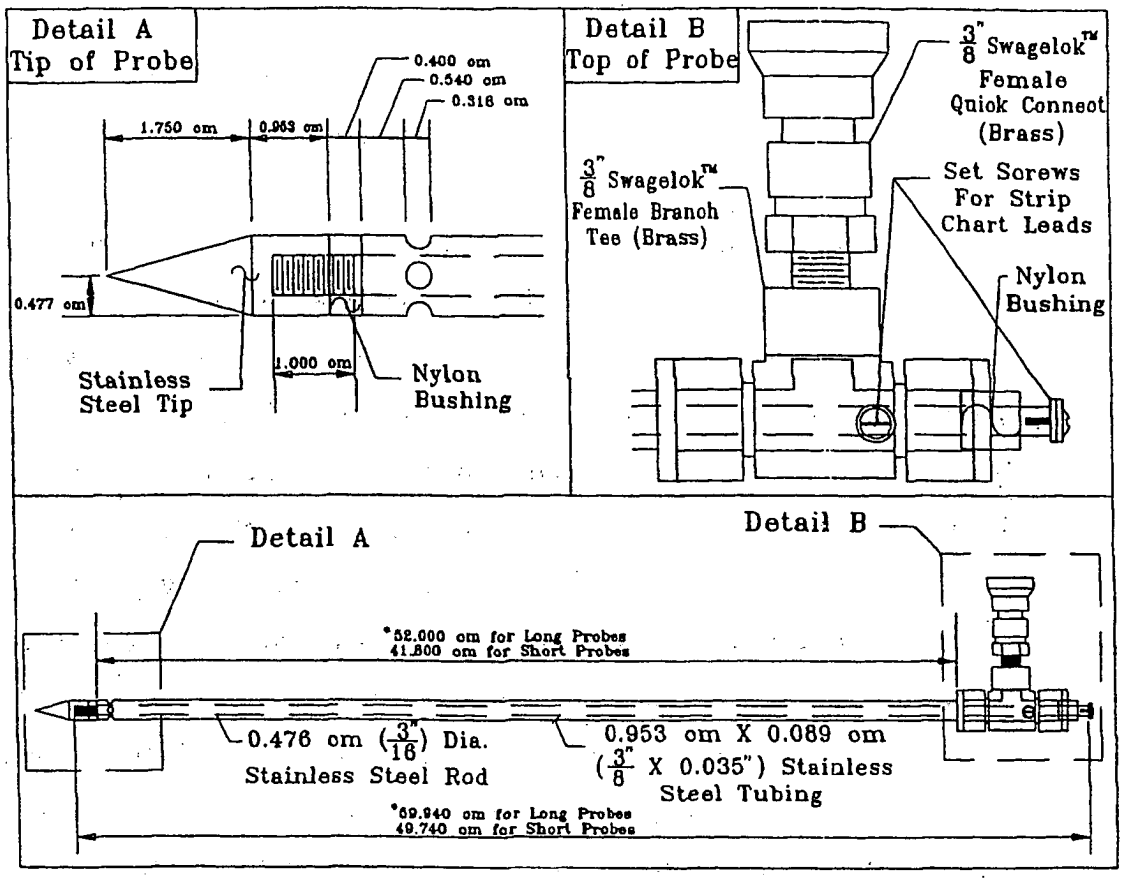

Figure 3-5: The probe system.

The second consideration in the determination of the discharge velocity was a device to measure and record the resistance of each probe versus time. In previous research conducted by Moulton and Seals (1979), the two probes were each connected to microammeters. When an abrupt change in resistance was detected on the upstream microammeter a timer was started. Likewise, when an abrupt change was indicated on the downstream microammeter the timer was stopped.

There are three possible problems that could occur using a similar technique in the development of an in situ device for coarse materials, 1) drift of the microammeters may trip the timer, 2) the mechanical dispersion effect is neglected, and 3) sudden sporadic jumps in resistance may also trip the timer.

The first problem mentioned was drift of the microammeter or other sensing devices. The drift, a linear change in resistance versus time not due to the electrolytic

solution, can be a problem when it is large enough to trip the sensing device timer. If the drift of the device sets off the timing device before or after the tracer has reached the probes, erroneous results of hydraulic conductivity could be obtained.

The second problem mentioned was the mechanic dispersion effect of the tracer as it passes through the base. Starting the timer when an abrupt change in resistance occurs indicates when a sharp front of the plume of the tracer reaches the probe and not when the median resistance passes the probe. This effect may not have affected the results greatly in fine grained materials, but in coarse grained materials this effect could be great. The dispersion effect of the tracer is directly related to the velocity of the fluid traveling through the base. The higher the velocity of the fluid traveling through the base, the greater the dispersion effect, and therefore the less pronounced the plume front. High velocities will be developed in coarse, open graded materials. Therefore, the dispersion effect needs to be accounted for.

The final problem mentioned was sudden unexplained sporadic jumps in resistance. Recording the resistance of each probe versus time will enable the experimenter to decide whether these jumps in resistance are due to the passing of the tracer, due to natural changes in water resistance or due to mechanical imperfections in the sensing device.

Measuring the resistance directly using digital multimeters and recording these resistances at specified time intervals using a stop watch was determined to be the most inexpensive solution to determining resistance versus time at each probe. Although the use of digital multimeters is more work for the field testing team, it is a viable and effective method.

3.3.4 Design of a device to measure differential pressure

Moulton and Seals (1979) found that the best way to determine the differential pressure was to measure directly between two points within the base. There were two aspects considered in this design, 1) the probe system and 2) the measuring device.

The probe system was the first aspect considered. At the bottom of the probes near the tip four 3.18 millimeter diameter holes were drilled to allow water in and out of the probes to sense the piezometric level of the water above the tips (Refer back to Figure

3-5). The three-eighths inch Swagelok female branch tee and a Swagelok female quick connect fitting made it possible for the probes to be directly attached to a pressure sensing device via one quarter inch tubing.

The differential pressure device was the last aspect considered. The first idea to measure differential pressure was the use of an electronic differential pressure transducer. The cost of this single device was quite high and the required precision could not be guaranteed so another option was sought. The idea that was used was a closed loop differential pressure manometer. This manometer was designed to use water and air to measure the differential pressure. This was an accurate and inexpensive alternative.

The differential pressure manometer has a one quarter inch line which directly attaches to the freshwater tank fitting via a Swagelok quick connect fitting (Figure 3-6). This line feeds into the bottom of a one-quarter inch Whitey three-way ball valve. On one side of the three-way valve is a one-quarter inch line with a Swagelok quick connect fitting which is used as a bleed line for the probes. On other side of the three-way valve is a one-quarter inch Nupro plug valve. This plug valve feeds into the side of a one-quarter inch tee. On the side of the tee is a one-quarter inch Hoke needle valve. Coming out of the bottom of the tee is a one-quarter inch line that feeds into a one quarter inch to one eighth inch Swagelok male branch tee. On each side of the male branch tee are one-eighth inch lines that feed directly to each of the probes via Swagelok quick connect fittings. The one-eighth inch lines are attached to a board that is oriented at a thirty degree angle with the horizontal to form a manometer. Mounted on the board is a centimeter scale to measure the difference in the differential pressure between the two probes. The differential pressure reading's accuracy is increased by a factor of two due to the oriented angle. This angle causes the differential pressure reading to be twice the actual difference. This allows the experimenter to read small differences more accurately.

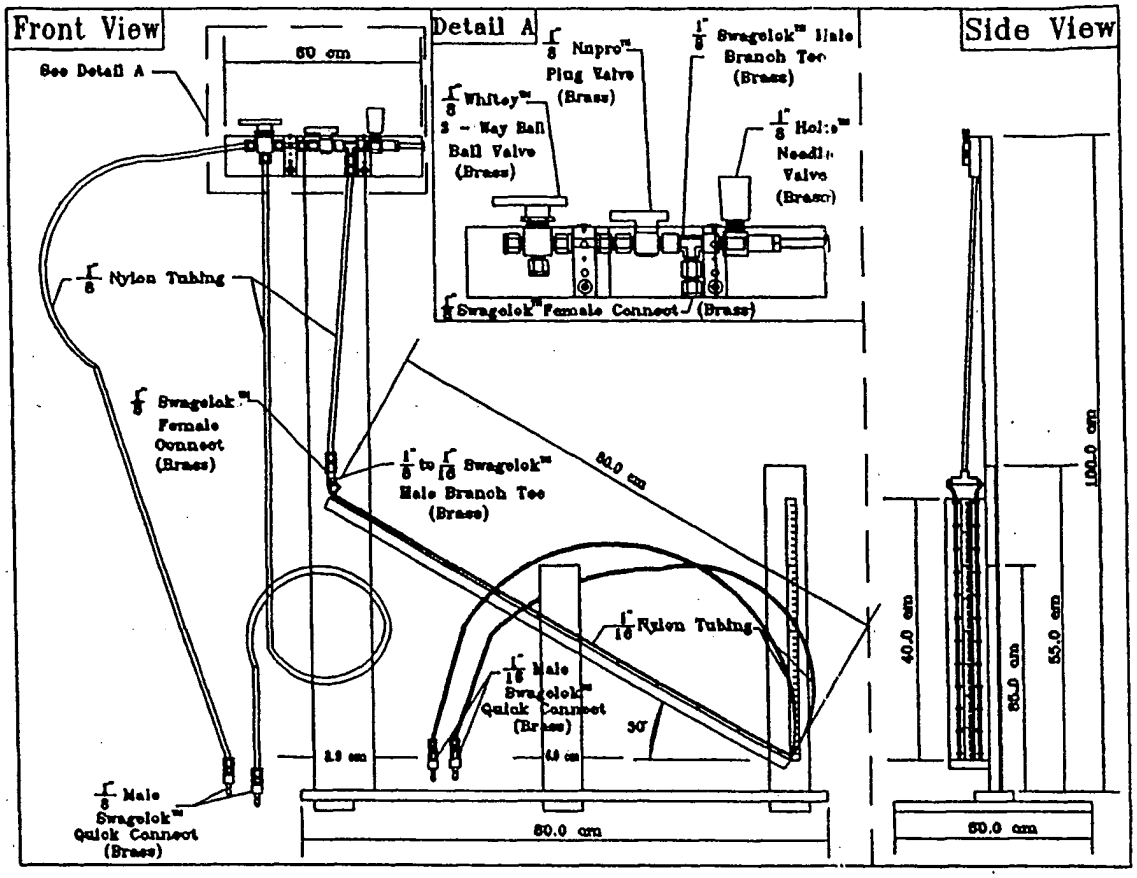

Figure 3-6: The closed loop differential pressure manometer.

When the three-way valve is thrown to one side, the probe's bleed line can be directly attached to the probes one at a time to flush entrapped air out of the probes. When the three-way valve was thrown to the other side, entrapped air can be bled out of the differential pressure lines. The differential pressure lines can then be attached to the probes. The plug valve is then closed and the needle valve slowly opened to allow air into both the manometer lines. Air is introduced via the needle valve, until the water levels in the manometer appear on the scale where differential pressure reading can be read. Once the water levels appear to settle, the differential pressure can then be directly measured and recorded.

3.4 Procedure

The operation of the in situ hydraulic conductivity device and test procedure is as follows:

1. Locate the position for the standpipe. This test should not occur in superelevated sections. This test should occur on normally crowned pavements with a grade of one percent or less. Core a four inch diameter hole in the pavement and through the thickness of the base material to be tested. The preferable position for the standpipe is the middle of the rightmost lane at the midpoint between joints, if present. Avoid highly cracked regions of the pavement.

2. Determine the in-place density of the base material. To do this, collect all the base material dislodged during the coring procedure and determine the weight. Estimate the volume of the hole that the base material came from.

3. Put the standpipe stand on the standpipe. Place the removable standpipe overflow collar onto the standpipe and place it at the desired height of the static head. Place rubber stoppers in the holes below the collar. Place the standpipe into the cored hole and inflate the rubber membrane until the standpipe is firmly sealed in place. Adjust the standpipe stand to the desired position and tighten the thumbscrews. Note that under high static head conditions, the standpipe may have to be wired down to eyebolts. These eyebolts can be screwed into concrete anchors that can be placed in holes that are drilled into the pavement.

4. Determine the positions to place the probes. Drill a one half-inch diameter hole vertically at each of these positions with a hammer drill and carbide masonry bit. Next, place appropriate sizes of neoprene O-rings around the probes to create a seal in the one half inch diameter hole. Place the probes into the holes and seal tightly by rolling the O-rings into the annular space between the probe and the pavement.

5. Place the water control system next to the standpipe. Secure all appropriate hoses to their proper positions for the testing configuration to be run. Place the differential manometer and the electrical resistivity sensing system next to the probes.

6. Measure the appropriate amount of ammonium chloride (to be determined by experimentation) (NH_4Cl) and add it to the salt water tank. Mix the solution with a stirring rod in the drill until the ammonium chloride is dissolved. Based on previous research by Moulton and Seals (1979), ammonium chloride was determined to be the best salt to use for this test method. However, table salt ($NaCl$) was found to produce an

acceptable electrolyte solution in this research. Note that the concentration will need to be adjusted depending upon the sensitivity of the equipment that is used to measure resistance. Trial tests should be run in order to determine the most effective concentration to be used for the specific equipment.

7. Open the valve to the fresh water tank to establish steady state flow in the base material. This process may take some time before steady state is achieved but is a necessary step.

8. Connect the fresh water bleed lines to the probes. This should take place just prior to running the test. Allow water to flow through the bleed lines until all of the entrapped air is removed from the probes. Place the probes into the holes while the water is flowing. Disconnect the bleed lines.

9. Connect the electrical resistance sensing system to the probes. Check for sensitivity and stability of the device.

10. Attach the differential manometer to the fresh water supply and bleed the entrapped air out of both legs of the differential manometer. Connect these lines to the probes.

11. The change in pressure between the two points can now be measured. This is accomplished by closing the plug valve and opening the needle valve slowly on the differential pressure manometer to introduce air. The needle valve can be closed once the air bubble travels past the tee and into the two one eighth inch lines leading to the probes. Do not let the water/air interface levels fall below the inclined scale readings. Read the difference between the two water levels in each of the two lines. Take the value and divide it by the scaling factor for the inclined manometer (2.0 in this case) and record it as the differential head.

12. The electrical resistance sensing system should again be checked for stability prior to the introduction of the electrolyte solution into the system. Open the valve to the salt water tank to begin the test. Record the resistances for both probes at uniform time increments.

13. Once the resistance readings have reached a steady minimum level, the valve to the salt water tank may be closed and fresh water reintroduced back into the test material.

The fresh water is allowed to flush the salt solution from the base, thus causing the resistance readings to return to near their original values.

14. Once the system returns to its original condition, the flow (and, thus, the differential head) are adjusted and another test can be conducted.

The data that is needed for calculations of the hydraulic conductivity are:

(a) the travel time, t (in seconds) between the midpoint resistance to be registered at the two probes.

(b) the differential head, Δh (in centimeters); and

(c) the probe spacing, L (in centimeters).

Appendices C and D list an in situ hydraulic conductivity test checklist and a typical data sheet set for this test, respectively.

3.5 Results

The in situ hydraulic conductivity testing device was used to determine the hydraulic conductivity of highway test section bases located on State Route 2. Trials of the device were conducted in summer and autumn of 1994. Data collected during testing consisted of differential pressure change between the two probes, probe locations, standpipe locations, standpipe potential, resistance versus time readings, location of the test, material being tested, water temperature, volume of material recovered from the hole, and weight of the material recovered from the hole.

Tests were performed on Ohio State Route 2 in Lorain County. The exact test locations, the type of materials tested, the date the material was tested and the number of tests performed at each location are listed in Table 3-6.

Table 3-6: Material test sites (note: all stationing is within Lorain County, Ohio)

Material	Location	Date	No. of Tests	Hole No.
No. 310	4+00	09/07/94	2	1
Iowa Mix	6+00	09/08/94	2	2
PCC No. 57	83+00	09/12/94	3	6
No. 304	64+00	09/13/94	1	3
Asp No. 57	80+00	09/14/94	2	5
N.J. Mix	72+00	09/14/94	2	4
No. 304	64+00	09/15/94	1	3

To illustrate how the in situ hydraulic conductivity was determined from the data collected, sample calculations are outlined here for ODOT specification No. 310, test no. 2. The first step in the calculation procedure was to take the resistance versus time readings and enter those readings into a spreadsheet (Note: all material field data are taken from Appendix E for No. 310). The graphs of the resistance versus time for both the upstream and downstream probes could then be plotted. By using engineering judgment, the beginning and ending breaks in the resistance versus time curves were then determined for both the upstream and downstream probe. A parallel line to the abscissa axis was then drawn from these two points on each curve to intersect the ordinate axis. A median value of resistance was determined at the midpoint between these two lines. A line was then drawn from the median value of resistance back to the curve. From this new point on the curve a line was drawn perpendicular to the abscissa axis. The intersection with the abscissa was then determined to be the time of the fifty percent resistance of the electrolytic solution passing each of the probes (See Figures 3-7 and 3-8). The times for the fifty percent resistance to pass each probe in No. 310, test no. 2 were:

$$t_{50\%\,up} = 435\ s$$

$$t_{50\%\,dn} = 1230\ s$$

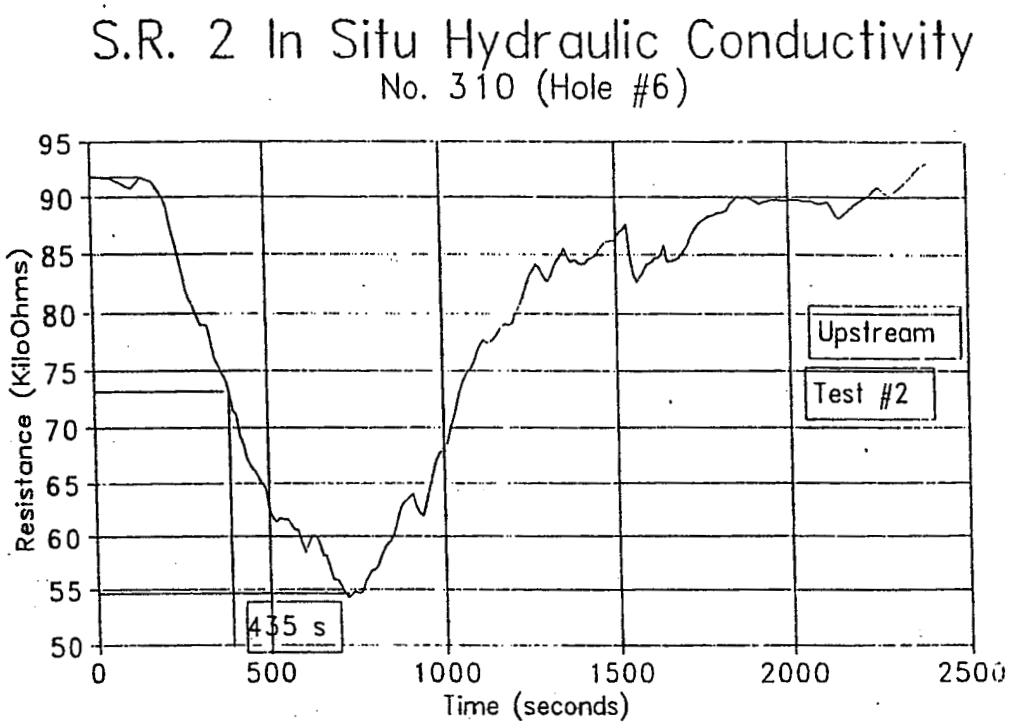

Figure 3-7: Resistance versus time for No. 310, Test No. 2, upstream probe.

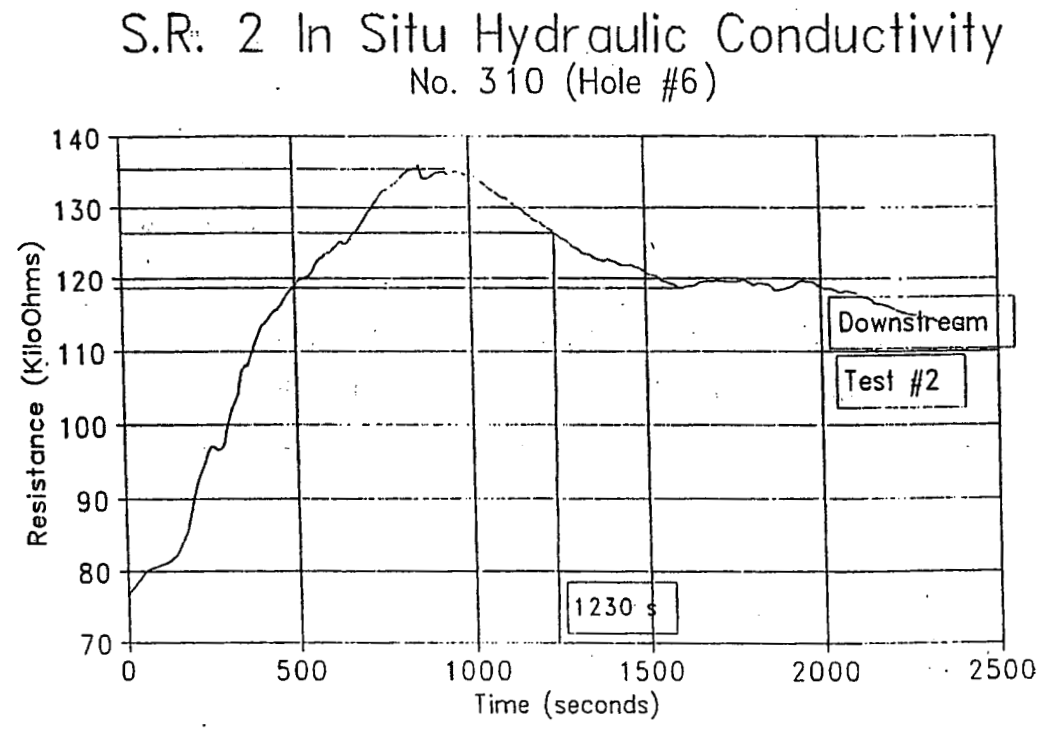

Figure 3-8: Resistance versus time for No. 310, Test No. 2, downstream probe.

The difference between these two times was taken to be the macroscopic time it took for water to travel from the upstream probe to the downstream probe. This time was calculated as follows:

$$t_{No.\,310} = 795\ s$$

The distance between the two probes was taken as the absolute difference between the upstream and downstream probe locations. This was as follows:

$$L = |L_{up} - L_{dn}| = |20\ cm - 30\ cm| = 10\ cm$$

Typically, the change in potential between the probes is found by taking an average of the change in potential readings before and after the electrolytic solution was allowed to flow into the base. For this case a single reading was taken after the electrolyte was released. The change in potential reading was divided by two because of the designed inclination of the closed-loop differential manometer. Therefore, the change in potential between the probes is:

$$\Delta\phi = 17.95\ cm$$

The hydraulic conductivity was then determined by using equation 2.19:

$$K = \frac{L^2}{t\,\Delta\phi} = \frac{(10\ cm)^2}{(795\ s)(17.95\ cm)} = 0.0158\ cm/s$$

Since the temperatures of the water used in each of the tests were not the same (depending on the ambient weather), the values of hydraulic conductivity were adjusted to a standard temperature of twenty degrees Celsius. This was achieved by the use of equation 2.8. The adjusted value of hydraulic conductivity for ODOT specification No. 310 was then determined as:

$$K_{20\,^{\circ}C} = 0.0154\ cm/s$$

The field test data are listed for each material in Appendices E through J. The materials' results, including No. 310, are summarized in Tables 3-7 and 3-8.

Table 3-7: Field test conditions.

Material	$\gamma_D(\frac{kN}{m^3})$	Test No.	Upstream Probe Location	Downstream Probe Location
No. 310	17.69	1	15 cm	30 cm
No. 310	17.69	2	15 cm	30 cm
Iowa	22.19	1	15 cm	30 cm
Iowa	22.19	2	15 cm	30 cm
PCC No. 57	15.34	1	30 cm	120 cm
PCC No. 57	15.34	2	30 cm	120 cm
PCC No. 57	15.34	3	30 cm	75 cm
No. 304	17.61	1	20 cm	30 cm
Asp No. 57	16.21	1	35 cm	120 cm
Asp No. 57	16.21	2	35 cm	120 cm
N.J. Mix	25.05	1	30 cm	55 cm
N.J. Mix	25.05	2	30 cm	55 cm
No. 304	17.61	2	20 cm	30 cm

Material	Water Temp. $(°C)$	Test No.	Upstream $t_{50\%}$ (sec)	Downstream $t_{50\%}$ (sec)
No. 310	21	1	-	1230
No. 310	21	2	435	-
Iowa	22	1	100	496
Iowa	22	2	87	200
PCC No. 57	20	1	423	536
PCC No. 57	20	2	353	400
PCC No. 57	20	3	39	350
No. 304	25	1	2082	2352
Asp No. 57	23.5	1	71	500
Asp No. 57	23.5	2	77	600
N.J. Mix	22	1	-	-
N.J. Mix	22	2	200	1015
No. 304	25	2	1219	2000

Table 3-8: Field test results.

Material	Test No.	Time	ϕ_w (m)	$\Delta\phi$ (cm)	L (cm)
No. 310	1	11:20 a	1.041	21.3	15
No. 310	2	12:08 p	1.041	17.95	15
Iowa 41-21	1	11:40 a	1.054	1.18	15
Iowa 41-21	2	1:10 p	1.054	0.80	15
PCC No. 57	1	11:30 a	Unk.	25.65	90
PCC No. 57	2	1:20 p	Unk.	29.45	90
PCC No. 57	3	2:02 p	Unk.	26.70	45
No. 304	1	11:32 a	1.270	1.20	10
Asp No. 57	1	10:45 a	Unk.	3.95	85
Asp No. 57	2	11:20 a	Unk.	3.93	85
N.J. Mix	1	1:00 p	0.743	3.45	25
N.J. Mix	2	1:30 p	Unk.	1.20	25
No. 304	2	11:45 a	2.724	22.66	10

Material	Test No.	Time	t (sec)	K_T (cm/s)	$K_{20°C}$ (cm/s)
No. 310	1	11:20 a	-	-	-
No. 310	2	12:08 p	795	0.0158	0.0154
Iowa 41-21	1	11:40 a	396	0.482	0.461
Iowa 41-21	2	1:10 p	113	2.49	2.38
PCC No. 57	1	11:30 a	113	2.79	2.79
PCC No. 57	2	1:20 p	47	5.85	5.85
PCC No. 57	3	2:02 p	311	0.244	0.244
No. 304	1	11:32 a	197	0.423	0.376
Asp No. 57	1	10:45 a	429	4.26	3.93
Asp No. 57	2	11:20 a	523	3.52	3.25
N.J. Mix	1	1:00 p	-	-	-
N.J. Mix	2	1:30 p	815	0.639	0.611
No. 304	2	11:45 a	781	0.00565	0.00503

4. LABORATORY HYDRAULIC CONDUCTIVITY TESTING

4.1 Introduction

The hydraulic conductivity of a granular material is determined in the laboratory by means of a device called a permeameter. There are two methods used to measure hydraulic conductivity in a laboratory permeameter. They are the constant head method and the falling head method. Because of the difficulty of measuring a small rate of flow in the constant head method, and the considerable reduction of hydraulic conductivity due to the presence of silts and fines, the constant head permeameter is usually used to measure soils with hydraulic conductivity not less than about 10^{-2} *cm/s* (Head, 1982). These are typically soils such as clean sands and gravels. The falling head permeameter is used for measuring those clayey soils of low and very low hydraulic conductivity.

The accepted standard methods of measuring hydraulic conductivity of granular materials in the laboratory are ASTM D2434-68 (1974) and AASHTO T215-70 (1984), which both use the constant head method. The principle underlying both standards is to reproduce the flow pattern which was incorporated in the derivation of Darcy's Law (Bear, 1972). The flow is steady state, laminar flow. The hydraulic gradient is constant during a test. The sample is compacted to a desired degree with the density constant throughout the sample and then is completely saturated before a test. During a test, the sample undergoes no volumetric change. Therefore, the permeameter and ancillary apparatus, the preparation of samples, and the procedures are carefully designed to create the required conditions.

The standard methods impose limits for coarse aggregates (ASTM D2434-38, 1974). To reduce the effect of sample variability and permeameter sidewall leakage, the minimum diameter of a permeameter cell is required to be from 8 to 12 times the maximum particle size, depending on the gradation distribution of the sample. Coarse

materials commonly used in bases and subbases contain a significant percentage of particles of 38 mm (1.5 inch) in diameter. Thus, a large scale permeameter must be fabricated. The maximum size particle which can be used in the standard permeameter is specified as 19 mm (3/4 inch), while most of the materials used as drainage layers in pavement construction contain a significant percentage of particles greater than this.

In the standard methods, a vertical permeameter is used, and the sample is compacted vertically. Thus, the hydraulic conductivity obtained is the vertical hydraulic conductivity. However, in pavement bases and subbases, the main direction of flow is horizontal, and the base materials are compacted vertically. Thus, the hydraulic conductivity used to calculate drainage rates in pavement bases and subbases should be horizontal hydraulic conductivity with vertical compaction. Research has shown a marked difference between horizontal and vertical hydraulic conductivity for coarse materials under the same conditions (Floss and Berner, 1989; Muskat, 1937; Wu, et al., 1978). The ratios of horizontal to vertical hydraulic conductivity of sand ranged from 1 to 42, according to Muskat's research results of 65 pairs of samples. Piersol, et al. (1940) mention ratios of horizontal to vertical hydraulic conductivity of sandstone of from 1.5 to 3.0. Thus, a large scale horizontal permeameter is needed to obtain a realistic, representative measure of the hydraulic conductivity of coarse materials used in pavement bases and subbases.

The principle of the large scale horizontal test is the same as for the standard hydraulic conductivity test on sands. However, uncertainties arise for testing in such a large scale horizontal permeameter for highly permeable materials. These include the control of saturation, lateral short circuiting along the walls of the permeameter, the significance of head loss through flow tubes and porous stones, and, more importantly, how to choose hydraulic gradients during testing for different materials to assure a laminar flow pattern is created and to obtain valid, reproducible results. Attention must

be paid to the testing apparatus, sample preparation, testing procedures and data interpretation.

In summary, the hydraulic conductivity of base and subbase materials is the key in calculating the drainage capacity, and the permeameter and the testing procedure used in the laboratory should be carefully designed to duplicate the field conditions as closely as possible to obtain accurate results.

4.2 Materials Tested

The gradations of the materials investigated are Ohio Department of Transportation (ODOT) specifications No. 304 and No. 310 soils, AASHTO M 43 specification No. 57 and No. 67 aggregates, the New Jersey test base materials (NJ Mix) and the Iowa Department of Transportation granular base specification 41-21 (IW Mix). Their gradation specifications are listed in Table 4-1.

Three types of materials were tested. They are crushed limestone, natural sand and gravel and crushed, air cooled blast furnace slag. Asphalt treated #57 and #67, and Portland cement treated #57 and #67 were also tested. The materials were provided by the Ohio Department of Transportation from commercial suppliers.

To obtain the range of the hydraulic conductivity within different gradation envelopes, the bulk materials were sieved and grouped in different particles sizes, then recombined according to the gradation specification into three target gradings: fine, medium and coarse. The fine gradation represents the upper grading limits in Table 4-1. The coarse gradation stands for the lower grading limits. The medium gradation is taken as the average of the upper and lower grading limits. The hydraulic conductivity tests that were conducted are listed in Table 4-2.

Table 4-1 Gradation Specifications - Percent Finer by Weight

SIEVE	No. 304	No. 310	No. 57	No. 67	NJ Mix	IW Mix
2 1/2"		100				
2"	100					
1 1/2 "			100		100	
1"	70-100	70-100	95-100	100	95-100	100
3/4"	50-90			90-100		
1/2"			25-60		60-80	50-80
3/8"				20-55		
#4	30-60	25-100	0-10	0-10	40-55	
#8			0-5	0-5	5-25	10-35
#16					0-8	
#30	7-30					
#40		5-50				
#50					0-5	0-15
#200	0-13	0-10			0	0-6

Table 4-2: Materials Tested for Laboratory Hydraulic Conductivity

	Limestone	Slag	Gravel
AC No.57	PF57LA PM57LA PC57LA	PM57SA	PM57GA
AC No. 67	PM67LA	PM67SA	PM67GA
PC No.57	PM57LP	PM57SP	PF57GP PM57GP PC57GP
PC No.67	PM67LP	PM67SP	PM67GP
No.57	PM57LN	PF57SN PM57SN PM57SN	PM57GN
No.67	PM67LN	PM67SN	PM67GN
NJ MIX	PMNJMLN	PMNJMSN	PNJMGN
IW MIX	PFIWMLN PMIWMLN PCIWMLN	PFIWMSN PMIWMSN PCIWMSN	PFIWMGN PMIWMGN PCIWMGN
NO. 304	PF304LN PM304LN PC304LN	PF304SN PM304SN PC304SN	PF304GN PM304GN PC304GN
NO.310	PF310LN PM310LN PC310LN	PF310SN PM310SN PC310SN	PF310GN PM310GN PC310GN

Legend:

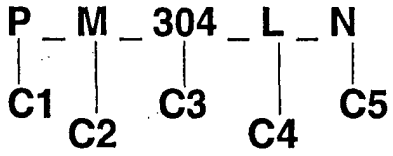

C1 = Testing type P = Permeability test
C2 = Target grading F = Fine grading limit of a gradation envelope
M = Middle grading of a gradation envelope
C = Coarse grading limit of a gradation envelope
C3 = Gradation type (see Table 4-1)
C4 = Material type L = Limestone
S = Slag
G = Gravel
C5 = Binder type N = Non-stabilized
P = Portland cement stabilized
A = Asphalt stabilized

4.3 Permeameter Design Considerations

The range of possible testing conditions was first estimated before beginning the design of the laboratory permeameter. The hydraulic conductivity of each specimen type in Table 4-2 was estimated using Hazen's equation to define the range of possible conditions that the laboratory permeameter must handle. Estimated values ranged from 0.0036 to 27.0 cm/s (10 to 76,700 ft/day). Upper limit hydraulic gradients were also estimated using equation 2.5 for a Reynold's number of 10. Estimated limiting values ranged from 0.0029 for the lower gradation No. 57 to 4650 for the upper gradation No. 304.

The constant head method is recommended to measure hydraulic conductivity for granular materials or materials with hydraulic conductivity not less than about 0.01 cm/s. Virtually all of the materials that were investigated in this study were estimated to have a higher value of hydraulic conductivity than this. Therefore, the constant head method was adopted for the measurement of hydraulic conductivity of these coarse grained materials.

Note that some materials in Table 4-1 may have particles over 51 mm (2 inches). However, most of the materials have 38 mm (1.5 inch) particles or smaller. Therefore, a large scale permeameter was needed for materials containing particles up to 38 mm (1.5 inch) in diameter. The minimum cross-sectional dimension of the permeameter cell is required to be from 8 to 12 times the maximum particle size. Thus, the permeameter cell was designed to be nominally 12 inches across.

For the laboratory measurement of hydraulic conductivity in a rigid wall permeameter, sidewall leakage is a significant source of error because of the large void spaces created along the boundaries. Special consideration was given to reduce this effect.

In the field, the flow direction is nearly horizontal, while the base and subbase materials are compacted vertically. To accurately determine the drainage rates in pavement bases and subbases, the measured hydraulic conductivity should be obtained in a horizontal permeameter, in which water flows horizontally and the samples are compacted vertically. To facilitate the vertical compacting and horizontal flow, a square cross section was selected for the permeameter.

4.3.1 Procedure Related Variables

The degree of saturation of the tested sample is crucial in the measurement of hydraulic conductivity. Lack of complete saturation reduces the measured value of hydraulic conductivity. The achievement of complete saturation is dependent on the saturation method and type of water used.

To increase saturation at the beginning of a test a vacuum was applied to the sample before and during filling with water, and the water was introduced from the bottom upward under a hydraulic gradient greater than 1.

When tap water is used directly in testing, the air bubbles in the tap water can be trapped in the samples if the void spaces are relatively small. An erroneously low value of hydraulic conductivity would then be obtained. Settled water has been used in previous research to reduce errors due to excessive air. Tap water was settled in a tank to allow the air bubbles to rise out of the water. Then, the settled water was pumped to the upstream constant head tank to create a head difference. It has been shown that test results with the use of settled water are satisfactory (Jones and Jones, 1989).

Moist compaction reflects field practice, but it runs the risk of preventing full saturation and yielding underestimated hydraulic conductivities. Dry compaction may result in segregation problems, however, it yields maximum density for coarse materials. Considering the impact of saturation on the results of hydraulic conductivity, dry compaction was chosen for this study.

Darcy's law is invalid when specific discharges exceed the upper-limit for linear flow. Practically, the flow deviates from linear flow when Reynold's number is some value between 1 and 10. Accordingly, each tested sample has an upper-limit of hydraulic gradient for linear flow. If the applied hydraulic gradient is greater than the upper-limit, and it is misinterpreted as linear flow, then the calculated hydraulic conductivity will be lower than the true hydraulic conductivity that is likely to be encountered in situ, where natural gradients are usually much lower. A range of resulting measured specific discharges have to be plotted against the applied hydraulic gradients to visualize the linear and non-linear portions of the data. The hydraulic conductivity can then be

determined from the slope of the linear part of this curve. Moreover, the upper-limit of hydraulic gradient for linear flow can be found from the plot. The plotting of i/q versus q serves as a more precise method to determine the upper limit hydraulic gradient for linear flow.

Plotting i/q (vertical axis) versus q (horizontal axis) yields a sloped straight line for nonlinear flow, and a horizontal line intercepting the i/q axis at 1/K for linear flow. A typical plot of i/q vs. q for flow progressing from linear laminar flow to nonlinear laminar flow is shown in Figure 4-1.

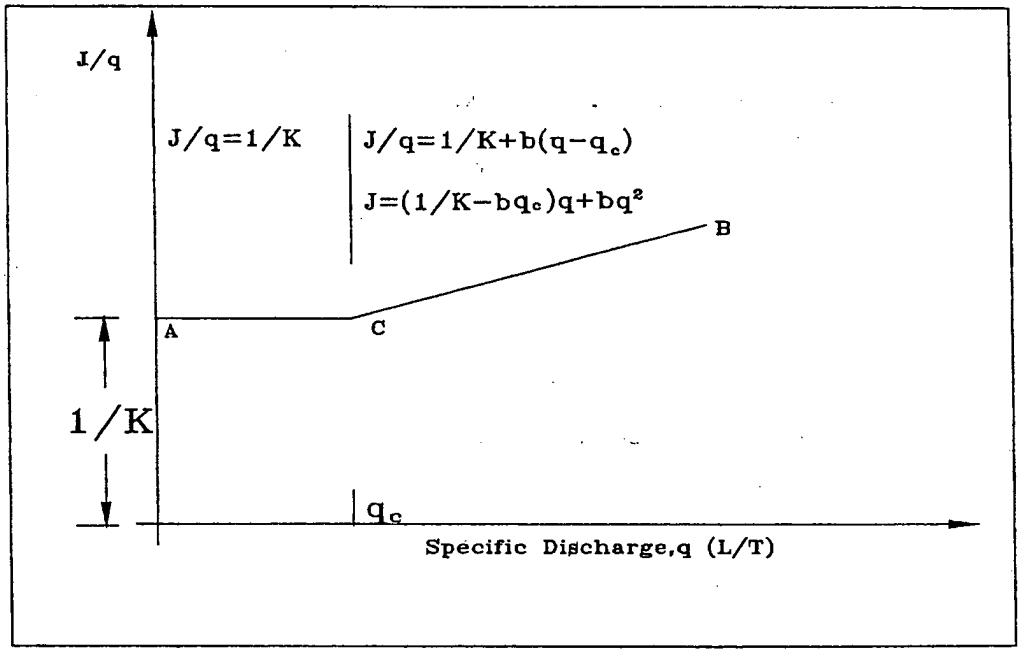

Figure 4-1: Typical Relation of i/q vs. q

In Figure 4-1, q_c is the specific discharge at the dividing point of linear and nonlinear flow regions. The upper limit of the hydraulic gradient can be obtained by taking q_c from the plot of i/q vs. q back to the i vs. q plot, if data in both the linear flow region and nonlinear flow region are available. The hydraulic gradient corresponding to q_c is the upper limit.

4.3.2 Permeameter Design

A permeameter was designed and constructed as shown in Figure 4-2. It consists of a permeameter cell, two standpipes, and accessories such as a vacuum pump, a level and a platform balance. The permeameter cell and the lid are shown in Figure 4-3. The

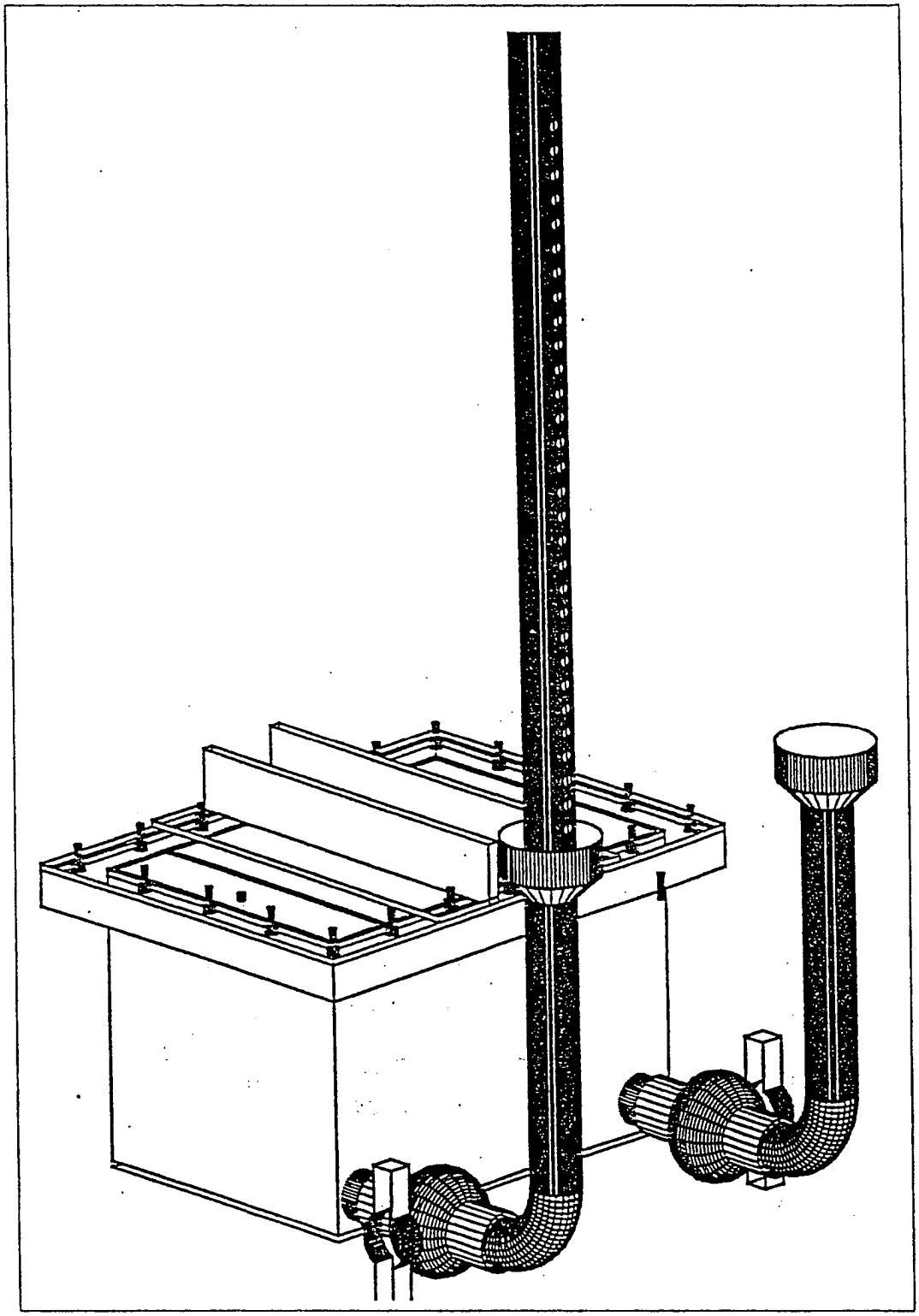

Figure 4-2: Schematic of the Permeameter

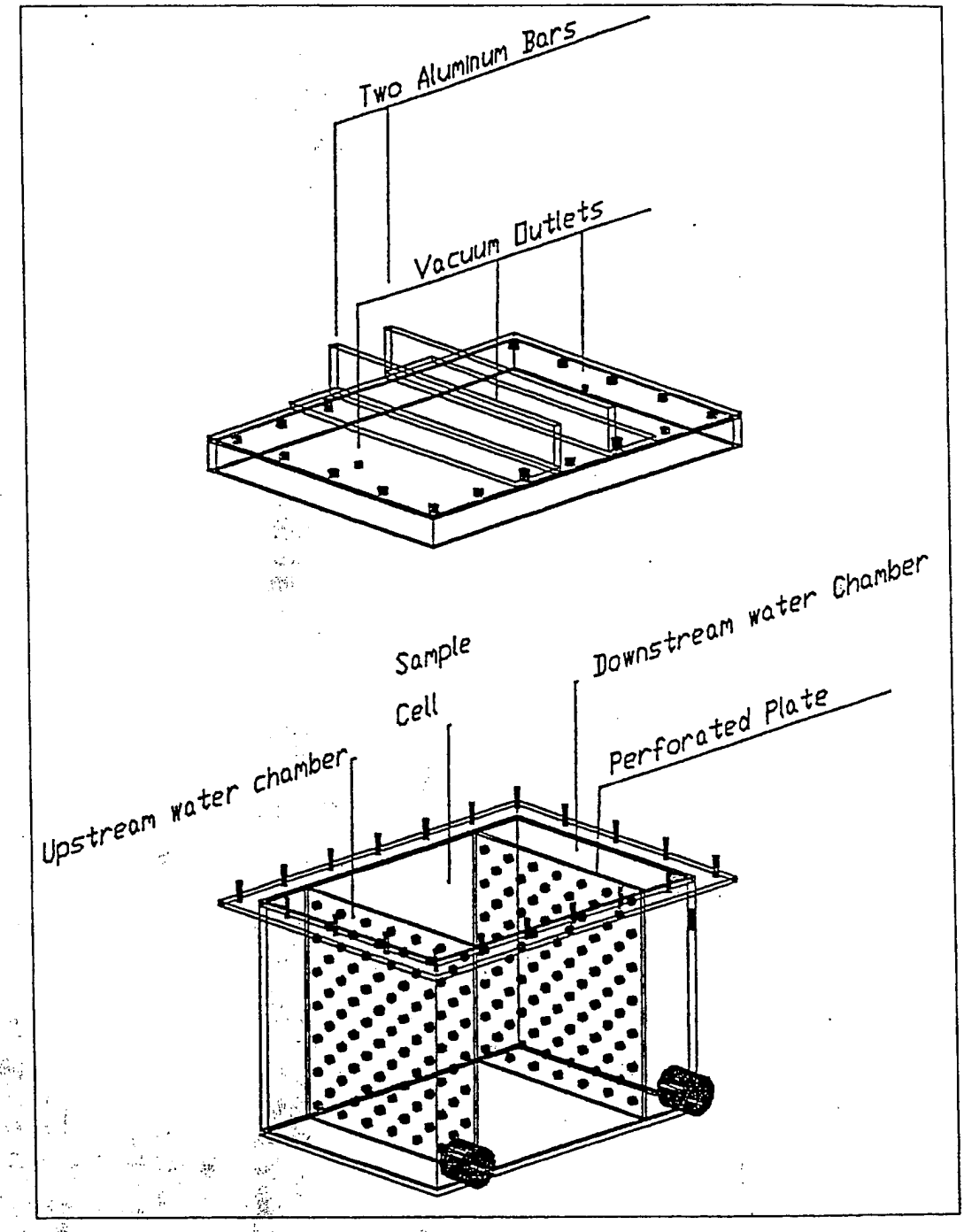

Figure 4-3: Transparent View of the Permeameter Cell

cross-sectional area of the sample cell is 30.5 cm by 30.5 cm (12 inches by 12 inches). The permeameter cell is 45.7 cm (18 inches) long. It was fabricated from 6 mm (1/4 inch) thick polyvinyl chloride (PVC) sheets. The flange around the top of the permeameter cell is used to secure the lid with nylon studs and wing nuts. Two aluminum angle stiffeners

are bolted across the lid to reduce bowing. Two perforated PVC plates separate the permeameter cell into water chambers at the two ends of the cell and a sample cell in the middle.

The length of the sample cell is 30.5 cm (12 inches). The determination of the length of the sample cell was dependent on the hydraulic conductivities of the materials to be tested, the desired accuracy of the computed gradient and the precision of the meter used to measure head differences. Once the length of the sample chamber of the permeameter was decided, there exists a critical head difference for the material tested in the permeameter due to the upper limit hydraulic gradient for that type of material. This is equal to the sample length times the critical hydraulic gradient. When the applied head difference is greater than the critical head difference the flow is nonlinear. For a given material, the critical head difference can be raised by increasing the sample length. In order to obtain an accurate value of the hydraulic conductivity, at least three different head differences below the critical head difference had to be applied across the sample. Moreover, the applied head difference increments have to be significant enough to be accurately determined by the available equipment used to measure the head differences. This imposes a practical minimum value on the critical head difference for the materials tested in the permeameter.

The lowest estimated upper limit hydraulic gradient was 0.0029 for coarse No. 57. The precision of the available device to measure head differences is 0.0254 mm (0.001 inch). Thus, the minimum critical length was estimated to be 8.8 cm (3.4 inches). Considering other factors, such as the effect of sample variation and the head difference which can be achieved in the laboratory, the sample length was selected as 30.5 cm (12 inches).

The permeameter is fitted with two perforated plates to create the sample cell. The plates are riddled with 9 mm holes. These are designed for relatively coarse materials such as No. 57 and No. 67. Fine screens were used over the perforations for relatively fine materials. There are two water chambers between the perforated plates and the ends of the box. The upstream water chamber is designed to distribute the inlet water evenly on the upstream face of the sample. The downstream chamber collects the water flowing through the sample.

One-centimeter thick flexible, closed-cell polypropylene foam sheets were glued to all sides of the sample cell except the two perforated end plates. This created a sample chamber with a 28.5 cm × 29.5 cm (11.2 inches × 11.6 inches) cross section. During compaction, the aggregate presses into the foam and the flexible material intrudes into the interstitial spaces to simulate adjacent coarse particles. A piece of foam was also glued to the inside of the lid to reduce short circuiting along the top of the sample and provide a gasket seal for the lid of the box.

A number of 9 mm diameter nylon studs were installed on the flange of the permeameter cell to align with holes in the lid. Stainless steel wing nuts are used to secure the lid and make the permeameter watertight. Two aluminum angles cross the lid surface and are firmly attached to the flange studs. They press the lid against the sample, preventing any volumetric change and eliminating short-circuiting along the top of the sample. Three vacuum outlets with valves are installed in the lid, with two in the top of the water chambers, and one in the top of the sample cell. They are used to attach a vacuum pump to evacuate the sample under full vacuum and improve the degree of saturation before making a measurement. The valves are closed when the vacuum line is disconnected.

The 5 cm (2 inches) diameter inlet and outlet standpipes are shown in Figure 4-2. The inlet standpipe has a valve and elbow on the lower end that can be removed from the short inlet pipe protruding from the bottom of the upstream water chamber. Double O-rings were installed on its lower end to provide a seal yet allow disassembly from the inlet pipe of the permeameter cell. The inlet standpipe is fitted with an adjustable overflow cup, which can be moved up and down along the standpipe. An O-ring installed on the inside of the overflow cup provides a water-tight seal with the standpipe. Overflow caught in the cup is carried to a drain by a flexible hose. There are a number of 1 cm holes at various heights in the inlet standpipe. Used with stoppers and the adjustable overflow cup, these holes are designed to change the water level in the inlet standpipe.

A short outlet standpipe with a valve and an elbow on its lower end can be removed from the short outlet pipe protruding from the bottom of the downstream water chamber. An O-ring is fitted on the inside of the bottom end of the standpipe so that the

joint with the outlet of the downstream water chamber remains sealed while rotating the standpipe to measure the outflow rate and alter the head difference.

Tap water is stored in a 1230-liter (325 gallon) tank to settle before passing via an intermediate hose to the base of the inlet standpipe. A valve in the hose can be used to adjust the flow.

In the standard permeability test methods, two piezometers are installed in the sample chamber and head differences are read from the piezometer levels. This reading is the true head difference in the sample between the two points at which the piezometers are inserted. However, the head difference measured between the two standpipes includes head losses occurring in the pipeline connections, valves, screens, perforated plates, etc. It introduces error if the head difference between the two standpipes is taken as the head difference of the sample. The error is significant when the flow rate is high.

Since the head differences were read directly from the water levels in the standpipes, they had to be calibrated to obtain the true head differences attributable to the sample. The head losses due to the system at different flow rates were measured, and then plotted versus the flow rates. This was done by measuring the head differences between the inlet and outlet pipes at different flow rates when the permeameter was filled with water only. This head loss was found to be linearly proportional to flow rate. The plot can be found in Appendix L. The relation for system head loss was obtained from the data sets as follows:

$$\Delta h_l = 0.000579Q(cm) \qquad 4.1$$

for Q in cm^3/s. The head loss due to the permeameter system can be found by substituting the measured flow rate into this equation. Therefore, the net head difference between the two ends of the sample was obtained by deducting the head loss due to the permeameter and the connections under a certain flow rate from the total head difference. The net head difference across the sample is caused by the resistance from the soil only. It is used to calculate the hydraulic conductivity of the soil.

A datum beam was constructed to measure the head differences between the inlet and outlet standpipes. An aluminum beam was constructed with a sensitive level bubble and clamp. It was attached to the two standpipes and taken as the datum for measuring the head difference between the inlet standpipe and the outlet standpipe. A dial gauge

with a precision of 0.0254 mm (0.001 inch) was used to measure small head differences by touching a pinpoint to the water surface in each overflow cup. A steel ruler with a precision of 0.254 mm (0.01 inch) was used to measure relatively large head differences.

A large bucket was used to catch the outflow, which was weighed on a balance with capacity of 13.6 kg (30 pounds) and precision of 0.0045 kg (0.01 pound). The permeameter sat on a platform scale with precision of 0.0045 kg (0.01 pound) to measure the mass of the system at different stages of the test. A stopwatch was used to record elapsed time of outflow. Water temperature was measured with a thermometer.

4.4 Outline of Procedure

The testing procedure is detailed in Appendix K. The major steps of the procedure include:

- Sieving and recombining to reach target gradation.
- Compaction.
- Saturation.
- Measuring head differences and flow rates under a range of gradients.
- Draining the sample.

During each test and before disassembling the system, the following data was recorded:

- M1: The mass of the dry permeameter cell without the lid and the standpipes.
- M2: The wet mass of the empty permeameter cell without the lid and the standpipes.
- M3: The mass of the permeameter full of water with the lid, the standpipes and the connections. The water levels in the upright standpipes are at the bottom of the hole in the overflow cup on the outlet standpipe.
- M4: The mass of the dry sample after compaction in the dry permeameter cell without the lid and the standpipes.
- M5: The mass of the permeameter and the saturated sample with the lid, the standpipes and the connections. The water levels in the upright

standpipes are at the bottom of the hole in the overflow cup on the outlet standpipe.

- M6: The mass of the sample after draining in the permeameter cell without the lid and the standpipes.

4.5 Data Interpretation

1. Calculation of Volumetric Flow Rates and Hydraulic Gradient

Mass flow rates were first converted to volumetric flow rates using the following equation

$$Q_v = \frac{Q_w}{\rho_w} = \frac{M}{\rho_w \cdot \Delta t} \qquad 4.2$$

where M = mass of water.

Then, q and i were calculated with equations given previously:

$$q = \frac{Q}{A}$$

$$i = \frac{\Delta h}{L}$$

2. Plot of q vs. i

Values of q vs. i were plotted to obtain hydraulic conductivity. By visualizing the plot, the curve can be distinguished into two parts, a linear part and a nonlinear part. Figure 4-4 shows a typical plot. The hydraulic conductivity is the slope of the linear part of the curve. The slope can be obtained by performing a linear regression for the data points on the linear part. Typical test data are shown in Table 4-3.

3. Plot of i/q vs. q

i/q vs. q was plotted to obtain the upper limits of hydraulic gradient and specific discharge for linear laminar flow. Refer to Figure 4-5 for a typical plot of i/q vs. q. The curve consists of two parts, a horizontal line and a sloped straight line. The horizontal line represents the linear flow that observes Darcy's Law. The sloped straight line represents the nonlinear laminar flow. The intersecting point of the two lines is the critical point distinguishing the two flow regions. The specific discharge of this point,

Table 4-3: Hydraulic conductivity testing data & results of P_M_304_L_N.

Hydraulic Conductivity Testing Data & Results

Test Identification **PM57LN**

Data

Item	Data	Unit		Delta H,cm	t, sec.	Water, V, cm^3
Sample Length	11.844	inch				
Sample Height	11.594	inch		0.2286	116	9090.00
Sample Width	11.813	inch		0.3175	82.63	9090.00
				0.396875	61.16	9090.00
Dry weight of permeameter box	21.2	lb		0.5842	60.91	9090.00
Wet weight of permeameter box	21.6	lb		0.714375	53.19	9090.00
Saturated weight of system w/ water	130.8	lb		0.7874	44.53	9090.00
				0.873125	48.41	9090.00
Dry soil with box	115.3	lb		1.031875	45.93	9090.00
Saturated weight of system w/ soils	191.6	lb		1.1509375	44.99	9090.00
Wet weight of soils w/box after drain	120.2	lb		1.3462	56.38	14089.50
Water temperature T	21	Degree C				

Results

Dry Density	99.2378	lb/ft^3
Degree of Saturation	1.038	
Porosity	0.432	
Effective Porosity	0.356	
Void Ratio	0.762	
Hydraulic Conductivity, K	12.526	cm/s
	35506.5	ft/day
The Upper Limit of Hydraulic Gradient	0.012	

Hydraulic Conductivity at 20 degree

K_20 =	12.227	cm/s
	34658.6	ft./day

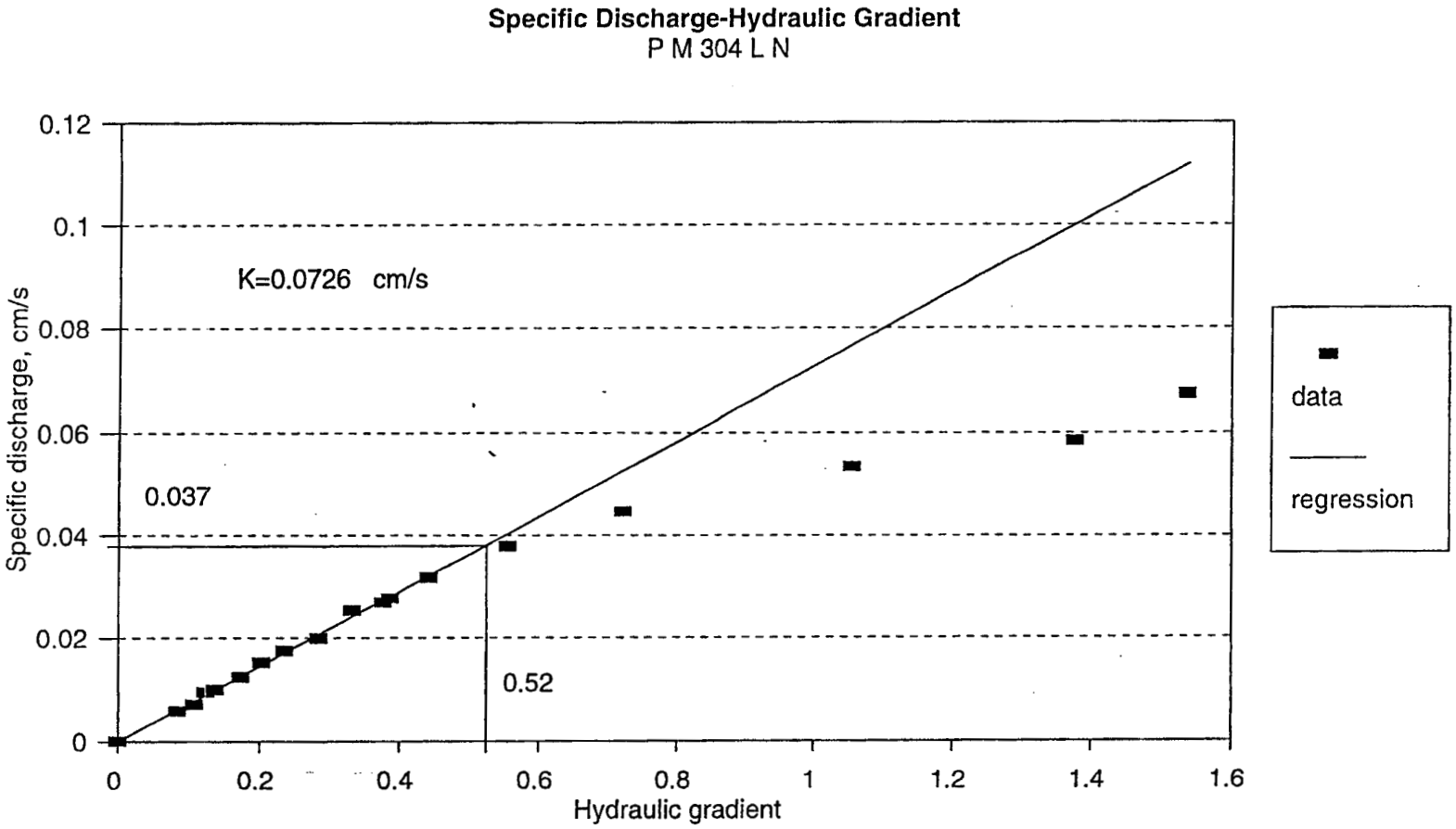

Figure 4-4: q-i plot of middle-grading limestone ODOT 304.

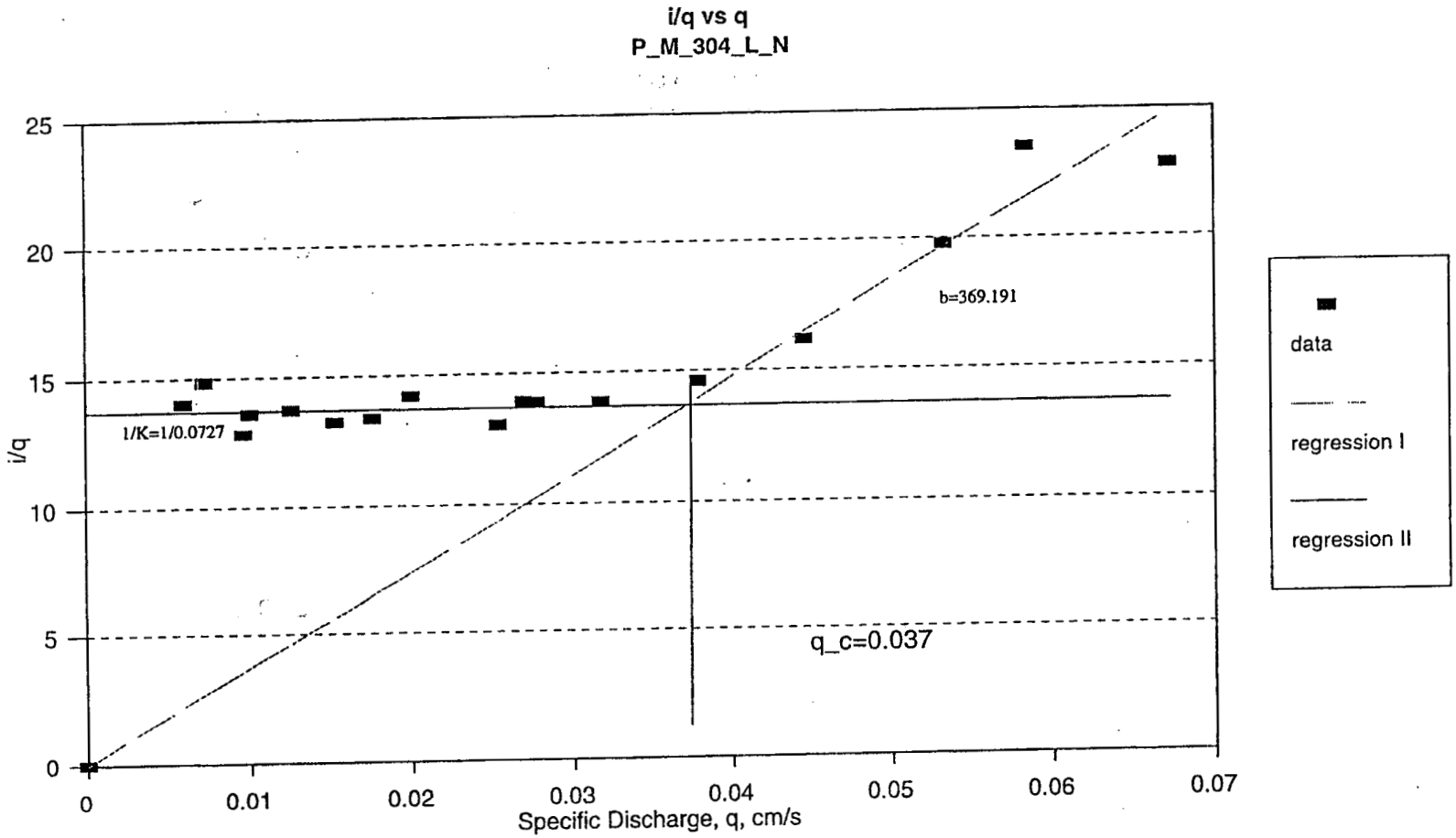

Figure 4-5: i/q vs. q of middle-grading limestone ODOT 304.

q_c, was plotted on the q vs. i plot seen in Figure 4-4. The hydraulic gradient corresponding to q_c is the upper limit of hydraulic gradient for linear laminar flow.

4. Calculation of Degree of Saturation

The degree of saturation was estimated using the equation

$$S_r = \frac{V_w}{V_v} = \frac{M_w}{\rho_w V_v} = \frac{M_{tot} - M_e + V\rho_w - M_s}{V\rho_w - \frac{M_s}{G}} \qquad 4.3$$

where:

$$M_{tot} = M5$$

$$M_e = M3$$

and M3 and M5 are defined in section 4.4. V is the volume of the sample cell. Specific gravity values and moisture contents of all samples were tested before the calculation of degree of saturation. Dry soil mass (oven-dried base) was obtained as follows

$$M_s = \frac{M4 - M1}{1 + \omega} \qquad 4.4$$

where M4 and M1 are as defined in section 4.4.

ω is the moisture content of the sample.

With data of all parameters in the right side of Equation 4.3, degree of saturation can be calculated.

5. Calculation of Porosity

Porosity was estimated using the following equation

$$n = \frac{V_v}{V} = \frac{V\rho_w - \frac{M_s}{G}}{V} \qquad 4.5$$

6. Calculation of Effective Porosity

Effective porosity was approximated as follows

$$n_e = \frac{M_{ms} - (M6 - M2)}{\rho_w V} \qquad 4.6$$

where M_{ms} is the mass of saturated soil sample including soil and the water filling voids:

$$M_{ms} = M_{tot} - (M_e - V\rho_w) \qquad 4.7$$

M6-M2 represents the soil mass after draining. M6 and M2 were defined in section 4.4. This definition of effective porosity is consistent with Moulton (1980).

4.6 Modifications for Stabilized Materials

4.6.1 *Portland cement stabilized materials*

To compare laboratory test results with the field test results, the mix design used in the field construction was used in the laboratory. The minimum requirement of cement content was 130.5 kg/cubic meters (220 pounds per cubic yard). The water/cement ratio by weight was 0.36, exclusive of that absorbed by the aggregates. The mix design calculations are presented in Table 4-4. The Portland cement stabilized aggregate used in the field was No. 57 limestone with an as-built unit weight found to be 15.3 kN/m^3 (97.7 pcf). First, the air volume percentage of the field mixture was calculated. Using the same air volume percentage for No. 57 limestone (middle grading), the weight of aggregates for 1 cubic foot of stabilized limestone was calculated as 43.3 kg (95.4 pounds). Compared to its maximum unstabilized dry density (59.5 kg/cubic meter or 100.2 pounds per cubic foot) obtained in the laboratory, the amount of limestone in 1 unit volume of concrete based on the field mix design was 95.2% of the maximum amount of non-stabilized limestone.

No field sections were constructed from slags, gravels or No.67 limestone. Assuming 95.2% as the ratio of the amount of aggregate in 1 unit volume of Portland cement stabilized base to the maximum dry density of non-stabilized base, the amounts of aggregate for slags, gravels and No.67 limestone were approximated by multiplying their maximum dry density by 95.2%. Then, the amount of cement and water were calculated. The percentages of voids were also calculated for the mixtures. This is equivalent to withdrawing 4.8% of the aggregate from a compacted non-stabilized sample and substituting 130.5 kg/cubic meters of cement and water (8.15 pounds per cubic foot). The cement and water can also occupy some of the permeable voids in the aggregate. Compared with the void space between particles in a non-stabilized sample,

Table 4-4: Mix design for 1 cubic foot of Portland cement stabilized bases and subbases.

		Moist Content %	Absorption %	Bulk S.G. Aggregate	Compacted Agg. Density,lb/ft^3	Aggr./(ft^3-concret.) lb/ft^3(Natural)	Cement lb/ft^3	Water to add lb/ft^3	Air volumn %	Non-Stab. Voids%
Field	ODOT 57	1.86	1.64	2.64		95.56	8.15	2.73	34.53	43.05
Limestone	ODOT 57_C	1.01	1.79	2.67	97.7	92.95	8.15	3.31	35.22	41.86
	ODOT 57_M	1.01	1.65	2.67	100.2	95.40	8.15	3.23	34.53	40.50
	ODOT 57_F	1.01	1.51	2.68	101.0	96.14	8.15	3.17	33.88	40.22
	ODOT 67_M	1.01	1.65	2.67	100.5	95.60	8.15	3.24	33.92	40.38
SLAG	ODOT 57_C	1.78	2.48	2.23	80.7	76.85	8.15	3.18	36.51	42.99
	ODOT 57_M	1.78	2.52	2.21	82.9	78.88	8.15	3.14	34.63	40.95
	ODOT 57_F	1.78	2.56	2.19	83.5	79.48	8.15	3.15	33.68	39.98
	ODOT 67_M	1.78	2.52	2.21	84.0	79.99	8.15	3.15	33.82	40.12
Gravel	ODOT 57_C	1.87	5.24	2.60	106.7	101.54	8.15	3.87	28.11	35.35
	ODOT 57_M	1.87	5.36	2.59	109.5	104.22	8.15	4.17	25.97	33.59
	ODOT 57_F	1.87	5.47	2.59	101.0	96.14	8.15	4.24	30.71	38.69
	ODOT 67_M	1.87	5.36	2.59	107.6	102.40	8.15	4.10	27.18	34.75

Water/Cement 0.36

Weight in 1-ft^3 concrete/Maximun non-stabilized density 0.95

the introduction of cement and water to substitute for 4.8% of the aggregate does not reduce the void ratio significantly.

The samples were mixed using conventional techniques. The compaction effort was adjusted to simulate field conditions as mentioned in Appendix K for unstabilized aggregates. The sample length was reduced to half that of non-stabilized samples (15 cm) to facilitate the preparation of samples. They were compacted in wooden molds lined with polypropylene foam sheets to approximate field boundary conditions around the sample. After 24 hours of curing, the samples were removed with the foam sheets attached and placed into the permeameter for testing.

An impermeable concrete block wrapped with foam sheets was made using the same procedure. It was positioned in the permeameter to test the foam's ability to prevent short circuiting around the sample. Various head differences were applied across the concrete block. Water flowed out of the downstream standpipe although the block was theoretically impermeable. This was due to leakage between the foam sheets wrapped around the sample and the inside of the permeameter. The leakage rates were calibrated at different applied head differences. The data were plotted (Appendix L) and leakage rates were found to be linearly proportional to the driving hydraulic gradient in the range of 0 to 2.5. This was used to calculate the leakage rate at any applied head difference. Assuming the same leakage occurs when all other tests were performed, the calculated leakage rates were deducted from the total flow rates. The leakage rates were approximately 0.3 % of the total flow rates for the stabilized materials tested.

4.6.2 *Asphalt stabilized materials*

Published field tests on asphalt stabilized bases identified the requirement of asphalt percentage by weight as 2.3% of the total weight of the mixture. This was also used to prepare laboratory samples for testing. Taking the maximum dry density of non-stabilized aggregates as the amount of aggregate contained in 0.0283 cubic meter (1 cubic foot) of asphalt stabilized bases, the amount of asphalt needed in 0.0283 cubic meter (1 cubic foot) was calculated. The required amount of mixture was prepared for each sample, allowing 5 percent loss of materials during mixing. Compactive effort was

adjusted to fill the sample mold with this required amount of materials flush to the top of the mold without over-using or under-using material. The asphalt stabilized aggregate used in the field was No. 57 limestone with an as-built unit weight found to be 16.2 kN/m^3 (103.2 pcf). The mix designs for 0.0283 cubic meter (1 cubic foot) of stabilized materials are shown in Table 4-5.

Table 4-5: Mix design for 1 cubic foot of asphalt stabilized materials

Asphalt Percentage **2.3%**

		Compacted Agg. Density,lb/ft^3	Mix weight lbs	Asphalt lbs
Limestone	ODOT 57_C	97.7	100.0	2.30
	ODOT 57_M	100.2	102.6	2.36
	ODOT 57_F	101.0	103.4	2.38
	ODOT 67_M	100.5	102.8	2.36
Slag	ODOT 57_C	80.7	82.6	1.90
	ODOT 57_M	82.9	84.8	1.95
	ODOT 57_F	83.5	85.5	1.97
	ODOT 67_M	84.0	86.0	1.98
Gravel	ODOT 57_C	106.7	109.2	2.51
	ODOT 57_M	109.5	112.1	2.58
	ODOT 57_F	101.0	103.4	2.38
	ODOT 67_M	107.6	110.1	2.53

The temperature during mixing and placement was 110° C (230° F), 17° C (30° F) higher than used in field mixing. This was done to account for heat loss during mixing such a small amount of material. Other procedures were similar to those for Portland cement stabilized materials.

4.6.3 *Data Output*

The saturation procedure developed during testing non-stabilized materials was carefully followed. This procedure produced degrees of saturation from 90% to 100% (Table 4-4). The degrees of saturation of stabilized materials were not determined.

However it is believed that satisfactory saturation was obtained during testing. The density was measured after compacting. Laboratory specimens closely matched the as-built compacted density for both types of stabilized bases, which is an important factor affecting the value of the hydraulic conductivity.

4.7 Testing of Drainage

Data of drainage rates of most samples were collected by recording the overall system weight with time while draining the samples. System weight was plotting against the elapsed time. Typical plots are presented and discussed in section 4.10.

4.8 Discussion of Results for Non-Stabilized Materials

The test results for ODOT 304 limestone (middle grading) are presented in detail as a representative example of all results. The data and output are listed in Table 4-3. The plot of specific discharge (q) versus hydraulic gradient (i) is in Figure 4-4. i/q is plotted versus q in Figure 4-5. The q-i relationship is linear before i reaches 0.52 and q reaches 0.037, which are the critical hydraulic gradient and critical specific discharge for linear laminar flow, respectively. The slope of the linear portion of the q-i line is the value of Darcy's hydraulic conductivity, which is 0.0727 cm/s. When the applied hydraulic gradient exceeds i_{upper} = 0.52, the q-i relation deviates from linear to non-linear flow. The relationship is similar to the one predicted theoretically in Figure 2-1.

q_c in Figure 4-5 is the critical specific discharge dividing linear and nonlinear flow regimes. Again, it is equal to 0.037. When specific discharge is less than this value, the i/q-q relation observes

$$\frac{i}{q} = \frac{1}{0.0727} = \frac{1}{K} \qquad 4.8$$

Taking q_c=0.037 back to Figure 4-4, the corresponding hydraulic gradient is the critical hydraulic gradient. In this example, the upper limit of hydraulic gradient for linear flow is 0.52. This is a typical example of other tested samples. The results and plots of other laboratory testing can be found in Appendices M, N, O and P.

4.8.1 Result comparison between different gradation types

The results of hydraulic conductivity tests for non-stabilized materials are listed in Table 4-6. For some gradation types, only middle grading samples were investigated while for others the fine, middle and coarse grading were all tested. To facilitate the comparison of hydraulic conductivity between different gradation types, the hydraulic conductivity of middle grading is taken as a representative value for each type of gradation envelope. The variation of hydraulic conductivity within each type of gradation envelope is also discussed below. Relating this variation to the width of the gradation envelope, a relative envelope width at D10 is defined as

$$W_{D10} = \frac{D10_C - D10_F}{D10_F} 100\% \qquad 4\text{-}9$$

where $D10_C$ is the effective grain size of the coarse grading of a gradation envelope, and

$D10_F$ is the effective grain size of the fine grading of a gradation envelope.

Also, the relative variation of hydraulic conductivity within a gradation envelope is defined as

$$W_K = \frac{K_C - K_F}{K_F} \qquad 4\text{-}10$$

where K_C is the hydraulic conductivity of the coarse grading sample in a gradation envelope, and

K_F is the hydraulic conductivity of the fine grading sample in a gradation envelope.

The relative envelope width at D10 of each type of gradation and the relative variation of K are calculated and listed in Table 4-6.

Table 4-6: Test results for non-stabilized materials

Type	Grading	D10	D60	Cu	W_D10	Density	Sat.Deg.	K_20		W_K	i_upper
		mm	mm		%	lb/ft^3		cm/s	ft/day		
310_L	F	0.072	0.7	9.7		118.6	101.8%	0.01	20		
310_L	M	0.1	4	40.0	108.0%	128.2	101.3%	0.04	102	634.0	0.650
310_L	C	0.18	18	100.0		124.0	94.5%	4.45	12,600		
310_G	F	0.072	0.7	9.7		117.5	94.9%	0.01	14		
310_G	M	0.1	4	40.0	108.0%	124.9	92.4%	0.01	31	488.7	
310_G	C	0.18	18	100.0		123.4	91.3%	2.45	6,940		0.041
310_S	F	0.072	0.7	9.7		113.9	96.9%	0.01	23		
310_S	M	0.1	4	40.0	108.0%	115.4	88.4%	0.27	757	576.7	0.190
310_S	C	0.18	18	100.0		96.1	97.8%	4.63	13,100		0.027
304_L	F	0.06	4.5	75.0		131.6	90.5%	0.04	111		0.075
304_L	M	0.12	12.7	105.8	100.0%	130.6	98.3%	0.07	201	9.6	0.520
304_L	C	0.18	21	116.7		125.3	96.8%	0.42	1,170		0.230
304_G	F	0.06	4.5	75.0		126.1	105.2%	0.02	60		
304_G	M	0.12	12.7	105.8	100.0%	126.2	95.9%	0.41	1,150	94.4	0.090
304_G	C	0.18	21	116.7		123.7	95.1%	2.01	5,680		0.048
304_S	F	0.06	4.5	75.0		120.8	72.6%	0.03	91		1.100
304_S	M	0.12	12.7	105.8	100.0%	109.1	94.6%	0.55	1,570	139.0	0.160
304_S	C	0.18	21	116.7		95.5	103.8%	4.51	12,700		0.023
57_L	M	5.2	16	3.1		99.2	103.8%	12.23	34,600		0.012
57_G	M	5.2	16	3.1		107.5	98.4%	11.95	33,800		0.014
57_S	F	4.8	13	2.7		82.1	92.2%	15.57	44,100		0.010
57_S	M	5.2	16	3.1	42.3%	81.4	92.8%	19.89	56,300	0.5	0.011
57_S	C	7	19	2.7		79.3	98.8%	23.88	67,600		0.007
67_L	M	5.2	12.5	2.4		99.4	101.3%	16.96	48,000		0.006
67_G	M	5.2	12.5	2.4		105.6	99.9%	9.47	26,800		0.018
67_S	M	5.2	12.5	2.4		82.6	95.0%	19.57	55,400		0.007
N.J.Mix_L	M	1.8	8.5	4.7		108.4	93.5%	2.63	7,450		0.070
N.J.Mix_G	M	1.8	8.5	4.7		109.4	94.9%	1.64	4,640		0.052
N.J.Mix_S	M	1.8	8.5	4.7		93.8	86.8%	2.86	8,100		
IW.Mix_L	F	0.13	6	46.2		121.0	90.2%	0.47	1,320		0.250
IW.Mix_L	M	0.4	11	27.5	517.5%	118.1	98.5%	0.89	2,530	6.5	0.170
IW.Mix_L	C	2.2	16	7.3		106.0	92.7%	3.48	9,850		0.042
IW.Mix_G	F	0.13	6	46.2		128.2	91.0%	0.23	649		0.250
IW.Mix_G	M	0.4	11	27.5	517.5%	124.0	95.9%	2.38	6,730	27.3	0.037
IW.Mix_G	C	2.2	16	7.3		114.9	98.6%	6.52	18,400		0.016
IW.Mix_S	F	0.13	6	46.2		107.1	95.4%	1.39	3,930		0.050
IW.Mix_S	M	0.4	11	27.5	517.5%	98.1	90.6%	3.10	8,790	5.4	0.038
IW.Mix_S	C	2.2	16	7.3		87.9	101.2%	8.89	25,200		0.015

For comparison, one can classify all samples into three groups based on their magnitude of hydraulic conductivity at the middle grading (see Table 4-7).

Table 4-7: Gradation Groups Based On Ranges of Hydraulic Conductivity Values

Groups	Gradation Types	K of Middle Grading, ft/day
Group 1	ODOT 304, ODOT 310	less than 2000
Group 2	N.J. Mix, Iowa Mix	from 2000 to 10000
Group 3	No. 57, No. 67	greater than 10000

The Group 1 types are traditional gradation types for base and subbase materials. ODOT 304 and ODOT 310 are very similar to each other, based on their grain size distribution curves, which may be found in Appendix L. The D10 values of Group 1 are all less than 0.2 mm, but they contain a wide range of particles as indicated by their coefficient of uniformity in Table 4-6. For their fine grading and middle grading, the values of hydraulic conductivity are all less than 2000 ft/day. However, the hydraulic conductivity for the coarse grading is much higher. The K value for ODOT 310 ranges from 0.007 cm/s (20 ft/day) to 4.2 cm/s (12000 ft/day). This variation is very large compared to other gradation types. This is attributed to its wide envelope of gradation specification as indicated by the value of relative envelope width at D10, which is the largest value among all types of gradations studied. The K value of the middle grading sample is far lower than the average K value of the fine and coarse gradings. Note that the variation of hydraulic conductivity within a gradation envelope is nonlinear. Such a large variation of K value within a gradation envelope further confirms that satisfying a gradation specification does not automatically satisfy drainage requirements.

The D10 value of Group 3 middle grading reaches 5.2 mm, which is over one order of magnitude higher than the other Groups. Group 3 K values are the highest among the three groups. The variation of K in the gradation envelope is much lower than Group 1 or Group 2. Group 3 has the lowest value of relative envelope width at D10, as indicated in Table 4-6. All Group 2 values are in between those of Group 1 and Group 3.

The discussion above shows that the gradation types with high values of D10 have high values of hydraulic conductivity. D10 is an important parameter used in Hazen's Formula as well as Moulton's chart to predict hydraulic conductivity. The values of hydraulic conductivity for nonstabilized materials obtained in this research were plotted against their D10 in Figure 4-6. In addition, the predicted values from Hazen's empirical equation were plotted. Generally, K values increase with D10 in a nonlinear trend. Local deviation occurs as D10 increases, without altering the overall trend. Local deviation can be ascribed to the variation of compaction effort, degree of saturation and particle shape and texture. As shown, Hazen's formula matches the tested values well when D10 is in the range between 1.8 and 2.2. It predicts a lower value for D10 less than 0.5 mm and a higher value when D10 is over 2.2 mm.

In Cedergren's chart (Figure 2-8), two gradation curves in the open-graded group have close values of D10 but have far different values of K due to the different uniformity of the grain size distribution curves. The one with a lower D60 value has a K value of 4.9 cm/s (14,000 ft/day), and the one with higher value of D60 has a value of 7.1 cm/s (20,000 ft/day). This indicates that D60 also has an effect on hydraulic conductivity. The K values obtained in this study were also plotted against their D60 values (Figure 4-7). K tends to increase with D60, but the curve shows an irregular shape at large D60 values. Therefore, D60 cannot be uniquely related to hydraulic conductivity, while D10 shows a more direct relation to hydraulic conductivity in Figure 4-6.

The plot of hydraulic conductivity against the product of D10 by D60 is shown in Figure 4-8. The introduction of D60 does not change the general trend of Figure 4-6. This reveals that D10 has a major effect on the K values and the effects of D60 on K are secondary. Empirical prediction using D10 to describe the effect of grain size distribution on hydraulic conductivity, such as Hazen's equation, provides an expedient way to predict hydraulic conductivity. However, the accuracy is undermined due to its simplicity as indicated in Figure 4-6 and Jones and Jones (1989). The introduction of D60 certainly describes the grain size distribution better than relying on D10 solely. Considering D60 or the coefficient of uniformity together with D10 may provide a better means of predicting hydraulic conductivity. Compared to the linear regression of the

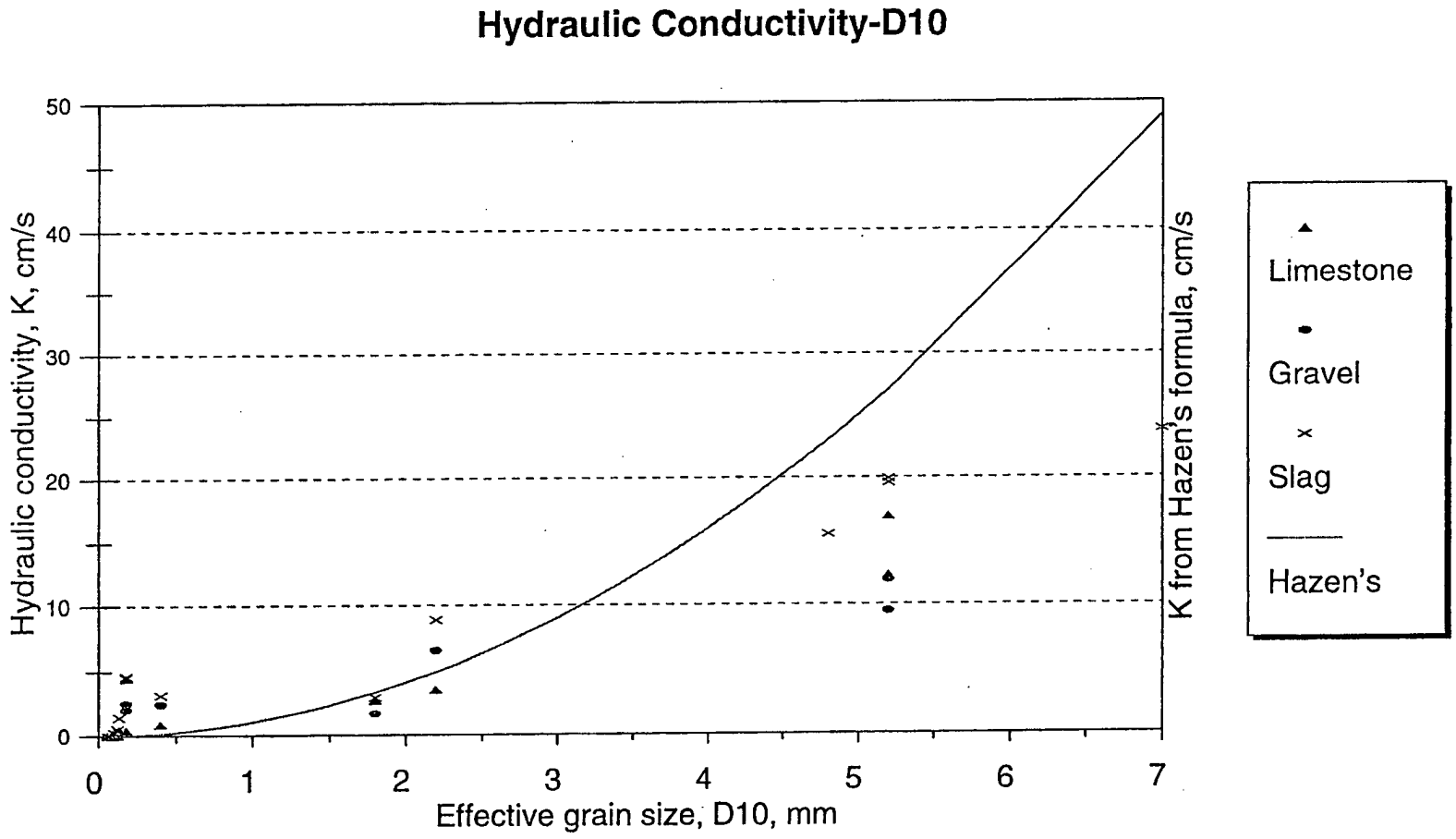

Figure 4-6: The plot of hydraulic conductivity against effective grain size

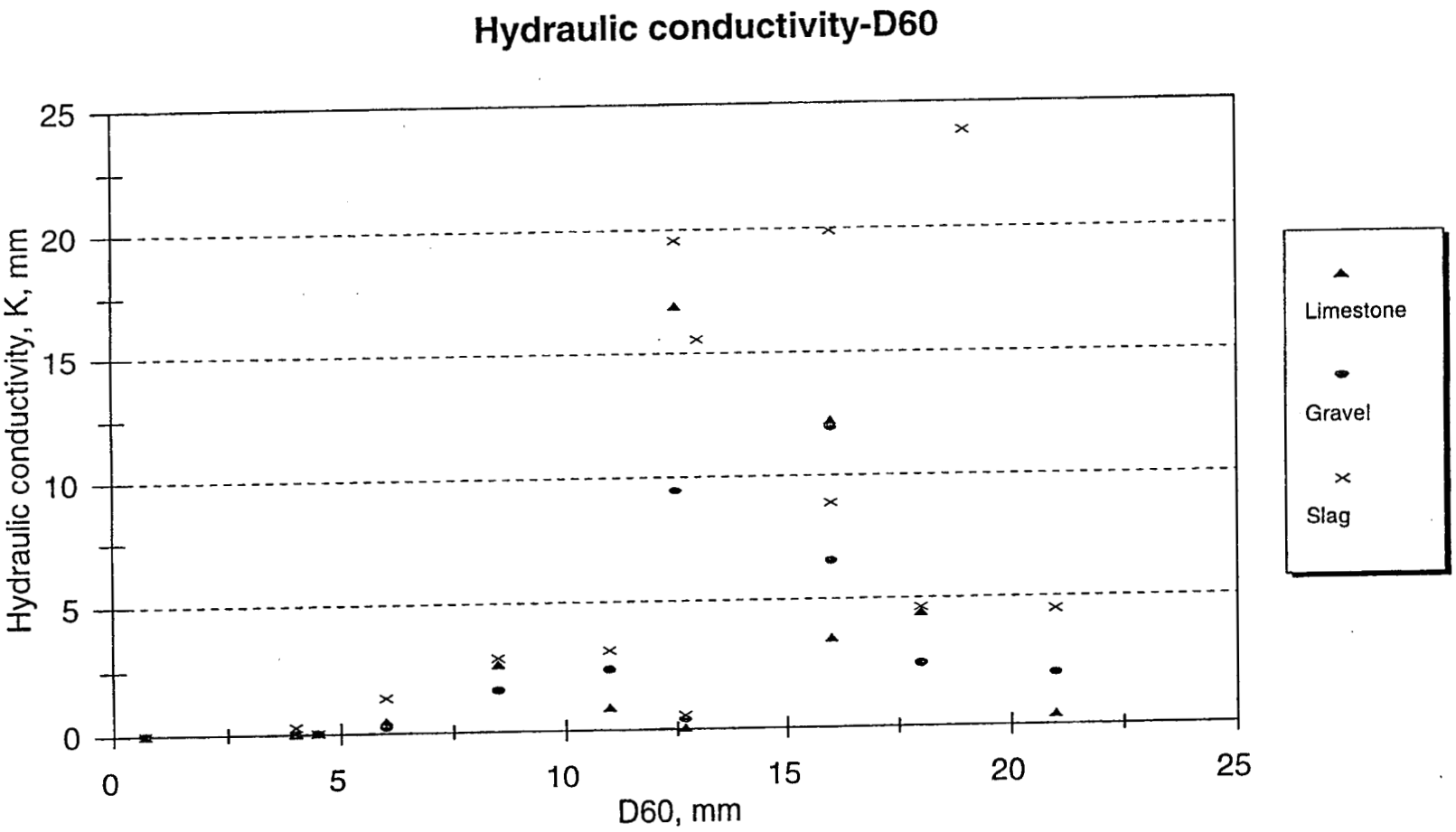

Figure 4-7: The plot of hydraulic conductivity against D60

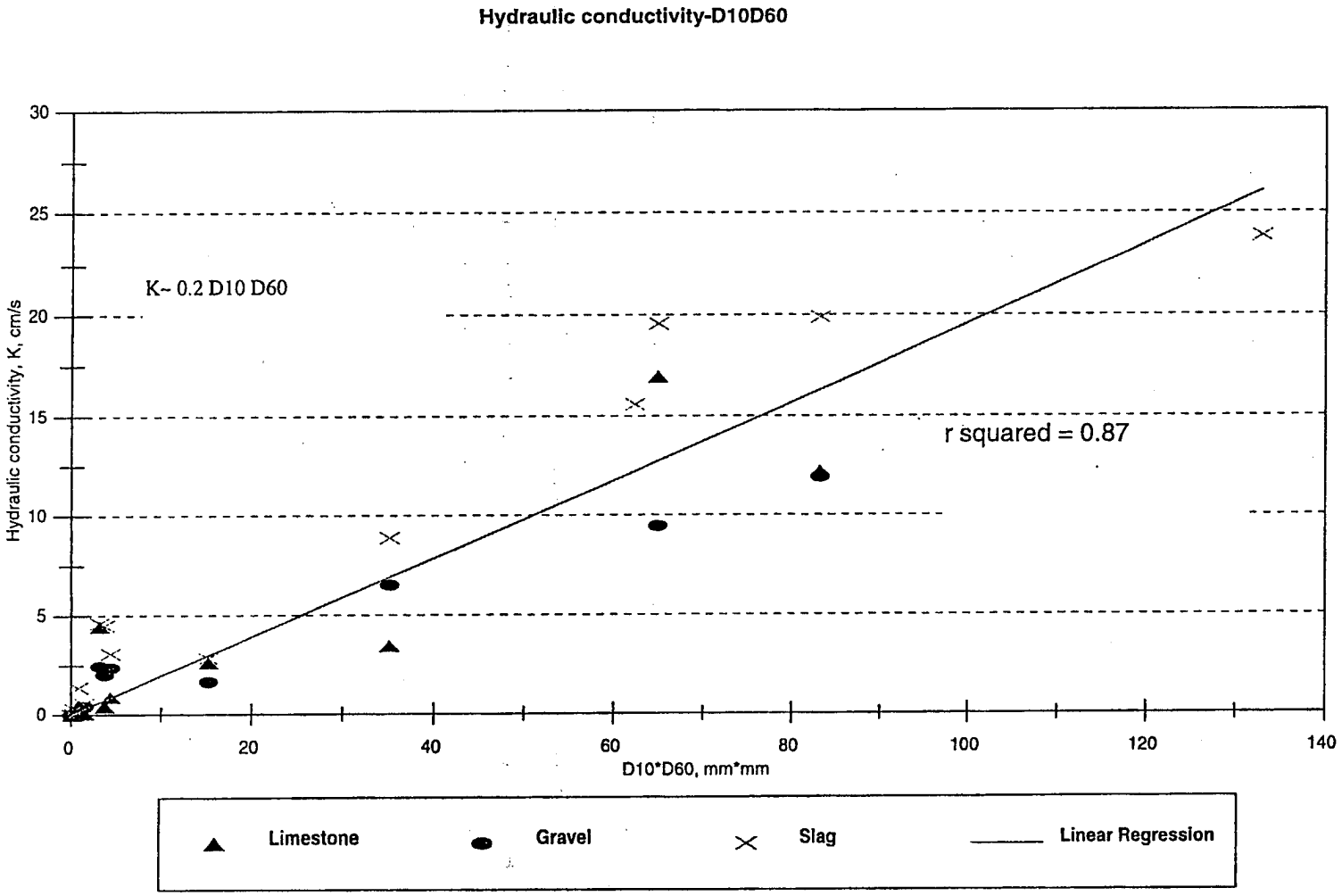

Figure 4-8: The plot of hydraulic conductivity against the multiplicand of D10 by D60

available data as shown in Figure 4-8, hydraulic conductivity was related to the product of D10 by D60 as follows with a R^2 value of 0.87.

$$K \cong 0.2D10 \cdot D60 \qquad 4\text{-}11$$

The units of D10 and D60 are millimeters. The units of K are cm/s. However, the correlation of D10 and D60 to hydraulic conductivity needs to be further investigated.

4.8.2 Comparison of results between material types

It can be observed that for the same grading, the values of hydraulic conductivity of slags are always higher than those of limestones and gravels. For No. 57, 67 and 310 and the NJ Mix, limestones had a higher value of hydraulic conductivity than those of gravels. For ODOT 304 and the Iowa Mix, gravels have higher values of hydraulic conductivity than limestone aggregates.

Gravels have relatively round shapes and smooth surfaces. The shapes of slags are angular, and the surfaces are rough with numerous permeable voids. Limestones are also angular, but the smoothness of the surfaces are between gravels and slags. Angular shapes make the flow paths more tortuous and rough surfaces create frictional resistance to flow. Both angular shape and rough surface play an adverse effect on hydraulic conductivity. Slags are the most likely to have an adverse effect of shape and texture on hydraulic conductivity, limestones rank second, and gravels provide the most smooth path for flow. Considering only the effect of shape and texture, gravel should provide the highest conductivity, then limestone and slags. However, the results show a reverse order.

Hydraulic conductivity depends on both soil matrix and fluid properties. Since the hydraulic conductivities in Table 4-6 have been standardized to the same temperature, the differences of hydraulic conductivities are due to soil matrix properties. These are grain size distribution, void ratio and particle shape and texture. For two samples with the same gradation curve but different material types, the differences of hydraulic conductivities must be due to void ratio, particle shape and texture. The effect of void ratio in addition to particle shape and texture needs to be considered.

Compaction effort affects void ratio. Usually, dry density after compaction is taken as an index of compaction efficiency. The dry densities of slag samples are the

lowest among the three types of materials for the same grading. The dry densities of gravel samples tend to be higher than limestone, except for ODOT 304 and ODOT 310. Plotting the values of hydraulic conductivity against dry density in Figure 4-9, it is found that overall, the K values decrease with increasing dry density, but some data points show significant deviation from this descending trend.

Dry density is a good indication of void ratio for the same type of material. For different types of materials, this distinction is blurred by the discrepancy of specific gravity between different types of materials. This is the reason for much of the scatter in Figure 4-9. The void ratio of each sample was calculated using bulk specific gravity and included with hydraulic conductivity in Table 4-8. The void ratios of 13 out of 14 slag samples are higher than their identical gradation counterparts of limestone or gravel. This explains why the hydraulic conductivity of slags are higher than other materials with the same gradation curve.

For ODOT 310, fine grading and middle grading of gravels have higher void ratios but lower K values than fine and middle grading of limestones while coarse grading of gravels has a lower value of void ratio and a lower value of hydraulic conductivity. The differences of hydraulic conductivity between samples with the same gradations are within one order of magnitude. For ODOT 304, gravels have higher void ratios and higher K values than limestones. For No. 57, 67 and the NJ Mix, limestones have higher void ratios and higher K values than their gravel counterparts. For the Iowa Mix, middle and coarse grading of limestones have higher void ratios and lower K values than their identical gravel counterparts while the fine grading of limestone has a higher void ratio and higher value of hydraulic conductivity than its gravel opponent. Hydraulic conductivity is positively related to void ratio. Samples of ODOT 304, No. 57, No. 67, NJ Mix, fine grading of Iowa Mix, and coarse grading of ODOT 310 all observe this relation. However, the fine and middle grading of ODOT 310 and the middle and coarse grading of Iowa mix do not comply with this relation.

The fine and middle grading of ODOT 310 are relatively fine materials, and the difference of K between similar samples of gravels and limestone are within a half

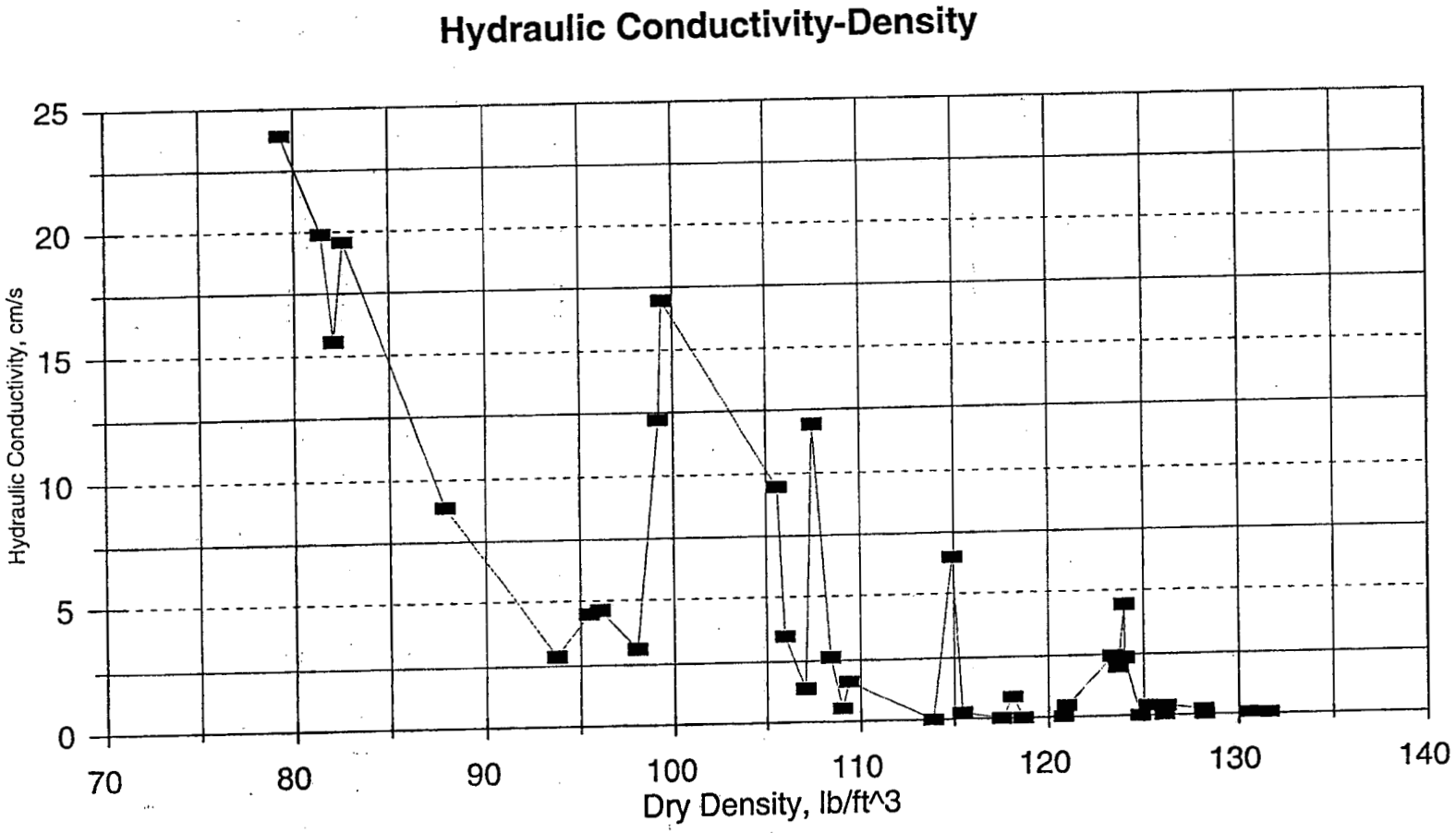

Figure 4-9: Hydraulic conductivity vs. dry density

Table 4-8: Hydraulic conductivity with void ratio

Type	Gradation	D10	Density		BK,S.G.	Void ratio	Sat.Deg.	K_20	
		mm	lb/ft^3	Kg/m^3				cm/s	ft/day
310_L	F	0.072	118.6	1901	2.53	33.2	101.8%	0.007	20
310_L	M	0.1	128.2	2054	2.59	25.8	101.3%	0.036	102
310_L	C	0.18	124.0	1987	2.64	32.9	94.5%	4.451	12,617
310_G	F	0.072	117.5	1883	2.63	39.5	94.9%	0.005	14
310_G	M	0.1	124.9	2000	2.61	30.6	92.4%	0.011	31
310_G	C	0.18	123.4	1977	2.60	31.5	91.3%	2.450	6,945
310_S	F	0.072	113.9	1824	2.65	45.1	96.9%	0.008	23
310_S	M	0.1	115.4	1849	2.46	32.8	88.4%	0.267	757
310_S	C	0.18	96.1	1539	2.29	48.7	97.8%	4.634	13,136
304_L	F	0.06	131.6	2108	2.59	22.7	90.5%	0.039	111
304_L	M	0.12	130.6	2092	2.61	24.9	98.3%	0.071	201
304_L	C	0.18	125.3	2007	2.64	31.3	96.8%	0.416	1,179
304_G	F	0.06	126.1	2020	2.61	29.3	105.2%	0.021	60
304_G	M	0.12	126.2	2022	2.61	28.9	95.9%	0.409	1,159
304_G	C	0.18	123.7	1982	2.60	31.2	95.1%	2.005	5,683
304_S	F	0.06	120.8	1935	2.45	26.4	72.6%	0.032	91
304_S	M	0.12	109.1	1747	2.37	35.7	94.6%	0.554	1,570
304_S	C	0.18	95.5	1530	2.31	50.7	103.8%	4.513	12,793
57_L	M	5.2	99.2	1590	2.67	68.1	103.8%	12.227	34,659
57_G	M	5.2	107.5	1722	2.59	50.6	98.4%	11.947	33,866
57_S	F	4.8	82.1	1315	2.23	69.6	92.2%	15.574	44,147
57_S	M	5.2	81.4	1304	2.21	69.4	92.8%	19.890	56,381
57_S	C	7	79.3	1271	2.19	72.3	98.8%	23.881	67,694
67_L	M	5.2	99.4	1593	2.67	67.7	101.3%	16.956	48,064
67_G	M	5.2	105.6	1692	2.59	53.3	99.9%	9.470	26,844
67_S	M	5.2	82.6	1323	2.21	67.0	95.0%	19.573	55,483
N.J.Mix_L	M	1.8	108.4	1737	2.61	50.2	93.5%	2.630	7,455
N.J.Mix_G	M	1.8	109.4	1752	2.61	48.8	94.9%	1.638	4,643
N.J.Mix_S	M	1.8	93.8	1502	2.39	58.8	86.8%	2.861	8,110
IW.Mix_L	F	0.13	121.0	1938	2.60	34.0	90.2%	0.469	1,329
IW.Mix_L	M	0.4	118.1	1892	2.62	38.4	98.5%	0.893	2,531
IW.Mix_L	C	2.2	106.0	1698	2.64	55.5	92.7%	3.476	9,853
IW.Mix_G	F	0.13	128.2	2054	2.61	27.1	91.0%	0.229	649
IW.Mix_G	M	0.4	124.0	1987	2.61	31.1	95.9%	2.375	6,732
IW.Mix_G	C	2.2	114.9	1841	2.60	41.2	98.6%	6.516	18,471
IW.Mix_S	F	0.13	107.1	1715	2.42	40.9	95.4%	1.388	3,934
IW.Mix_S	M	0.4	98.1	1571	2.36	49.8	90.6%	3.101	8,790
IW.Mix_S	C	2.2	87.9	1408	2.30	62.9	101.2%	8.892	25,206

order of magnitude. The deviation between two pairs of ODOT 310 samples can be explained by the fact that the degree of saturation of the two limestone samples are higher than the two gravel samples and it overrides the effect of void ratio. The deviation between two pairs of the Iowa mix is uncertain. Possible reasons include measurement error and inherent variability within samples.

In short, for the same gradation distribution and under similar compaction effort, slag samples have higher void ratios and thus higher hydraulic conductivities than gravels and limestones. Some limestone samples have higher void ratios and hydraulic conductivities than their gravel counterparts while others do not. The effect of angularity of slags dominates over other factors influencing void ratio. The effect of particle shape and texture for gravels and limestones is obscured or even overwhelmed by other factors such as gradation distribution, compaction effort, etc..

For the same gradation distribution, most samples with higher void ratios have higher K values. In order to judge whether this is universally true between all materials without the limitation of the same gradation, the values of hydraulic conductivity for non-stabilized samples are plotted against

$$e' = \frac{e^3}{1+e} \qquad 4\text{-}12$$

in Figure 4-10. Note that K generally increases with e', however local irregularities exist. This is due to the effects of grain size distribution, particle shape and texture and variations of the degree of saturation. The smoothness of the relationship is comparable to the plot of hydraulic conductivity vs. D10 (Figure 4-6). This substantiates that void ratio is an important factor for estimating hydraulic conductivity.

Considering the effect of D10, D60 and void ratio, the values of hydraulic conductivity for non-stabilized materials are plotted against $D_{10} \cdot D_{60} \cdot \frac{e^3}{1+e}$ on Figure 4-11. This plot reflects the conjunctive effect of D10, D60, and e on hydraulic conductivity. By obtaining the linear regression of the available data as shown in Figure 4-11, hydraulic conductivity was related to D10, D60, and e as follows

$$K = 0.000044 \cdot D_{10} \cdot D_{60} \cdot \frac{e^3}{1+e} \qquad 4\text{-}13$$

with a R^2 value of 0.84. The units of D10 and D60 are millimeters. The units of K are cm/s. It is observed that Equation 4-11 (i.e. linear regression in Figure 4-8) predicts values of K higher than over 50% of the data points while Equation 4-13 (i.e. linear regression in Figure 4-11) predicts values of hydraulic conductivity lower than most of the data points.

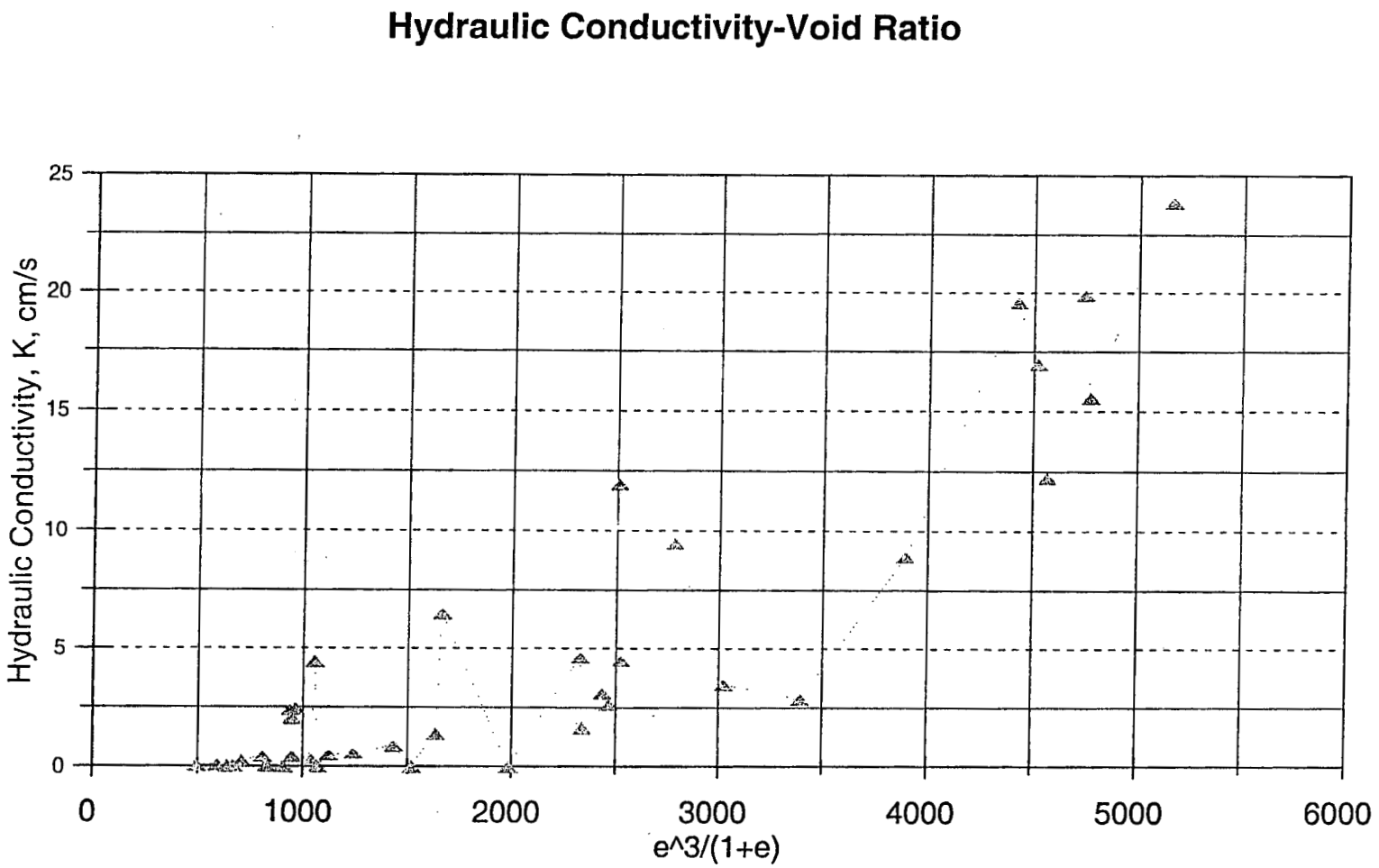

Figure 4-10: Hydraulic conductivity vs. void ratio

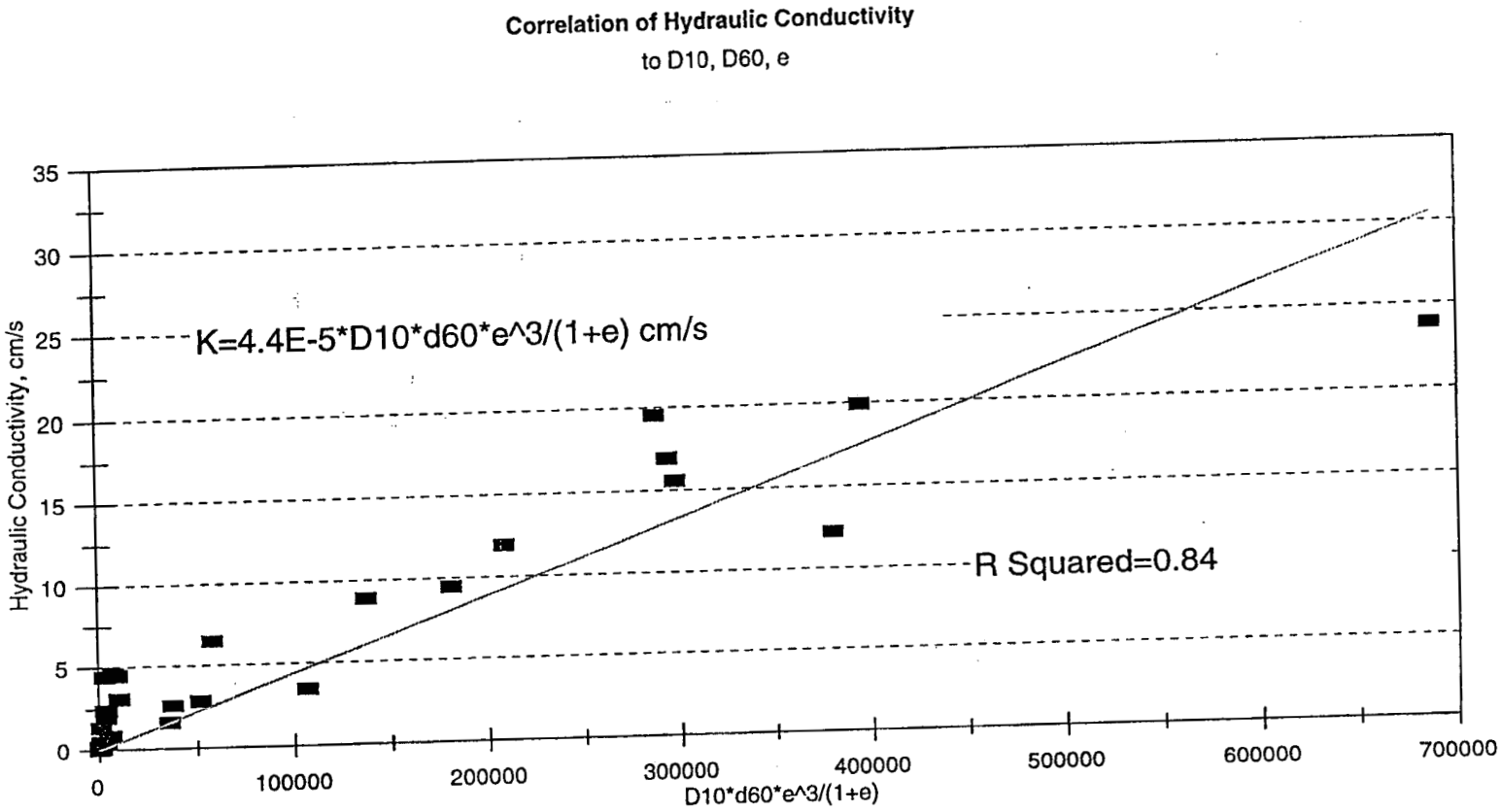

Figure 4-11: Correlation of hydraulic conductivity to D10, D60, and e.

4.8.3 Comparison with Moulton's Chart

The values of hydraulic conductivity of non-stabilized limestone samples in this study were compared with their values predicted from Moulton's (1980) chart presented in section 2.4. Moulton's chart is based on D10, dry density and percentage finer than the No.200 sieve and assumes the specific gravity of all samples is 2.70. The values of hydraulic conductivity for both sources are listed in Table 4-9. For relatively fine materials, such as ODOT 304, ODOT 310 and the Iowa mix, tested values are all much higher than Moulton's chart. Conversely, for open-graded materials such as No.57 and No.67, the values predicted from Moulton's chart are higher than tested values.

Moulton correlated the values of hydraulic conductivity of measured samples of granular base materials to effective grain size (D10), porosity n, and the percent passing the No. 200 sieve (P200). The correlation is as follows

$$K = \frac{6.214\times10^{5}\cdot D_{10}^{1.478}\cdot n^{6.654}}{P_{200}^{0.597}} \qquad 4\text{-}14$$

At first glance, the correlation is not defined for materials with P200 equal to 0. It is not suitable for predicting hydraulic conductivity of coarse materials having no particles passing the No. 200 sieve. However, the chart presented by Moulton (1980) only approximates Equation 4-14. Specific gravity was assumed to be 2.70 for all materials, so that dry density could be used instead of porosity. Moreover, P200=0 is presented in the chart. This is an extrapolation from the original data on which the equation is based. Even for materials with P200 greater than 0, one should be cautious using empirical relations. As indicated in Moulton's equation, grain size distribution and porosity are critical to hydraulic conductivity. Here, D10 and P200 are used to describe grain size distribution. There must exist a gradation bound for those original materials on which this correlation was based. As stated in Moulton (1980), the applicability is necessarily limited to similar types of materials. The importance of P200 for these types of materials is emphasized by placing it in the denominator. Hydraulic conductivity increases with D10 and void ratio as shown in Figure 4-6 and Figure 4-10. However, local deviations exist due to variations of grain size distribution, material shape and texture. When the gradation distribution curve is beyond Moulton's valid gradation

Table 4-9: Comparison of K values of limestones with K estimated from Moulton's chart

Type	Grading	D10	Dry Density	P200	Sat. Degr.	K of Moulton		Tested K	
		mm	lb/ft^3	%		ft/day	cm/s	ft/day	cm/s
57	M	5.2	99.2	0%	103.8%	90000	31.8	34,659	12.2
67	M	5.2	99.4	0%	101.3%	90000	31.8	48,064	17.0
N.J.Mix	M	1.8	108.4	0%	93.5%	8000	2.82	7,455	2.63
Iowa Mix	F	0.13	121.0	6%	90.2%	1.8	0.0006	1,329	0.47
	M	0.4	118.1	3%	98.5%	25	0.0088	2,531	0.89
	C	2.2	106.0	0%	92.7%	4000	1.41	9,853	3.48
304	F	0.06	131.6	13%	90.5%	0.1	0.00004	111	0.04
	M	0.12	130.6	7%	98.3%	0.4	0.00014	201	0.07
	C	0.18	125.3	0%	96.8%	17	0.0060	1,179	0.42
310	F	0.072	118.6	10%	101.8%	1.0	0.00035	20	0.01
	M	0.1	128.2	6%	101.3%	0.6	0.00021	102	0.04
	C	0.18	124.0	0%	94.5%	18	0.0064	12,617	4.45

bound, the adverse effect of P200 on hydraulic conductivity may be overestimated. In Table 4-9, only the result for the New Jersey mix matches Moulton's prediction well. Others are either significantly greater or less than Moulton's prediction.

4.8.4 Comparison with Jones and Jones' Results

Jones and Jones (1989) conducted research on the measurement of horizontal hydraulic conductivity of coarse materials as presented in section 2.5. The materials used in their research were limestone, sandy gravel and crushed granite. The gradation was British Department of Transportation Type 1. The specification envelope and medium grading of this type of gradation is shown in Figure 4-12. By superimposing these curves on the curves of the gradation types investigated in this study, it was found that the fine grading of their materials is very close to the fine grading of the Iowa mix and the coarse grading of their material approximates the coarse grading of ODOT 310. No gradation curve in this study matches their middle grading well. Variations of hydraulic conductivity exist for nominally identical samples in their results. The maximum values are 2 to 4 times higher than the minimum values in a group of identical samples. Jones and Jones attributed this to the variation of degree of saturation, compaction effort, and inherent variability within samples.

The results of Jones and Jones' study and the results of fine grading Iowa mix and coarse grading ODOT 310 from this study are listed in Table 4-10. Hydraulic conductivity values of fine grading Iowa mix of both limestone and gravel are in the ranges of the fine grading of Jones and Jones' materials. The same results can be seen for the coarse grading results for ODOT 310. It can be concluded that the results obtained in Jones and Jones' study are similar to the results obtained in this study for materials having comparable distribution curves.

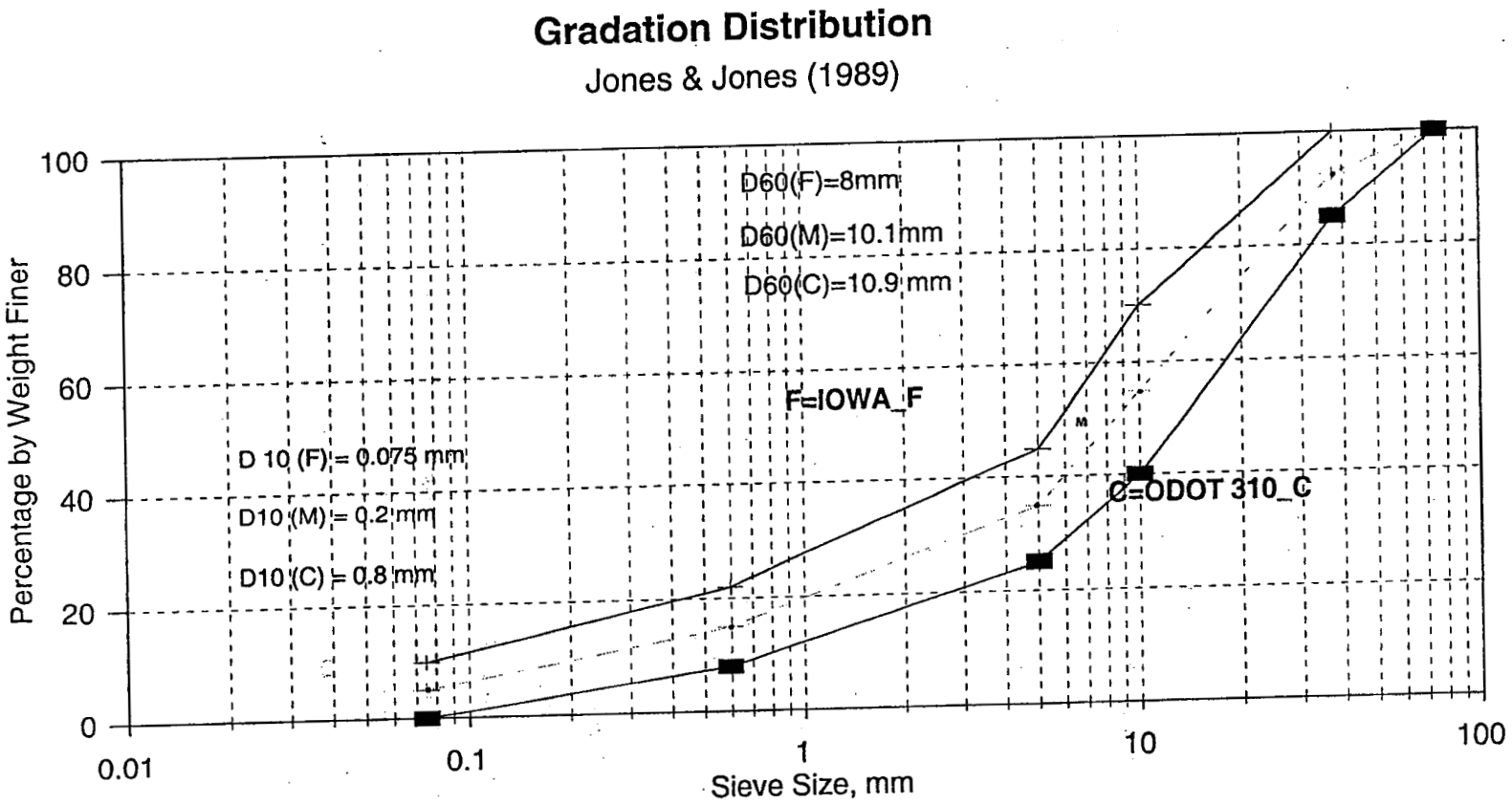

Figure 4-12: Gradation distribution of Jones and Jones' (1989) material

Table 4-10: Comparison of hydraulic conductivity with Jones and Jones's results

Jones & Jones' Results

		D10 mm	D60 mm	Dry density lb/ft^3	Total n %	K cm/s	K ft/day
Specification	F	0.075	8				
	M	0.2	10.1				
	C	0.8	10.9				
Limestones	F1	0.125		142.2	19.2	0.28	794
	F2	0.077		142.9	18.8	1.00	2,835
	F3	0.062		144.3	18.0	0.50	1,417
	M1	0.16		143.2	18.7	0.87	2,466
	M2	0.15		141.8	19.4	0.24	680
	M3	0.125		140.7	20.1	0.50	1,417
	C1	1.21		133.4	24.2	2.30	6,520
	C2	0.895		133.4	24.2	3.20	9,071
	C3	0.62		135.8	22.9	4.40	12,472
	C4			134.8	23.4	3.00	8,504
Sandy Gravel	F1	0.185		144.0	13.3	0.14	397
	F2	0.099		144.5	13.0	1.00	2,835
	M1	0.288		144.3	13.1	0.46	1,304
	M2	0.212		143.3	13.7	1.60	4,535
	C1	0.647		136.5	17.8	3.20	9,071
	C2	0.728		137.3	17.3	5.80	16,441

Results obtained in this research

Limestones	IWA_F	0.13	6	121.0	31.4	0.47	1,329
	310_C	0.18	18	124.0	29.3	4.45	12,617
Gravels	IWA_F	0.13	6	128.2	25.7	0.23	649
	310_C	0.18	18	123.4	28.6	2.45	6,945

4.8.5 Comparison with Cedergren's chart

Cedergren (1974) provided a chart for predicting hydraulic conductivity of filter materials and open-graded bases (Figure 2-8). In his chart, the gradation distribution curve is used to estimate hydraulic conductivity. Comparing the gradation curves in his chart with the curves in this research, it can be seen that the study materials have a wider range of particles than his materials. The shapes of the gradation distribution curves in this study do not match well to those in his chart.

For comparison purposes, define the left most curve in his chart as the fine limit curve and the right most curve as the coarse limit curve and the gradation envelope bounded by these curves as Cedergren's envelope. The value of hydraulic conductivity

for the fine limit curve is 0.00071 cm/s (2 ft/day), and the value of hydraulic conductivity for the coarse limit curve is 42.3 cm/s (120,000 ft/day). Most of the samples in this study are within Cedergren's gradation envelope, except for the fine grading of ODOT 310, which is located to the left of Cedergren's fine limit curve, yet can be considered comparable. The values of hydraulic conductivity for the samples in this study range from 0.0049 cm/s (14 ft/day) to 20.1 cm/s (57,000 ft/day), and are all within the K range of Cedergren's envelope. Therefore, the results obtained in this study are consistent with Cedergren's range of results.

4.9 Discussion of Results for Stabilized Materials

A summary of test results for stabilized base and subbase materials are presented in Table 4-11. Data and results for individual tests can be found in Appendix P. The density in Table 4-11 was measured immediately after mixing and compacting. The void ratio is based on this density. The amounts of aggregate, cement and water or asphalt were calculated according to their proportion in the mix design. The volume of each component in a sample was then calculated using its specific gravity. The apparent specific gravity as given in Appendix L was used for aggregates instead of the bulk specific gravity, since the cement would fill up those permeable voids in the aggregates. Also, the results for their non-stabilized counterparts are again listed in Table 4-11 for comparison. The volumes of aggregates of non-stabilized materials are based on bulk specific gravities. The void ratio of non-stabilized materials includes only the voids between particles, and does not include the permeable voids in the particles which do not contribute to the flow path.

In general, asphalt stabilized samples on average show higher values of void ratio and hydraulic conductivity than Portland cement stabilized samples. Both asphalt stabilized and Portland cement stabilized samples have lower values of void ratio and hydraulic conductivity than non-stabilized samples.

Table 4-11: Results for stabilized materials

Stabilized Samples

Test I.D.	Mix. Density	Void Ratio	K at 20		i_upper
	lb/ft^3	e	cm/s	ft/day	
P_F_57_L_A	101.5	0.654	10.0	28,400	0.011
P_M_57_L_A	99.5	0.685	11.2	31,800	0.011
P_C_57_L_A	101.7	0.647	13.2	37,500	0.008
P_M_67_L_A	105.1	0.595	13.4	37,900	0.013
P_M_57_S_A	90.0	0.679	12.4	35,200	0.011
P_M_67_S_A	93.1	0.624	9.8	27,600	0.012
P_M_57_G_A	115.4	0.442	8.1	23,000	0.015
P_M_67_G_A	109.8	0.516	12.3	34,900	0.008
P_M_57_L_P	111.5	0.491	11.9	33,700	0.011
P_M_67_L_P	110.7	0.508	7.6	21,500	0.023
P_M_57_S_P	101.2	0.499	9.5	26,900	0.018
P_M_67_S_P	101.7	0.491	11.9	33,600	0.010
P_F_57_G_P	117.4	0.395	11.7	33,100	0.010
P_M_57_G_P	121.1	0.357	8.7	24,800	0.012
P_C_57_G_P	121.8	0.355	10.6	30,000	0.008
P_M_67_G_P	116.7	0.406	10.0	28,400	0.016

Non-stabilized Counterparts

P_M_57_L_N	99.2	0.681	12.2	34,600	0.012
P_M_67_L_N	99.5	0.677	17.0	48,000	0.006
P_M_57_S_N	81.4	0.694	19.9	56,300	0.071
P_M_67_S_N	82.6	0.670	19.6	55,400	0.007
P_M_57_G_N	107.5	0.506	11.9	33,800	0.014
P_M_67_G_N	105.6	0.533	9.5	26,800	0.018

In the Portland cement stabilized group, the values of K range from 7.60 cm/s (21,500 ft/day) to 11.9 cm/s (33,700 ft/day). Void ratios range from 0.36 to 0.50. The K value of fine grading No. 57 gravel is higher than those of middle grading and coarse grading No.57 gravel. This is attributed to variations of compaction effort as indicated by their values of void ratio. The fine grading No. 57 gravel has a higher void ratio than the others. In general, the void ratios and hydraulic conductivities of Portland cement stabilized samples are lower than the non-stabilized samples and so are the values of hydraulic conductivity of asphalt stabilized samples. The impact of stabilization on

hydraulic conductivity varies from lowering hydraulic conductivity approximately 50% to increasing hydraulic conductivity 20%. The two critical factors are compaction effort and mix design.

The specification for cement content is 130.5 kg/cubic meters (220 pounds per cubic yard) of stabilized material, and the water/cement ratio by weight is 0.36. The amount of aggregate contained in 1 cubic yard of Portland cement stabilized base or subbase material is not specified. Since these lab results were to be compared with field results of K, the field mix design was used in the laboratory, in which the amount of aggregate contained in a unit volume of material is 95.2% of the maximum density of the corresponding non-stabilized sample. As shown in Table 4-11, the stabilization of base materials does not significantly lower hydraulic conductivity for these mix designs and compaction effort. However, charts such as Moulton (1980) and Cedergren (1974) appear to be greatly affected by mix design. Hence, the effect on hydraulic conductivity needs to be further investigated if compaction effort and mix design change.

4.10 Discussion of Time to Drain and Effective Porosity

A typical plot of permeameter system weight vs. time during draining is presented in Figure 4-13. The horizontal axis represents elapsed time, and the vertical axis represents system weight, which decreases with time as drainage takes place. Figure 4-13 is the draining curve of sample ODOT 304 gravel at coarse gradation. The system weight decreases with time nonlinearly. The rate of decrease of the system weight drops with time. At the tail of the curve, the system weight tends to stabilize. The characteristics shown in the figure were observed during the experiments for all the materials. At the instant of opening the downstream valve, large amounts of water flowed out at high velocity. After this fast discharge, flow decreased gradually to dripping.

All the draining curves have similar characteristics to Figure 4-13. The differences are the rates of decrease. The rate of decrease in Figure 4-13 was clearly lower than in similar curves for materials such as No. 57 gravel. The hydraulic

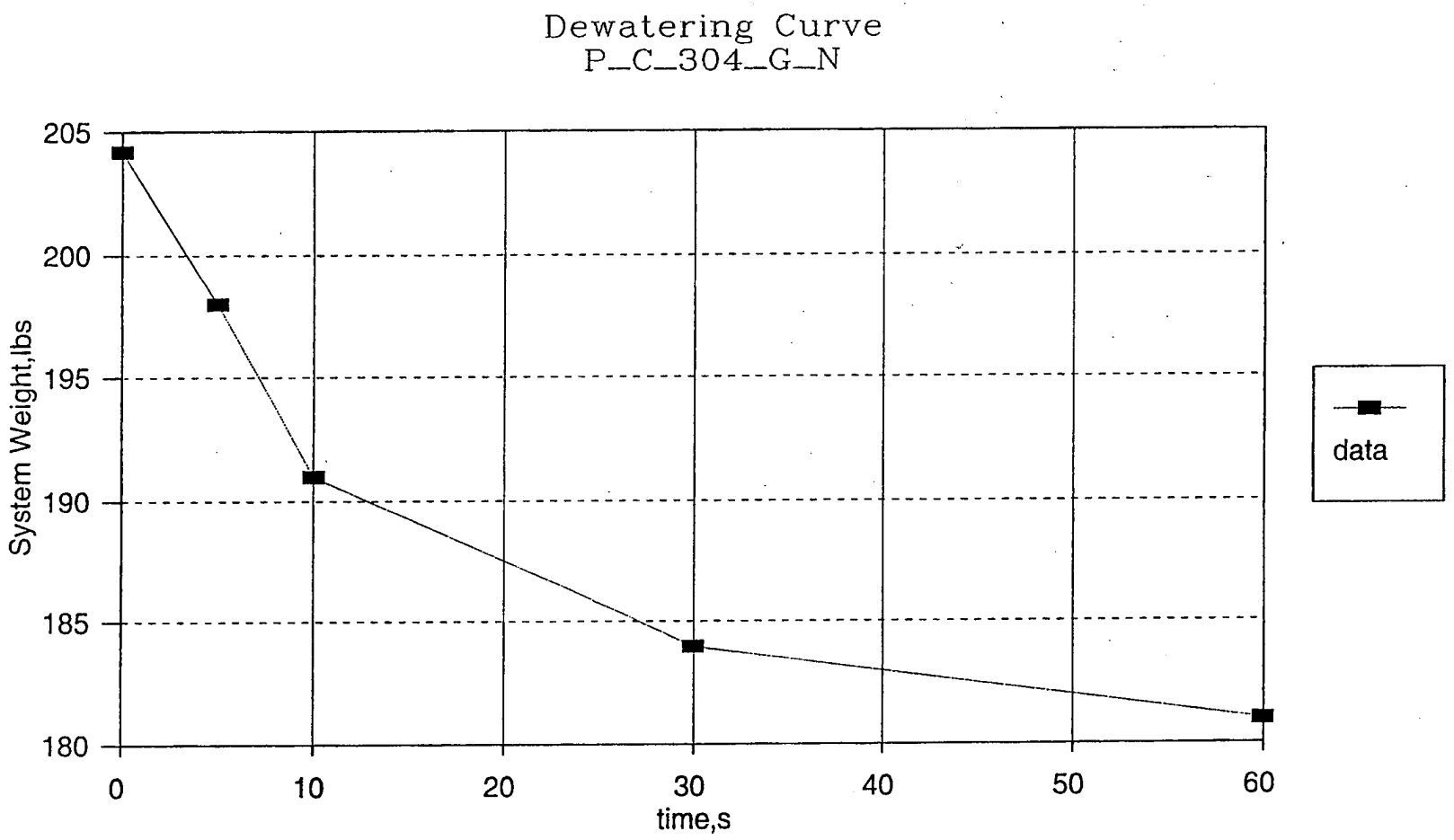

Figure 4-13: Dewatering curve.

conductivity of ODOT 304 gravel at coarse gradation is 2 cm/s. The hydraulic conductivity of No. 57 gravel at coarse gradation is 12 cm/s. As is expected, materials having higher hydraulic conductivity drain faster than low hydraulic conductivity materials. However, the degree to which drainage occurs is dependent on gradation.

The effective porosities, as described in section 4.5, can be found in Table 4-12. Typical values ranged from 6% for fine grading of ODOT 304 limestones to 35.6% for middle grading of No. 57 limestones, from 9% for fine grading of ODOT 310 slags to 41.7% for coarse grading of No. 57 slags, and from 8.4% for fine grading of ODOT 310 gravel to 39% for middle grading of No. 67 gravel. Volumetric percentages of water remaining in samples after drainage are also included on Table 4-12. Percentages of water remaining in samples ranged from 7.3% to 27.9%. Under normal drainage conditions, the amount of water contained in aggregates within pavements will not go below the percentages of water remaining in the samples as shown on Table 4-12. For instance, for the fine grading of ODOT 304 limestone, 26% of the total volume is void space, yet only 6% of the total volume drains freely. This means that 76% of the void space remains filled with water, leading to a pavement layer that is quickly resaturated when surface or subgrade moisture becomes available.

Type	Grading	Porosity n	Effective Porosity, n_e	Undrained Volume of Water in Base	
		% of total	% of total	% of total vol.	% of pore vol.
310_L	F	33%	10%	23%	69%
310_L	M	27%	11%	17%	60%
310_L	C	29%	13%	17%	56%
310_G	F	32%	8%	23%	74%
310_G	M	28%	8%	20%	72%
310_G	C	29%	21%	8%	28%
310_S	F	37%	9%	28%	76%
310_S	M	32%	10%	23%	70%
310_S	C	40%	27%	13%	33%
304_L	F	26%	6%	20%	76%
304_L	M	26%	10%	16%	61%
304_L	C	29%	12%	17%	59%
304_G	F	27%	11%	16%	60%
304_G	M	27%	11%	16%	58%
304_G	C	29%	16%	13%	44%
304_S	F	29%	12%	17%	60%
304_S	M	34%	16%	18%	53%
304_S	C	41%	24%	17%	42%
57_L	M	43%	36%	8%	18%
57_G	M	38%	29%	9%	22%
57_S	F	48%	32%	16%	33%
57_S	M	48%	36%	12%	26%
57_S	C	49%	42%	7%	15%
67_L	M	43%	35%	8%	19%
67_G	M	39%	30%	9%	22%
67_S	M	47%	34%	13%	28%
N.J.Mix_L	M	NA	NA	NA	NA
N.J.Mix_G	M	37%	29%	8%	22%
N.J.Mix_S	M	NA	NA	NA	NA
IW.Mix_L	F	31%	12%	19%	61%
IW.Mix_L	M	33%	17%	16%	47%
IW.Mix_L	C	40%	26%	14%	34%
IW.Mix_G	F	26%	8%	18%	68%
IW.Mix_G	M	28%	14%	14%	50%
IW.Mix_G	C	34%	23%	10%	30%
IW.Mix_S	F	36%	NA	NA	NA
IW.Mix_S	M	41%	23%	18%	44%
IW.Mix_S	C	46%	NA	NA	NA

Table 4-12: Effective Porosities and Undrained Volumes of Unstabilized Materials

5. STABILITY TESTING

The testing for this project consisted of a laboratory investigation utilizing a triaxial pressure chamber and a closed-loop servo hydraulic test system. The testing included 15 sequences of repeated axial cyclic stress of fixed magnitude with a load duration of 0.1 second, and a total cycle duration of 1 second applied to a cylindrical test specimen. During testing, the specimens were subjected to a dynamic cyclic stress using arbitrary function generator software (AWFG) and a digital to analog card. Static confining stress was provided by means of a triaxial pressure chamber. The axial loads and deformations were measured with electronic transducers. Data was recorded with a computer data acquisition system. Generally, the laboratory preparation and testing procedures described in the SHRP P46 and P31 protocol (FHWA, 1992) and AASHTO Designation T 274 - 82 (AASHTO, 1986) were followed.

5.1 Stability Tests

The aggregates used for the testing were supplied by the ODOT. The types of aggregates included crushed limestone, natural sand and gravel and air-cooled blast furnace slag. The material gradations shown in Table 5-1 are ODOT specifications No. 304 and No. 310 soils, AASHTO M43 specification No. 57 and No. 67 aggregates, the New Jersey test base materials (NJ MIX) and the Iowa Department of Transportation granular base specification 41-21 (Iowa Mix). The lower and upper bound gradations were the minimum and maximum percentages permitted by the specifications, respectively. The central gradation percentages are the averages of the lower and upper bounds. The central gradations were used for all test specimens for specification No. 57 and the NJ Mix. A total of 56 test specimens were prepared of which 44 were non stabilized aggregates and 12 were stabilized (See Table 5-2).

Table 5-1: Specifications for material gradations (percent finer by weight)

	No.304			No. 310			Iowa Mix			NJ Mix	No. 57
Sieve	C	M	F	C	M	F	C	M	F		
2 1/2"	-	-	-	100	100	100	-	-	-	-	-
2"	100	100	100	-	-	-	-	-	-	-	-
1 1/2"	-	-	-	-	-	-	-	-	-	100	100
1"	70	85	100	70	85	100	100	100	100	95-100	95-100
3/4"	50	70	90	-	-	-	-	-	-	-	-
1/2"	-	-	-	-	-	-	50	65	80	60-80	25-60
3/8"	-	-	-	-	-	-	-	-	-	-	-
#4	30	45	60	25	62.5	100	-	-	-	40-55	0-10
#8	-	-	-	-	-	-	10	22.5	35	5-25	0-5
#16	-	-	-	-	-	-	-	-	-	0-8	-
#30	7	18.5	30	-	-	-	-	-	-	-	-
#40	-	-	-	5	27.5	50	-	-	-	-	-
#50	-	-	-	-	-	-	0	7.5	15	0-5	-
#200	0	6.5	13	0	5	10	0	3	6	0	-

Legend: C – Coarse gradation limit; M – Middle gradation; F – Fine gradation limit

Table 5-2 Resilient modulus tests

Specification	Gradation	Limestone	Gravel	Slag
AC Stabilized No. 57	Middle	SM57LA(D,M)	SM57GA(D,M)	SM57SA(D,M)
PC Stabilized No. 57	Middle	SM57LP(D,M)	SM57GP(D,M)	SM57SP(D,M)
No. 57	Middle	SM57LN(D,M)	SM57GN(D,M)	SM57SN(D,M)
New Jersey Mix	Middle	SMNJLN(D,M)	SMNJGN(D,M)	SMNJSN(D,M)
	Coarse	SCIWLN(D,M)		
Iowa Mix	Middle	SMIWLN(D,M,W)	SMIWGN(D,M)	SMIWSN(D,M)
	Fine	SFIWLN(D,M)		
	Coarse		SC304GN(D,M)	
No. 304	Middle	SM304LN(D,M,W)	SM304GN(D,M)	SM304SN(D,M)
	Fine		SF304GN(D,M)	
	Coarse			SC310SN(D,M)
No. 310 (Grading A)	Middle	SM310LN(D,M)	SM310GN(D,M)	SM310SN(D,M)
	Fine			SF310SN(D,M)

Legend: S _ M _ 304 _ L _ N _ D
C1 C2 C3 C4 C5 C6

C1 = Test type	S = Stability
C2 = Target grading	C = Coarse grading limit of a gradation envelope M = Middle grading limit of a gradation envelope F = Fine grading limit of a gradation envelope
C3 = Gradation type	57, NJ Mix, IoWa Mix, No. 304 or No. 310
C4 = Material type	L = Limestone; G = Gravel; S = Slag
C5 = Binder type	N = Non-stabilized P = Portland cement stabilized A = Asphalt stabilized
C6 = Preparation moisture	D = Dry; M = Moist; W = Wet

5.1.1 Definitions of terms

The following terms describe the factors used to compute the resilient modulus of the aggregate base materials. The mathematical expressions required for the calculations are also provided.

(a) Haversine Shaped Load Form: the required load form for the standardized resilient modulus test. The load pulse is in the form $(1- \cos \theta)/2$ as shown in Figure 5-1.

(b) Maximum Applied Axial Load (P_{max}): the total load applied to the sample including the contact and cyclic loads.

$$P_{max} = P_{contact} + P_{cyclic}$$

(c) Contact Load ($P_{contact}$): vertical load placed on the specimen to maintain a positive contact between the specimen cap and the specimen.

$$P_{contact} = 0.1 P_{max}$$

(d) Cyclic Axial Load (P_{cyclic}): applied repetitive load to test a specimen.

$$P_{cyclic} = P_{max} - P_{contact} = 0.9 P_{max}$$

(e) Maximum Applied Axial Stress (S_{max}): the total stress applied to the sample including the contact and cyclic stresses.

$$S_{max} = P_{max}/A$$

(f) Contact Stress ($S_{contact}$): vertical stress placed on the specimen to maintain a positive contact between the specimen cap and the specimen.

$$S_{contact} = 0.1 S_{max}$$

(g) Cyclic Axial Stress (S_{cyclic}) : applied repetitive stress to test a specimen.

$$S_{cyclic} = S_{max} - S_{contact} = 0.9 S_{max}$$

(h) σ_d is the same as S_{cyclic}

(i) e_r is the recovered axial deformation due to S_{cyclic}

(j) ε_r is the recovered axial strain due to S_{cyclic}

$$\varepsilon_r = e_r / L_0$$

L_0 = initial sample length

(k) Resilient Modulus: determined based on the recoverable strain under repeated loads. The resilient modulus, M_r, is defined as

$$M_r = \sigma_d / \varepsilon_r = S_{cyclic} / \varepsilon_r$$

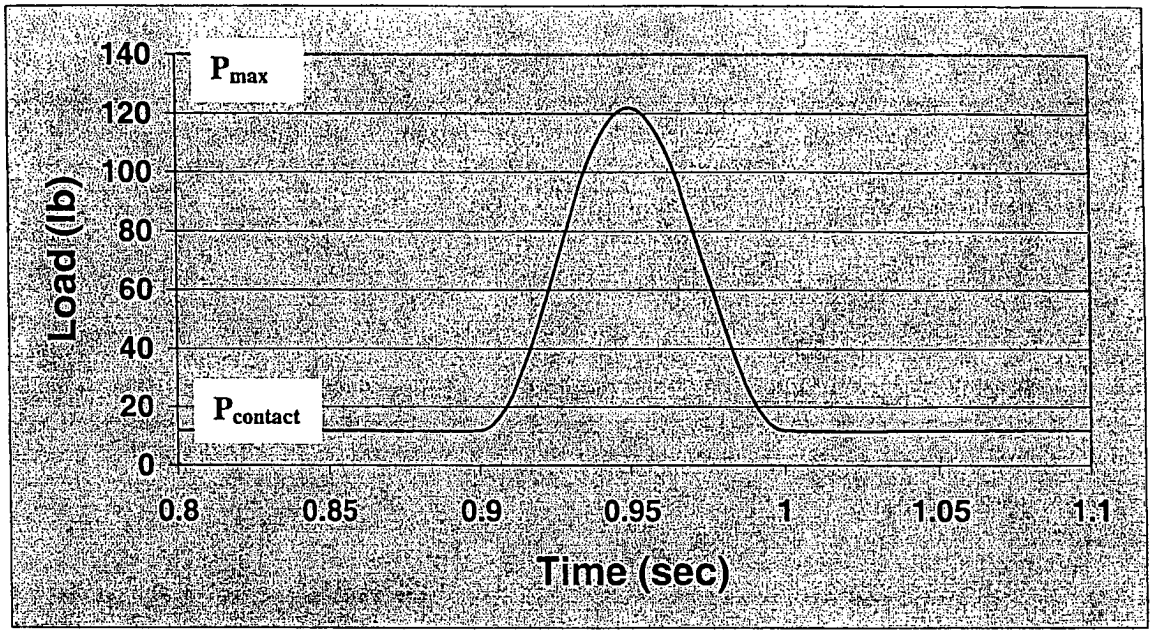

Figure 5-1 – Haversine load form

5.1.2 Test apparatus

The following test apparatus was used for the tests. All of the equipment functioned properly throughout the duration of the testing.

(a) Rubber membrane from 0.25 to 0.79 mm (0.01 to 0.031 inch) thickness, O-ring and pressure seal tape.

(b) Steel split molds.

(c) Vibration table for compacting the non stabilized specimens.

(d) Triaxial chamber, loading piston, porous plates (2), and top loading platen.

(e) Test frame with 1500 lb. axial load capacity.

(f) Computer system (386 DX-33) with the AWFG to send the load wave function to the hydraulic system servo-valve.

(g) Hydraulic system with hydraulic pump, servo-valve and hydraulic cylinder for applying loads to the specimen.

(h) Load cell and two LVDTs for use with the data acquisition system.

(i) Data collecting computer system (486 DX2-50) and data acquisition system.

5.1.3 Sample preparation

The following preparation was required for each test specimen that was tested in order to ensure proper results.

(a) Prepare enough material for one specimen as shown in Table 5-3. Mix the fine and coarse aggregate using a mechanical mixer.

(b) Place the rubber membrane and a bottom porous plate in the split steel molds. Place the material in the membrane using the vibration table to compact the specimen using several lifts.

(c) Place a porous plate on the top of the sample, then place the sample with the steel mold on the pedestal of the triaxial chamber. Carefully place an O-ring and seal tape on both the top and the bottom side of the rubber membrane.

(d) Apply vacuum of 15 psi to the specimen.

(e) Remove the steel molds.

(f) Assemble the triaxial chamber and insert the loading piston. Tighten the chamber tie rods firmly.

(g) Connect the air pressure supply line to the triaxial chamber. Apply a cell pressure of 10 psi and remove vacuum pressure. Check for leakage caused by poor connections, holes in the membrane, or imperfect seals at the cap and base.

(h) Slide the assembly apparatus into position under the loading frame and axial loading cell. Lower the loading piston of the triaxial cell to the top loading platen top and connect the two LVDTs to the top of the triaxial chamber.

Table 5-3: Sample preparation

Specifi-Cation	Grad.	Limestone		Gravel		Slag	
		Air Dry Density, (lb/ft^3)	Aggregate Bulk S.G.	Air Dry Density, (lb/ft^3)	Aggregate Bulk S.G.	Air Dry Density, (lb/ft^3)	Aggregate Bulk S.G.
[1]AC Stab. No. 57	M	100.2	2.67	109.5	2.59	82.9	2.21
[2]PC Stab. No. 57	M	97.7	2.67	106.7	2.60	82.9	2.23
No. 57	M	99.2	2.67	107.5	2.59	81.4	2.23
N.J. Mix	M	108.4	2.61	109.3	2.61	93.8	2.39
	C	106.0	2.64	114.3	2.60	87.9	2.30
Iowa Mix	M	118.1	2.62	124.0	2.61	98.1	2.36
	F	121.0	2.60	128.2	2.61	107.1	2.42
	C	125.3	2.64	123.7	2.60	95.5	2.31
No. 304	M	130.6	2.61	126.2	2.61	109.1	2.37
	F	131.6	2.59	126.1	2.61	120.8	2.45
No. 310	C	124.0	2.64	123.4	2.60	96.1	2.29
Grading A	M	128.2	2.59	124.9	2.61	115.4	2.46
	F	118.6	2.53	117.5	2.63	113.9	2.65

1 Asphalt percentage = 2.3%

2 Portland cement percentage = 8.1%

5.1.4 Resilient modulus testing

The test procedures were required for the resilient modulus testing. The test procedures were carried out throughout the testing to ensure appropriate results.

(a) Conditioning: Apply the pre-conditioning confining pressure of 15 psi. Then begin the sample conditioning by applying 500 repetitions of load sequence No. 0 (see Table 5-4).

(b) Apply 102 repetitions of the loads from sequence No. 1 to No. 15 (Table 5-3). These 15 sequences of repeated axial cyclic stress of fixed magnitude, load duration (0.1 second), and cycle duration (1 second) are applied to each cylindrical test specimen. During testing, the specimen is subjected to a static

confining stress provided by the triaxial cell pressure and a dynamic cyclic stress applied by the servo hydraulic system and AWFG.

(c) The loads and deformation time histories were measured using a 486 DX2-50 computer and the data acquisition system using the high speed mode option and stored in data files.

(d) At the completion of the 15 test sequences, reduce the confining pressure to zero and remove the sample from the triaxial cell.

Table 5-4: Test sequences

Sequence No.	Confining Stress kPa (psi)	Max. Deviator Stress kPa (psi)	Max. Cyclic Stress kPa (psi)	No. of Load Cycles
0	103.4 (15)	103.4 (15)	93.1 (13.5)	500
1	20.7 (3)	20.7 (3)	18.6 (2.7)	100
2	20.7 (3)	41.4 (6)	37.3 (5.4)	100
3	20.7 (3)	62.1 (9)	55.9 (8.1)	100
4	34.5 (5)	34.5 (5)	31.0 (4.5)	100
5	34.5 (5)	68.9 (10)	62.0 (9.0)	100
6	34.5 (5)	103.4 (15)	93.1 (13.5)	100
7	68.9 (10)	68.9 (10)	62.0 (9.0)	100
8	68.9 (10)	137.9 (20)	124.1 (18.0)	100
9	68.9 (10)	206.8 (30)	186.1 (27.0)	100
10	103.4 (15)	68.9 (10)	62.0 (9.0)	100
11	103.4 (15)	103.4 (15)	93.1 (13.5)	100
12	103.4 (15)	206.8 (30)	186.1 (27.0)	100
13	137.9 (20)	103.4 (15)	93.1 (13.5)	100
14	137.9 (20)	137.9 (20)	124.1 (18.0)	100
15	137.9 (20)	275.8 (40)	248.2 (36.0)	100

5.2 Test Results

The data acquisition system, electronic load cell and two electronic displacement transducers (LVDTs) were used to record the load-time and displacement-time histories. The actual applied loads, as measured by the load transducer, were used for all stress calculations. Values of maximum cyclic stress and resilient deformation were determined for each test sequence for each of the last five seconds (95 - 100 seconds) using the load-time and displacement-time histories and the averages of the two displacement transducers. Examples of the histories are shown in Figures 5-2 and 5-3. The computed cyclic stress and resilient strain were used to compute resilient modulus. An example of the results from one test specimen is shown in Table 5-5. The particular specimen is a crushed limestone aggregate prepared using the central bound of the No. 57 specification and tested at moist condition. The resilient modulus values were determined by averaging the last five load cycles from each load sequence. The minimum and maximum values of resilient modulus for all test specimens are shown in Tables 5.6a and 5.6b, and values of resilient modulus are provided for all test specimens for one Sequence No. 11. In all cases the minimum values of resilient modulus occurred during Sequence No. 1 and the maximum values were obtained during Sequence No. 15.

Results of all the testing are shown in Appendix Q. Tables Q.1 and Q.2 are results for stabilized bases. Tables Q.3 through Q.10 are for non-stabilized bases and subbases. Tables Q.11 and Q.12 summarize the results for all stability tests performed. The data in Tables Q.1 and Q.2 are sporadic due to difficulty with the servo-hydraulic system. The system could not respond quickly enough in order to apply the loads properly. The tests on non-stabilized aggregates did not experience the same difficulty because of the lower stiffness of the materials. Therefore, it was possible to observe consistent trends and to analyze the data. Additional details and analysis of the test results beyond the scope of this study have been presented elsewhere (Heydinger, et al., 1996; Xie, 1995).

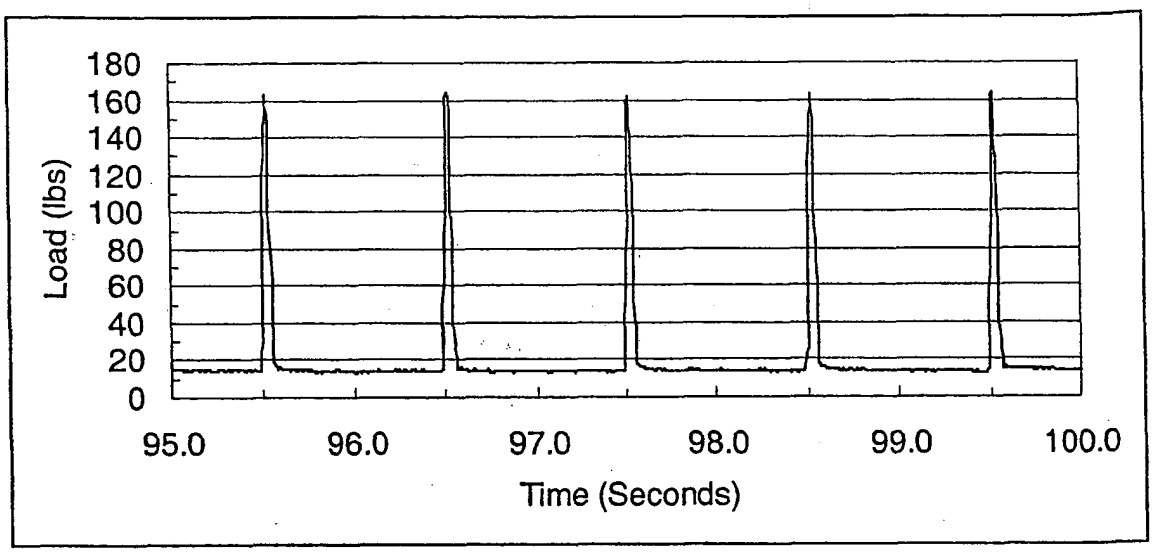

Figure 5-2 Example of load - time history

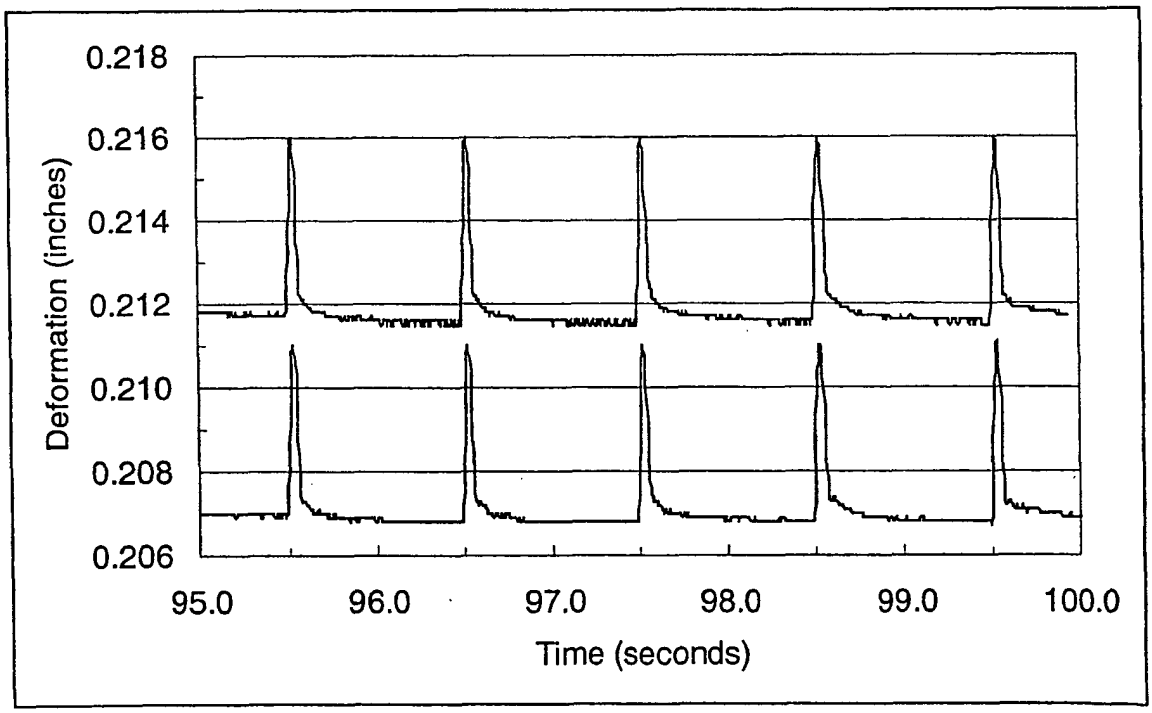

Figure 5-3 Example of displacement - time history

Table 5-5 Calculation of resilient modulus (SM57LNM)

Sequence.	Bulk Stress		Actual Maximum Cyclic Stress		Average Resilient Strain	Resilient Modulus	Resilient Modulus
No.	kPa	(psi)	kPa	(psi)	-	MPa	psi
1	81.2	(11.77)	17.0	(2.46)	0.000356	48	6910
2	101.9	(14.78)	36.3	(5.27)	0.000363	100	14500
3	123.0	(17.84)	55.9	(8.11)	0.000436	128	18600
4	141.8	(20.57)	35.4	(5.13)	0.000343	103	15000
5	175.7	(25.48)	66.1	(9.59)	0.000419	158	22900
6	216.6	(31.42)	103.1	(14.96)	0.000566	182	26400
7	275.9	(40.02)	62.0	(8.99)	0.000298	208	30100
8	339.8	(49.28)	120.0	(17.41)	0.000469	256	37100
9	411.8	(59.73)	183.8	(26.66)	0.000671	274	39700
10	382.3	(55.45)	64.5	(9.36)	0.000303	213	30900
11	414.9	(60.18)	93.1	(13.51)	0.000335	278	40300
12	507.7	(73.64)	175.3	(25.42)	0.000549	319	46300
13	526.3	(76.33)	101.1	(14.66)	0.000323	314	45500
14	543.5	(78.82)	114.3	(16.57)	0.000355	322	46700
15	702.0	(101.81)	257.1	(37.29)	0.000651	395	57300

Table 5-6a Summary of resilient modulus testing (MPa)

Specification	Gradation	Moist. Cond.	Limestone		Gravel		Slag	
			Range of M_r (MPa)	^1M_r (MPa)	Range of M_r (MPa)	^1M_r (MPa)	Range of M_r (MPa)	^1M_r (MPa)
No. 57	M	D	51 - 430	299	73 - 509	358.	30 - 195	164
	M	M	48 - 395	278	70 - 502	349	28 - 186	156
NJ Mix	M	D	61 - 412	306	79 - 461	381	30 - 197	164.
	M	M	59 - 387	288	71 - 439	363.	34 - 193	163
	C	D	42 - 283	215				
	C	M	43 - 262	206				
Iowa	M	D	45 - 279	215	70 - 461	345	37 - 232	188
Mix	M	M	44 - 284	213	59 - 431	314	35 - 237	188
	M	W	30 - 286	196				
	F	D	50 - 296	219				
	F	M	51 - 307	217				
	C	D			72 - 471	404		
	C	M			69 - 451	350		
	M	D	50 - 315	235	70 - 448	324	33 - 238	191
No. 304	M	M	48 - 300	238	58 - 427	317	33 - 252	188
	M	W	37 - 293	237				
	F	D			68 - 482	347		
	F	M			68 - 454	354		
	C	D					27 - 213	168
	C	M					30 - 216	162
No. 310	M	D	47 - 298	225	76 - 527	392	29 - 212	170
Grading	M	M	50 - 299	215	71 - 502	386	32 - 214	166
A	F	D					36 - 218	177
	F	M					35 - 220	173

^1M_r = Resilient modulus in MPa for Sequence No. 11 with both confining stress and maximum deviator stress equal to 15 psi (103.4 Mpa).

Table 5-6b Summary of resilient modulus testing (psi)

Specification	Gradation	Moist. Cond.	Limestone		Gravel		Slag	
			Range of M_r (psi)	^1M_r (psi)	Range of M_r (psi)	^1M_r (psi)	Range of M_r (psi)	^1M_r (psi)
No. 57	M	D	7460 - 62400	43300	10600 - 73900	51900	4420 - 28300	23800
	M	M	6910 - 57300	40300	10200 - 72800	50700	3990 - 26900	22700
NJ Mix	M	D	8830 - 59800	44300	11500 - 66800	55300	4400 - 28600	23800
	M	M	8520 - 56100	41800	10300 - 63700	52700	4870 - 28000	23700
	C	D	6040 - 41100	31200				
	C	M	6210 - 38000	30000				
Iowa	M	D	6580 - 40400	31200	10100 - 66800	50100	5390 - 33700	27300
Mix	M	M	6400 - 41200	31000	8520 - 62500	45500.	5110 - 34400	27300
	M	W	4310 - 41500	28500				
	F	D	7320 - 43000	31700				
	F	M	7400 - 44600	31400				
	C	D			10400 - 68300	58600		
	C	M			10000 - 65500	50700		
	M	D	7310 - 45700	34000	10200 - 65000	47000	4840 - 34500	27700
No. 304	M	M	6910 - 43600	34400	8460 - 62000	45900	4830 - 36600	27300
	M	W	5300 - 42600	34400				
	F	D			9820 - 69900	50400		
	F	M			9920 - 65800	51400		
	C	D					3910 - 30800	24400
	C	M					4310 - 31300	23500
No. 310	M	D	6880 - 43300	32600	11000 - 76400	57000	4260 - 30800	24700
Grading	M	M	7210 - 43400	31200	10300 - 72800	56000	4580 - 31000	24100
A	F	D					5250 - 31700	25700
	F	M					5060 - 31900	25000

^1M_r = Resilient modulus in psi for Sequence No. 11 with both confining stress and maximum deviator stress equal to 15 psi.

6. SUMMARY, CONCLUSIONS AND RECOMMENDATIONS

6.1 In Situ Hydraulic Conductivity Values and Test Method

There are two parts to the discussion of the in situ hydraulic conductivity test. The first part is a presentation of the field results and comparison to laboratory test results that simulate the field conditions. The second part includes observations, criticisms and suggested improvements to be made to the in situ hydraulic conductivity test device and method.

Estimations for the in situ hydraulic conductivity of the materials tested are based on the authors' judgments. Considerations that went into the selection of these values are 1) interpretation of the data collected in the field test, 2) as built density and gradation of the base materials, and 3) results of the limiting gradations for each material specification tested in the laboratory.

The first consideration to determine the overall field hydraulic conductivity of a particular material was interpretation of the data collected from the field test. If expected trends in the data did not occur and observations could not explain the behavior, then results from these tests were eliminated as faulty data of unknown origin.

The other consideration of the hydraulic conductivity testing in the field was comparison to the results for the limiting gradations that material's specification tested in carefully controlled laboratory experiments. One would expect that the in situ hydraulic conductivity of a certain material be within an order of magnitude of the laboratory value when the laboratory test simulates field conditions well (Bear, 1972), if the gradation and density are similar. The features constructed into the laboratory permeameter developed for this study appropriately represent field conditions, eliminate side wall leakage and minimize the adverse effect of non-representative samples in the laboratory.

Table 6-1 lists in situ hydraulic conductivities for each material tested. Table 6-2 lists the laboratory hydraulic conductivity results for these same material specifications and sources, as excerpted from Tables 4-8 and 4-11 (see also Cai, 1995; Steinhauser, 1995; Randolph, et al, 1996a,b). The laboratory device used to obtain the results in Table 6-2 measured horizontal hydraulic conductivity using a constant head test and conforms to ASTM standards for hydraulic conductivity testing. It was carefully designed to provide a realistic match to field conditions and minimal variability.

Table 6-1: Interpreted results of in situ hydraulic conductivity

Material	Predictions Using Moulton (1980) cm/s (ft/day)	Test No.	Field Hydraulic Conductivity cm/s (ft/day)
No. 310	0.00777 (22)	2	0.0154 (44)
No. 304	0.0184 (52)	2	0.00503 (14)
IDOT 41-21	0.0438 (124)	1	0.461 (1,306)
N. J. Mix	0.252 (714)	2	0.611 (1,731)
PCC No. 57	No Result	2	5.85 (16,572)
Asphalt No. 57	No Result	1	3.93 (11,133)

Table 6-2: Selected results of laboratory hydraulic conductivity (limestone).

Material	Gradation	Hydraulic Conductivity cm/s (ft/day)
No. 310	Upper Limit	0.0071 (20)
No. 310	Central Mix	0.035 (102)
No. 310	Lower Limit	4. 5 (12,600)
No. 304	Upper Limit	0.036 (111)
No. 304	Central Mix	0.074 (201)
No. 304	Lower Limit	0.42 (1,200)
Unstabilized No. 57	Central Mix	12.2 (34,600)
N.J. Mix	Central Mix	2.6 (7,450)
IDOT 41-21	Upper Limit	0.44 (1,320)
IDOT 41-21	Central Mix	0.90 (2,530)
IDOT 41-21	Lower Limit	3.5 (9,850)

By comparing Table 6-1 and Table 6-2 one can note that the field hydraulic conductivity results and the reported laboratory results compare favorably. However, in all cases the controlled laboratory test tended to overpredict hydraulic conductivity. These differences are logical, since it is unlikely that the in situ test was capable of fully saturating the base. An unsaturated medium always has a lower conductivity, all other conditions being equal. An unsaturated condition is most likely in the denser gradations such as No. 304, due to their smaller void spaces, hence the larger disparity for No. 304. This demonstrates the true value of an in situ test to provide realistic properties for design. Unfortunately, the uncertainty of in situ conditions during the tests makes finding a common condition for comparative studies difficult.

The differences seen for No. 57 are also logical. The No. 57 in the laboratory test was unstabilized and the No. 57 in the field test was either asphalt or Portland cement stabilized. Both values of hydraulic conductivity for this material were within an order of magnitude but less than the laboratory test value. This would be expected, since the asphalt and Portland cement binders take up void space within the material pore matrix. Subsequently, the material hydraulic conductivity would be lower due to the smaller void spaces.

Table 6-1 also lists predicted values of hydraulic conductivity based on Moulton's (1980) nomograph and the in situ hydraulic conductivity results of the same materials. Note that in determining hydraulic conductivity predictions for coarse materials, the nomograph may underestimate the actual hydraulic conductivity by as much as an order of magnitude, since it was developed for finer grained materials.

The results of the field tests were also compared to the laboratory results on No. 310, No. 304, and No. 57 reported by Majidzadeh and Elimitiny (1981), which were much lower. This is likely to be due to the fact that these researchers determined vertical hydraulic conductivity and not horizontal hydraulic conductivity. Other reasons could be small samples in the laboratory test (not complying with ASTM standards), a nonstandard method of compaction for these materials and the possibility of partially saturated conditions during laboratory testing. Many other researchers have shown that horizontal hydraulic conductivity is higher than the vertical hydraulic conductivity for compacted materials such as road bases (Bear, 1972). This is attributed in part to the

material particle orientation during compaction. It is difficult to compare these results completely due to the material anisotropy of hydraulic conductivity.

Agreement was very good between the in situ values and the values reported by McWaters (1994) for large scale horizontal tests of IDOT 41-21. Agreement was also good with the value of hydraulic conductivity for the New Jersey mix reported by Baumgartner (1992).

The second part of the discussion of the results of the in situ hydraulic conductivity test device contains criticisms and suggested improvements to be made to the device. The items that are discussed are the fresh water tank size, low range standing head, low hydraulic conductivity materials, passing trucks, data acquisition and placement of the salt injection port.

The first improvement to this field device would be to obtain a larger fresh water tank or to have the ability to fill the tank as it empties at the test site. Although this tank size proved to be large enough for low hydraulic conductivity materials, it was marginal for multiple tests of high hydraulic conductivity materials. Base material such as No. 57 can take on water so quickly that it was easy to empty the 1230 liter (325 gallon) tank within ten to fifteen minutes. While this speeds the test time, the limited tank size incurred more down time than anticipated due to necessary refilling of the tank to run more tests.

The second consideration of this device is that it may not be the best suited test to determine the properties of low hydraulic conductivity materials. In low hydraulic conductivity materials such as No. 304 it took a prohibitively long time to create steady state flow in the base. Also, when the air from the probes was bled out, water was introduced into the probe holes in the pavement. This water remained in the holes for a great deal of time because of the low hydraulic conductivity of the material. This extra water may or may not have had an effect on the differential pressure readings. If the water levels in the probe holes were not established by the flow of water underneath the pavement, but instead were establish by the water flushed through the probes, faulty differential pressure readings would occur. Because of the low hydraulic conductivity of these materials, it took a longer time to run these tests. Higher well potentials would have to be used, in order to run the test more quickly. These higher well potentials might

cause undue stress on the pavement and cause it to deflect upward allowing hydraulic short circuiting between the pavement and base. Therefore, a system to weigh down the pavement should be considered if higher well potentials are used.

The next consideration was the effect of heavy trucks passing on the pavement slab next to the one being tested. Each time a heavy truck passed by the experimental equipment a small downward deflection was experienced which sent shock waves to the adjacent slab where the experiment was taking place. This caused a slight brief change in the differential pressure readings. It may be worthwhile to complete a field investigation when heavy traffic is not allowed to pass to see if there are any adverse effects on the differential pressure and resistance versus time readings.

The next consideration would be to upgrade the method of recording the resistance readings at the specified time intervals. The method of writing each reading down by hand is cumbersome and also leaves the experimenter with less time to monitor valves that periodically need adjusting during the course of the test. Although this consideration is not critical to the integrity of the test, it is recommended that each probe be attached to a single channel LED readout device with the capability of storing the data electronically. Then the data could be imported to a computer to be reduced for test results.

The next consideration to upgrade the test is placement of the port for the salt water injection. On this device the salt water was injected into the water control system and then went into the standpipe. In high hydraulic conductivity materials this was adequate, but in low hydraulic conductivity materials this presented a problem. The low hydraulic conductivity materials such as No. 304 accepted less than four liters of water every ten minutes. Since the water control system and hoses from the salt water tank to the standpipe could hold ten or more liters of water, it took approximately one half hour to a full hour for the salt water to reach the base. Additional time was required for the salt water to reach each of the probes. Future designs should incorporate a means for the salt water to be injected directly to the standpipe with a valve located at this position to regulate the flow.

There are three conclusions to discuss regarding the in situ device and procedure: 1) the degree to which the device worked, 2) whether representative results were obtained and 3) the ease of operation of the device.

The first conclusion to discuss is the degree to which the device worked. The device did work as designed and proved to be durable under the conditions it was intended to handle. This test provided adequate results representative of the field conditions under which it was to perform. Correlation with laboratory tests was good. Although this device is capable of providing representative results, trained personnel are needed to perform the tests in order to obtain the true in situ hydraulic conductivity. This need for trained personnel limits the ease of operation of this device. Improvements have been suggested to increase the testing ease. The test is more correct for coarse drainable road bases than the Moulton and Seals (1979) method, based on comparisons of measured versus predicted values from Moulton's nomograph. Overall, based on the results obtained from this device and comparisons of these results with laboratory test results, the velocity technique proved to be a viable method of determining in situ hydraulic conductivity of coarse base materials. This test has the potential to be a valuable tool for condition assessment of bases under existing pavements. However, additional field testing is required to evaluate any instrument bias and result variability.

6.2 Hydraulic Conductivity and Drainability Variations Within Gradation Envelopes

Material specifications for bases and subbases allow a range of possible percentages passing each sieve size in the specification. Since the in situ test was limited to as-built gradations and densities only, the laboratory hydraulic conductivity test was developed to define the range of possible results for the limiting gradations of each material specification. Tables 4-8 and 4-11 clearly show the large differences possible for two materials that both satisfy the same specification. For example, air cooled blast furnace slag meeting ODOT specification 304 had measured hydraulic conductivities of 0.032 to 4.5 cm/s (91 to 12,800 ft/day), for the lower and upper limiting gradations, respectively. Most other materials and sources show less severe variations over their gradation envelopes. Those specifications that permit significant percentages of fine material, such as ODOT 310, ODOT 304 and IA 41-21 show the greatest variations. Note that based on the conclusions of the previous section, these laboratory values may

somewhat overestimate the in situ hydraulic conductivities under field conditions. However, relative comparisons and conclusions can be drawn. It is important to recognize that the selection of a specific specification still implies the possibility of a wide variation of resulting hydraulic conductivities in situ.

Within any gradation envelope, a logical variation of hydraulic conductivity was found. The variability of hydraulic conductivity is proportional to the relative envelope width at D10 as defined in section 4.8. Among six gradation types of non-stabilized materials, the permeability descends in the order of No. 57 and No. 67, New Jersey mix, IA 41-21, ODOT 304 and ODOT 310 (Table 4-8). For the same gradation type, the air cooled blast furnace slag showed higher values of hydraulic conductivity than limestone and gravel, which is attributed to a lower bulk density due to the highly angular particles. Hydraulic conductivity of stabilized materials are lower than their non-stabilized counterparts with identical gradation, however, the differences are small (Table 4-11). Portland cement stabilized samples show slightly lower K values than asphalt stabilized materials.

The hydraulic conductivity values of all samples were analyzed in conjunction with their grain size distribution and void ratio. It was found that grain size distribution and void ratio are two critical factors determining hydraulic conductivity. Among samples with identical gradation, those with high void ratio show a higher value of hydraulic conductivity. Hydraulic conductivity increases as void ratio and D10 increase, and is influenced by particle shape and texture.

Cedergren's (1974) chart favorably supports the overall range of the hydraulic conductivities obtained in this study. Jones and Jones' (1989) research agrees with these results for similar types of materials and gradations (Table 4-10). Comparison between field results and laboratory results on the same materials suggests the validity of the laboratory device and procedure. The agreement of the results with previous research indicates that the testing device and procedure work well with the tested materials. The features constructed into this horizontal permeameter appropriately represent field conditions, eliminate side wall leakage and minimize the adverse effect of non-representative samples in the laboratory.

Most of the results do not match well with empirical estimates such as Moulton's (1980) chart because the chart is limited to granular types of materials with significant amounts of fine materials (Table 4-9). The effect of P200 in his chart overestimated the hydraulic conductivity for coarse materials in this study and underpredicted values when many fines were present. Majizadeh and Elminity's (1981) results are all lower than this study. This is ascribed to size effects, incomplete saturation and the use of a vertical permeameter for base materials in which the natural flow direction is horizontal.

Note that among tested material types, No. 57 and 67 in both non-stabilized and stabilized form show values of hydraulic conductivity above 2.82 cm/s (8000 ft/day), while most other specifications fail to meet this value. The widely recommended design hydraulic conductivity of 0.353 cm/s (1000 ft/day) (FHWA, 1990, 1992b) can be met by all of the materials within some portion of their gradation envelope. However, ODOT 304 and 310 can only meet this recommendation for the lower boundary of the envelope, in which virtually all fine particles are eliminated. This guideline also neglects to consider the effective porosity, which has a significant influence on the amount of readily drainable water in the base layer.

Table 4-12 contains the effective porosities found for the tested materials. The combination of effective porosities and hydraulic conductivities found in this study can be used to design new pavement drainage layers and evaluate existing pavements for time to drain using methods in FHWA Technical Paper 90-01 *Subsurface Pavement Drainage* (FHWA, 1990) or FHWA *Drainable Pavement Systems* (FHWA, 1992b) from Demonstration Project 87. However, the time to drain calculations only determine the time necessary for a unit of water to move from the farthest point under the pavement to the outlet drain. This should not be interpreted to mean that the drainage layer is fully drained of pore water. Capillary attractions due to aggregate texture will prevent a significant amount of water from freely draining. This is reflected in the difference between the true porosity and the effective (free draining) porosity. When effective porosity is low, the benefit of a drainage layer is significantly reduced.

A significant result of the drainage study can be seen by examining the effective porosities in Table 4-12. Under normal conditions, the volumetric percentage of drained pore space in an aggregate base could range from only 6% for a fine gradation of No. 304

limestone to 42% for a coarse gradation of No. 57 slag. Although these bases are porous by design, their ability to drain is very sensitive to the presence of fine particles. As a result, pore spaces in the drainage layers below pavements virtually always contain a significant volume of water. This ranges from 76% of the void space filled with water for a drained fine gradation of No. 304 limestone to only 15% of the void space filled with water for a drained coarse gradation of No. 57 slag. This aspect must be considered when designing pavement drainage, since even from a drained condition the pavement base can resaturate quickly and be subject to potential distress. If the inflow of groundwater or infiltration is sufficiently high, or if the outlet drains lose capacity over time, the drainage layer may remain saturated for extended periods.

The results obtained in this study provide a basis for choosing base and subbase materials based on their hydraulic conductivities and effective porosities. Once the type of material is chosen, the range of hydraulic conductivities and effective porosities should be further investigated with the compacted density expected in the field for the range of allowable gradations under consideration. This would provide a more accurate range of values for drainage design.

6.3 Stability Tests

A mechanistic method for pavement design employing elastic-layer theories requires the determination of resilient moduli for pavement base and subbase materials. From the test and analysis results presented in Chapter 5 of this report, it can be seen that the repeated-load testing procedure of resilient moduli (AASHTO T-274-82) can be rather complicated and time-consuming. It is very difficult to perform the required preparation and procedures. Specimens can fail before or during the conditioning stage. The specified test procedure requires a highly trained technician. The equipment must be carefully designed to obtain accurate data. Extensive detailed standards are needed for sample preparation, sample conditioning, and load magnitude control. A simpler or modified procedure to test resilient moduli is needed for future research

Results of laboratory resilient modulus testing conducted on dense and open-graded aggregates are presented in this report (see Tables 5.6a and 5.6b). The testing program included three different aggregate materials (crushed limestone, natural stone and air

cooled blast furnace slag), five different gradation specifications (No. 57, New Jersey mix, IA 41-21, ODOT 304 and ODOT 310) and three different moisture conditions (dry, moist and saturated). Test specimens of the five aggregate specifications were prepared so that they would satisfy the fine, middle and coarse gradations of each material (see Table 5-3). Resilient modulus tests were conducted as closely as possible to SHRP Protocol P-46 (AASHTO designation T 294-92 I).

The resilient modulus of aggregates is shown to be dependent on material type, gradation and moisture condition. For the following observations, sequence number 11 of each test will be used as the basis of comparison (Tables 5.6a and 5.6b). The gravel aggregates consistently had the highest resilient moduli, followed by limestone and then slag. For the limestone aggregate, the open-graded specifications (No. 57 and NJ mix) had higher moduli than the dense-graded specifications (IA mix, ODOT 304 and 310). However, for the Iowa mix the moduli do not vary significantly with variations of gradation for similar moisture conditions. The open-graded specifications tend to be slightly more sensitive to changing moisture content. For the gravel aggregate, the maximum moduli were obtained from the dense-graded specimens (ODOT 304 and 310) tested dry. The lower bound gradation (coarser) of the No. 304 specification had the highest moduli, followed by the upper bound (finer) and then the central gradation. The open-graded specifications exhibited a decrease of modulus with increase of moisture as was expected. For the slag aggregate, again the Iowa mix, ODOT 304 and ODOT 310 specifications had higher moduli than the other specifications. The moduli were not greatly affected by gradation for the No. 310 specification. However, again there were slight reductions of moduli for all gradations of slag with increased moisture content.

The results of this testing program can only serve as a guide in selecting values for resilient modulus. The precision and bias of the test procedures are not known. There was only one source each for the crushed limestone, natural stone and slag aggregates that were used for the testing. One could expect deviations from the results for aggregates obtained from different sources. The deviations could be significant if an aggregate is close to being out of specification with respect to other material properties.

The results do provide relative resilient moduli values for key variables such as specification, gradation within the allowable envelope, material type and moisture

condition. With these relative comparisons and observations of stabile materials in use, anticipated stabilities for the other variables can be extrapolated. The following general conclusions can be drawn. The most stabile materials in each gradation are gravel, followed by limestone and slag. In many instances, slag had a modulus less than half that of gravel for similar conditions. There is not a dramatic variation in moduli for the upper and lower bounds within each gradation.

In virtually ever case, increasing the moisture content lowered the modulus. However, when one considers the conclusion of the previous section that all the tested drainable bases normally contain a significant moisture content in situ, there are moist combinations that are noteworthy for their significantly higher moduli. Under moist conditions, the various gradations of gravel showed essentially the same level of stability. For moist limestone, the open graded specifications (No. 57 and NJ mix) showed distinctly higher moduli, though still lower than all gravels tested. Under moist conditions the dense gradings provide somewhat higher moduli for slags, although the values were all lower than those for limestone and gravel.

6.4 Recommendations

Based upon the summary and conclusions presented, several recommendations can be made. Under the correct conditions, all of the specifications tested (No. 57, No. 67, New Jersey mix, IA 41-21, ODOT 304 and ODOT 310) can provide hydraulic conductivities in excess of 0.353 cm/s (1000 ft/day), a widely recommended design hydraulic conductivity for pavements (FHWA, 1990, 1992b). However, it is essential that the lower limit of the gradation envelope (coarser) be followed for ODOT 304 and ODOT 310, with the expressed purpose of minimizing particles passing the No. 200 sieve. A reduced envelope for the ODOT 304 specification should be considered, when it is designed as a layer to provide pavement drainage.

Any gradation within the specifications for No. 57 or No. 67, whether stabilized or unstabilized, yields a hydraulic conductivity far in excess of 0.353 cm/s (1000 ft/day). Stabilization does reduce the hydraulic conductivity by about half, but this is not overly detrimental considering the high values. These gradations also yield a much higher effective porosity than the other materials tested. No. 57 or No. 67, whether stabilized or

unstabilized, should be considered when drainage is critical, and when fine materials are present in the subgrade that could migrate to clog finer grained bases.

Effective porosity is at least as important as hydraulic conductivity for the long term in situ drainability of a pavement base. The values reported in this study should be used to predict the travel time to the outlet for water under the pavement. However, as has been shown, the base is unlikely to ever completely drain. The effective porosity is the appropriate measure of the capacity of a freely drained base to accept new inflow when it becomes available from infiltration or groundwater.

The nomograph by Moulton (1980) has been widely referenced as a means to predict the hydraulic conductivity of granular materials. Based on this study, it is recommended that this nomograph not be used to predict the hydraulic conductivity of the open graded materials tested. Instead, the in situ hydraulic conductivity test developed in this study should be used to assess a broad range of existing pavement bases throughout Ohio. When this is not practical, or for future specifications, the laboratory test developed here should be used to assess the hydraulic conductivity and effective porosity of representative specimens at realistic densities.

Unstabilized specification No. 57 was found to have an equal or higher resilient modulus than the dense graded bases tested (ODOT 304, 310 and IA mix) for the moist conditions likely to exist in situ. Coupled with its relatively high hydraulic conductivity and effective porosity, this suggests that No. 57 be considered a first choice for the drainage layer under future pavements. The source material for No. 57 should be gravel when possible, followed in preference by limestone and air cooled blast furnace slag. The slag provides a higher hydraulic conductivity that is not really needed, and has significantly lower moduli than the other materials.

ODOT 304 is present under many existing pavements. Based on this study, it is relatively stabile under the moisture conditions likely to occur in situ, especially if composed of gravel or limestone. However, the in situ hydraulic conductivity was found to be seriously inadequate to drain the pavement. Additional in situ testing should occur to examine the drainage capabilities of other bases that meet the ODOT 304 gradation envelope. Future construction with ODOT 304 should be restricted to the lower bound of

the gradation envelope and require adequate construction inspection to assure compliance with this restriction.

7.0 REFERENCES

AASHTO, (1984), *AASHTO T215-70*, "Standard Method of Test for Permeability of Granular Soils (Constant Head)", Standard Specifications for Transportation Materials and Methods of Sampling and Testing, Part 2, Washington, D. C.

AASHTO, (1986), American Association of State Highway and Transportation Officials, Standard Specifications for Transportation Materials and Methods of Sampling and Testing, Washington, DC.

AASHTO, (1993), American Association of State Highway and Transportation Officials. The AASHTO Guide for Design of Pavement Structures, Washington, DC.

Albright, S., (1986), Evaluation of Crushed Aggregate Specifications Used by the Alaska Department of Transportation and Public Facilities, Thesis, Oregon State University, in partial fulfillment of the requirements for the degree of Master of Science in Civil Engineering.

ASTM, (1989). Annual Book of ASTM Standards, Philadelphia, PA.

ASTM, (1990), *ASTM D2434*, "Standard Test Method for Permeability of Granular Soils (Constant Head)", Annual Book of ASTM Standards, Sect. 4, V. 04.08, Philadelphia, PA.

Amerman, C. R., (1983), "Advances in Infiltration", *Proceedings on National Conference on Advances in Infiltration*, Chicago, Illinois, pp. 201-214.

The Asphalt Institute, (1986), SOILS MANUAL For the Design of Asphalt Pavement Structures, Manual Series No. 10(MS-10), Fourth Edition, College Park, MD.

Barber, E. S., and Sawyer, C. L., (1952), "Highway Subdrainage", *Public Roads*, Vol.26, No. 12, February.

Baumgartner, N., D. E. Elrick, and K. L. Bradshaw, (1987), "In-Situ Hydraulic Conductivity Measurements of Slowly Permeable Materials Using a Modified Guelph Permeameter and Guelph Infiltrometer", *Proceedings of First National Outdoor Action on Aquifer Restoration*, Ground Water Monitoring and Geophysical Methods, pp. 469-483.

Baumgartner, R. H., (1992), "Overview of Permeable Bases", *Proceedings of the '92 Materials Engineering Congress on Materials: Performance and Prevention of Deficiencies and Failures*, Atlanta, GA, pp. 275-287.

Bear, J., (1972), Dynamics of Fluids in Porous Media, American Elsevier Co., New York.

Bear, J. and A. Verjuijt, (1987), Modeling Groundwater Flow and Pollution, D. Reidel Co., Dordrecht, Holland.

Boutwell, G. P., and R. K. Derick, (1986), "Groundwater Protection for Sanitary Landfills in the Saturated Zone", presented to Waste Tech '86, National Solid Waste Management Association, Chicago, Illinois.

Bouwer, H., (1986), "Intake Rate: Cylinder Infiltrometer", Methods of Soil Analysis, Part I, Physical and Mineralogical Methods, *Agronomy Monograph No. 9*, American Society of Agronomy, Madison, Wis., pp. 825-844.

Bowles, J. E., (1992), Engineering Properties of Soils and Their Measurement, McGraw-Hill, N. Y..

Cai, J., (1995), Development of a Laboratory Hydraulic Conductivity Test for Coarse Materials, Thesis, The University of Toledo, in partial fulfillment of the requirements for the degree of Master of Science in Civil Engineering.

Cedergren, H. R., (1974), Drainage of Highway and Airfield Pavements, John Wiley and Sons, New York.

Cedergren, H. R., (1977), Seepage, Drainage, and Flow Nets, John Wiley and Sons, New York.

Chapuis, P. R., Gill, E. D., Baass, K., (1989), "Laboratory Permeability Tests on Sand: Influence of the Compaction Method on Anisotropy", *Canadian Geotechnical Journal*, 26(1), pp. 614-622.

Chapius, P. R., Baass, K. (1989), "Granular Soils in Rigid-Wall Permeameters: Method For Determining The Degree of Saturation", *Canadian Geotechnical Journal*, 26, pp. 71-19.

Chen, H. W., and L. O. Yamamoto, (1987), "Permeability Tests for Hazardous Waste Management Unit Clay Liners", Geotechnical and Geohydrological Aspects of Waste Management, D.J.A. van Zyl et al., Lewis Publishing, Inc. Chelsea, Michigan, pp. 229-243.

Childs, E. C., (1953), "The Measurement of the Hydraulic Permeability of Saturated Soil In Situ, Part I", *Proceedings of the Royal Society of London*, 215(1), pp. 525-535.

Childs, E. C., A. H. Cole, and D. H. Edwards, (1953), "The Measurement of the Hydraulic Permeability of Saturated Soil In Situ, Part II", *Proceedings of the Royal Society of London*, 216(1), pp. 72-89.

Christiansen, J. E., (1944), "Effect of Entrapped Air Upon The Permeability of Soils," *Soil Science*, 58(1), pp. 355-365.

Chu, T. Y., Davidson, D. T., and Wickstrom, A. E., (1955), "Permeability Test For Sands", Permeability of Soils, ASTM Special Technical Publication No. 163, American Society for Testing and Materials, Philadelphia, PA.

Collins, R. E., (1961), Flow of Fluids Through Porous Materials, Reinhold, New York.

Daniel, D. E., (1983), "Permeability Test for Unsaturated Soils", *Geotechnical Testing Journal*, 6(2), pp. 81-86.

Daniel, D. E., (1984), "Predicting the Hydraulic Conductivity of Compacted Clay Liners", *Journal of Geotechnical Engineering*, ASCE, 110(2), pp. 285-300.

Daniel, D. E., (1989), "In Situ Hydraulic Conductivity Tests for Compacted Clay", *Journal of Geotechnical Engineering*, ASCE, 115(9), pp. 1205-1226.

Daniel, D. E., and S. J. Trautwein, (1986), "Field Permeability Test for Earthen Liners", *proceedings, In Situ '86*, Blacksburg, Virginia, pp. 146-160.

Daniel, D. E., D. C. Anderson, and S. S. Boyton, (1985), "Fixed-Wall Versus Flexible-Wall Permeameters, " Hydraulic Barriers in Soil and Rock, ASTM STP 874, ASTM, Philadelphia, pp. 107-126.

Day, S. R. and D. E. Daniel, (1985), "Hydraulic Conductivity of Two Prototype Clay Liners", *Journal of Geotechnical Engineering*, ASCE, 111(8), pp. 957-970.

Dudgeon, C. R., (1966), "An Experimental Study of the Flow of Water Through Coarse Granular Media", *La Houille Blanche 7*, 785-801.

Elrick, D. E., W. D. Reynolds, and K. A. Tan, (1988), "A New Analysis for the Constant Head Well Permeameter", *proceedings, Validation of Flow and Transport Models for the Unsaturated Zone*, University of New Mexico, Las Cruses, New Mexico.

Elsbury, B. R. and R. J. Smith, (1988), "Field and Laboratory Testing of a Compacted Soil Liner", *U.S. EPA*, Cincinnati, Ohio.

Fancher, G. H., and J. A. Lewis, (1933), "Flow of Simple Fluids through Porous Materials", *Industrial and Engineering Chemistry*, 25(10), pp. 1139-1147.

Fernuik, N., (1987), "In situ Permeability Testing of Soil Liners with Low Hydraulic Conductivity", Thesis, University of Saskatchewan, Saskatoon, Canada, in partial fulfillment of the requirements for the degree of Master of Science.

Fernuik, N. and M. Haug, (1990), "Evaluation of In Situ Permeability Testing Methods", *Journal of Geotechnical Engineering*, ASCE, 116(2), pp. 297-311.

FHWA, (1992), Federal Highway Administration, Resilient Modulus of Unbound Granular Base/Subbase Materials and Subgrade Soils--SHRP Protocol: P46 (AASHTO DESIGNATION: T 294-92 I).

Floss, R. and Berner, U., (1989), "A New Method for the Determination of Horizontal and Vertical Permeability of Cohesionless Basecourse Materials", *Proceedings of The 3rd International Symposium*, University of Nottingham, April 11-13.

Forchheimer, P., Wasserbewegung durch Borden, (1901), *Z. Ver. Deutsch. Ing.*, No. 45, pp. 1782-1788.

Hastings, C., (1955), Approximations for Digital Computers, Princeton University Press, Princeton, N. J.

Head, K. H., (1982), Manual of Soil Laboratory Testing, Chapter 10, vol. II, Pentech Press, Plymouth, London.

Heydinger, A.G., Q.L. Xie, B.W. Randolph and J.D. Gupta, (1996), "Analysis of Resilient Modulus of Dense and Open-Graded Aggregates," *Transportation Research Record, No 1547, Aggregate and Material Tests and Properties Related to Performance*, TRB, pp. 1-6.

Hicks, R.G. and C.L. Monismith, (1991), "Factors Influencing the Resilient Response of Granular Materials," *Highway Research Record No. 345*, TRB, National Research Council, Washington, DC.

Hoopes, J. A., and D. R. F. Harleman, (1967), "Dispersion in Radial Flow from a Recharge Well", *Journal of Geophysical Research*, 72(14), pp. 3595-3607.

Hsu, T. H., (1990), Structural Engineering and Applied Mechanics Data Handbook, Vol. III, Plates, Gulf Publishing, Houston, TX.

Hubbert, M. K., (1956), "Darcy's Law and The Field Equations of The Flow of Underground Fluids", *Trans. Amer. Inst. Min. Metal. Eng.* 207, 222-239.

Hvorslev, M. J., (1949), "Time Lag in the Observation of Ground-Water Levels and Pressures", U. S. Army Engineers Waterways Experiment Station, Vicksburg, Miss.

Irmay, S., (1954), "On the Hydraulic Conductivity of Unsaturated Soils", *Transactions, American Geophysical Union* 35, 463-468.

Jones, H. A. and Jones, R. H., (1989), "Technical Note: Horizontal Permeability of Compacted Aggregates", *Proceedings of the 3rd International Symposium*, University of Nottingham, April 11-13.

Kaspyapa, A.S. and Lytton, R.L., (1988), A Simplified Mechanistic Rut Depth Prediction Procedure for Low-Volume Roads, *Research Report 473-1*, Texas Transportation Institute, College Station, TX.

Kinzelbach, W., and R. Rausch, (1989), Aquifer Simulation Model "ASM" computer software, Gesamthochschule, Kassel - Universitat, Kassel, F.R.G.

Knight, R. B. and J. P. Haile, (1984), "Construction of the Key Lake Tailings Facility", *Proceedings International Conference on Case Histories in Geotechnical Engineering*, St. Louis, Missouri.

Kozlov, G. S., (1984), "Implementation of Internal Road Drainage Design and Application", *Transportation Research Record, No. 993*, pp. 35-46.

Lambe, T. M., (1958), "The Engineering Behavior of Compacted Clay", *Journal of the Soil Mechanics and Foundation Division, ASCE, 84*, No. SM-2, pp. 1654-1 to 1654-34.

Lindquist, E., (1933), "On The Flow of Water Through Porous Soil", *Premier Congres des Grands Barrages*, Stockholm, 5, 81-101.

Majidzadeh, K., and R. Elmitiny, (1981), "Development and Implementation of Pavement Drainage Design Guidelines in Ohio", *Report No. FHWA/OH - 81/007*, Ohio Department of Transportation, Federal Highway Administration, 80pp.

Maytin, I. L., (1962), "A New Field Test for Highway Shoulder Permeability", *proceedings, Highway Research Board, 41(1)*, pp. 109-124.

McWaters, B., (1994), *personal communication*, Iowa Department of Transportation Official.

McCarthy, D. F., (1988), Essentials of Soil Mechanics and Foundations, 3rd Edition, Prentice Hall, Englewood Cliffs, N. J..

Mitchell, J. K. and Younger, J. S., (1967), "Abnormalities in Hydraulic Flow through Fine-Grained Soils", *ASTM STP 417*, pp. 106-139.

Monismith, C.L., J.A. Epps, D.A. Kasianchuk and D.B. McLean. "Asphalt Mixture Behavior in Repeated Flexure," *Report No. TE 70-5*, University of California, Berkeley, January, 1972.

Moulton, L. K., (1980), "Highway Subdrainage Design", *Report No. FHWA-TS-80-224*, Federal Highway Administration, 162pp.

Moulton, L. K. and R. K. Seals, (1977), "In Situ Determination of Permeability of Bases and Subbases", Phase 1, Interim Report, *Report No. FHWA-RD-78-21*, Federal Highway Administration,104 pp.

Moulton, L. K. and R. K. Seals, (1979), "Determination of the In Situ Permeability of Base and Subbase Courses", Phase 2, *Report No. FHWA-RD-79-88*, Federal Highway Administration, 48 pp.

Moulton, L. K. and R. K. Seals, (1980), "Determination of the In Situ Permeability of Bases and Subbases", *Public Roads*, 43(4), pp. 134-143.

Muskat, M. M., (1937), The Flow of Homogeneous Fluids through Porous Media, McGraw-Hill, Inc., New York.

Ogata, A., (1958), "Dispersion in Porous Media", Dissertation, Northwestern University, in partial fulfillment of the requirements for the degree of Doctor of Philosophy in Civil Engineering.

Oglesby, C. H. and L. I. Hewes, (1963), Highway Engineering, John Wiley and Sons, New York.

Olson, R. E. and Daniel, D. E., (1979), "Field and laboratory measurements of the permeability of saturated and partially saturated fine-grained soils", *Symposium on Permeability and Groundwater Contaminant Transport*, ASTM, Philadelphia, Pennsylvania.

Olson, R. E. and D. E. Daniel, (1981), "Measurement of the Hydraulic Conductivity of Fine Grained Soils", *ASTM STP 746*, pp. 18-64.

Phillips, J. R., (1985), "Approximate Analysis of the Borehole Permeameter in Unsaturated Soil", *Water Resources Research*, 21(7), pp. 1025-1033.

Piersol, R. J., L. E. Workman, and M. C. Watson (1940), "Porosity, Total Liquid Saturation and Permeability of Illinois Oil Sands III", *Geology Survey*, Report 67(1).

Rada, G. and M.W. Witczak, (1981), "Comprehensive Evaluation of Laboratory Resilient Moduli Results for Granular Material," *Transportation Research Record 810*, TRB, National Research Council, Washington, DC.

Randolph, B. W., Steinhauser, E. P., Heydinger, A. G. and Gupta, J. D., (1996a), "In Situ Test for the Hydraulic Conductivity of Drainable Bases," *Transportation Research Record, No. 1519, Effectiveness of Subsurface Drainage*, TRB, pp. 36-41.

Randolph, B. W., Cai, J., Heydinger, A. G. and Gupta, J. D., (1996b), "Laboratory Study of Hydraulic Conductivity for Coarse Aggregate Bases," *Transportation Research Record, No. 1519, Effectiveness of Subsurface Drainage*, TRB, pp. 19-28.

Reynolds, W. D. and D. E. Elrick, (1986), "A Method for Simulations of In Situ Measurement in the Vadose Zone of Field-Saturated Hydraulic Conductivity, Sorptivity, and the Conductivity-Pressure Head Relationships", *Ground Water Monitoring Review*, 6(1), pp. 84-95.

Reynolds, W. D., D. E. Elrick, and B. E. Clothier, (1985), "The Constant Head Well Permeameter: Effect of Unsaturated Flow", *Soil Science*, 139(2), pp. 172-180.

Rose, H. E., (1945), "An investigation into the laws of flow of fluids through beds of granular material", *Proc. Inst. Mech. Eng.* No. 153, pp. 141-148.

Roy, M. and S. K. Sayer, (1989), "Technical Note: In Situ Permeability Testing of Subbases on the M5 Motorway", Unbound Aggregate in Roads, *Proceedings of the Third International Symposium*, University of Nottingham, Great Britain.

Sai, J. O. and D. C. Anderson, (1990), "Field Hydraulic Conductivity Tests for Compacted Soil Liners", *Geotechnical Testing Journal*, 13(3), pp. 215-225.

Sargand, S.M., G.A. Hazen, B.E. Wilson and A.C. Russ, (1991), "Evaluation of Resilient Modulus by Back-Calculation Technique," Dept. of Civil Engineering, Ohio University, Athens, OH, Oct.

Scheidegger, A. E., (1960), The Physics of Flow Through Porous Media, 2nd ed., University of Toronto Press, Toronto.

Smith, T. W., Cedergren, H. R., and Reyner, C. A., (1964), "Permeable Materials for Highway Drainage", *Highway Research Record No. 68*, Highway Research Board, Washington, DC.

Smith, R. M. and Browning, D. R., (1942), "Persistent water-unsaturation of natural soil in relation to various soil and plant factors", *Soil Science of American Proceedings*, 7, 114-119.

Soil Testing Engineers Inc., (1983), "STEI Two-Stage Permeability Test", Soil Testing Engineers Inc., Baton Rouge, Louisiana.

Spellman, D. L., (1972), "Faulting of Concrete Pavements", *Highway Research Record no. 407*, Highway Research Board, Washington, DC.

Steinhauser, E. P., (1995), " Development of an In Situ Hydraulic Conductivity Test for Coarse Materials", Thesis, The University of Toledo, in partial fulfillment of the requirements for the degree of Master of Science in Civil Engineering.

Stephens, D. B., K. Lambert, and D. Watson, (1987), "Regression Models for Hydraulic Conductivity and Field Test of the Borehole Permeameter", *Water Resources Research*, 23(12), pp. 2207-2214.

Stephens, D. B., (1988), "Vadose Zone Characterization of Low Permeability Sediments Using Field Permeameters", *Ground Water Monitoring Review*, 8(2), pp. 59-66.

Stephens, D. B. and S. P. Newman, (1982a), "Vadose Zone Permeability Tests: Summary", *Journal of Hydraulics*, ASCE, 108(5), pp. 623-639.

Stephens, D. B. and S. P. Newman, (1982b), "Vadose Zone Permeability Tests: Steady State Results", *Journal of Hydraulics*, ASCE, 108(5), pp. 640-659.

Stephens, D. B. and S. P. Newman, (1982c), "Vadose Zone Permeability Tests: Unsteady Flow", *Journal of Hydraulics*, ASCE, 108(5), pp. 660-677.

Stephens, D. B. and S. P. Newman, (1982d), "Free Surface and Saturated-Unsaturated Analysis of Borehole Infiltration Tests Above the Water Table", *Advanced Water Resources*, 5(1), pp. 111-116.

Stewart, J. P. and T. W. Nolan, (1987), "Infiltration Testing for Hydraulic Conductivity of Soil Liners", *Geotechnical Testing J.*, 10(2), pp. 41-50.

Strack, O. D. L., (1989), Groundwater Mechanics, Prentice-Hall, Inc., Englewood Cliffs, N. J.

Thompson, M.R., (1989), "Factors Affecting the Resilient Moduli of Soils and Granular Materials," Workshop on Resilient Modulus Testing, Oregon State University, Corvallis, OR.

Thompson, M.R. and K.L. Smith, (1990), "Repeated Triaxial Characterization of Granular Bases," *Transportation Research Record 1278*, TRB, National Research Council, Washington, DC.

Timoshenko, S. P. and S. Woinowsky-Krieger, (1959), Theory of Plates and Shells, McGraw-Hill, Inc., New York.

Torstensson, B. A., (1984), "A New System for Ground Water Monitoring", *Groundwater Monitoring Review*, 4(4), pp. 131-138.

Vennard, J. K. and R. L. Street, (1982), Elementary Fluid Mechanics, John Wiley and Sons, Inc., New York.

Wallace, M. I., (1948), "Experimental Investigation of the Effect of Degree of Saturation On the Permeability of Sand", Thesis, Department of Civil Engineering, Massachesetts Institute of Technology, Cambridge, MA.

Ward, J. C., (1964), "Turbulent Flow In Porous Media", *Proceedings of American Society in Civil Engineering* , No. HY5, 90, 1-12.

Wright, D. E., (1968), "Nonlinear Flow Through Granular Media", *Proc. of American Society of Civil Engineering, Hydraulic Division,* No. HY4, 94, 851-872.

Wu, T. H., Chang, N. Y., and Ali, E. M., (1978), "Consolidation and Strength Properties of A Clay", *Journal of the Geotechnical Engineering Division*, ASCE, V.104, N. GT7, pp. 889-905.

Wu, T. H., Randolph, B. W. and Huang, C. S., (1987), "Long Term Strength of Embankment Materials: Shale and Colluvium", *Report FHWA/OH-87/008*, Columbus, OH.

Wyckoff, R. D., and Botest, H. G. (1936), "The Flow of Gas-liquid Mixture Through Unconsolidated Sands," *Physics* 7, 325-345.

Xie, Q.L., (1995), "Investigation of Resilient Moduli of Pavement Base and Subbase Materials," Thesis, The University of Toledo, Toledo, OH , in partial fulfillment of the requirements for the degree of Master of Science in Civil Engineering.

Yoder, E. J. and M. W. Witczak, (1975), Principles of Pavement Design, John Wiley and Sons, Inc., New York, Second Edition.

Zhou, H., L. Moore, J. Huddleston and J. Gower, (1992), "Free Draining Base Materials Properties," Research Unit/Pavements Unit, Oregon Dept. of Transportation, Salem, OR, March.